

# CHAPTER 5

## MANIPULATOR DESIGN

**H.-J. Warnecke**

**R. D. Schraft**

**M. Hägele**

**O. Barth**

**G. Schmierer**

Fraunhofer Institute for Manufacturing  
Engineering and Automation (IPA),  
Stuttgart, Germany

### 1 INTRODUCTION

In 1996 some 680,000 industrial robots were at work and major industrial countries reported growth rates in robot installation of more than 20% compared to the previous year (see Figure 1). The automotive, electric, and electronic industries have been the largest robot users, their predominant applications being welding, assembly, material handling, and dispensing. The flexibility and versatility of industrial robot technology have been strongly driven by the needs of these industries, which account for more than 75% of the world's installation numbers. Still, the motor vehicle industry accounts for 33% of the total robot investment worldwide (IFR, 1997).

In their main application, robots have become a mature product exposed to enormous competition from internationally operating robot manufacturers, resulting in dramatically falling unit costs. A complete six-axis robot with a load capacity of some 10 kg was offered at less than \$60,000 in 1997. In this context it should be noted that the robot unit price accounts for only 30% of the total system cost. However, for many standard applications in such areas as welding, assembly, palletizing, and packaging, preconfigured, highly flexible robot workcells are offered by robot manufacturers, thus providing cost-effective automation, especially for small and medium-sized productions.

Robots are considered a typical representative of mechatronics, which integrates aspects of manipulation, sensing, control, and communication. Rarely are a comparable variety of technologies and scientific disciplines focused on the functionality and per-

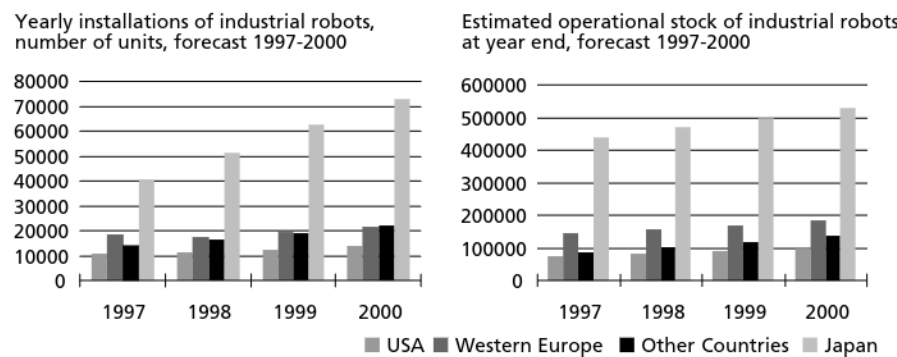


**Figure 1** Yearly installation numbers and operational stock of industrial robots worldwide (source: World Industrial Robots 1997, United Nations, and IFR).

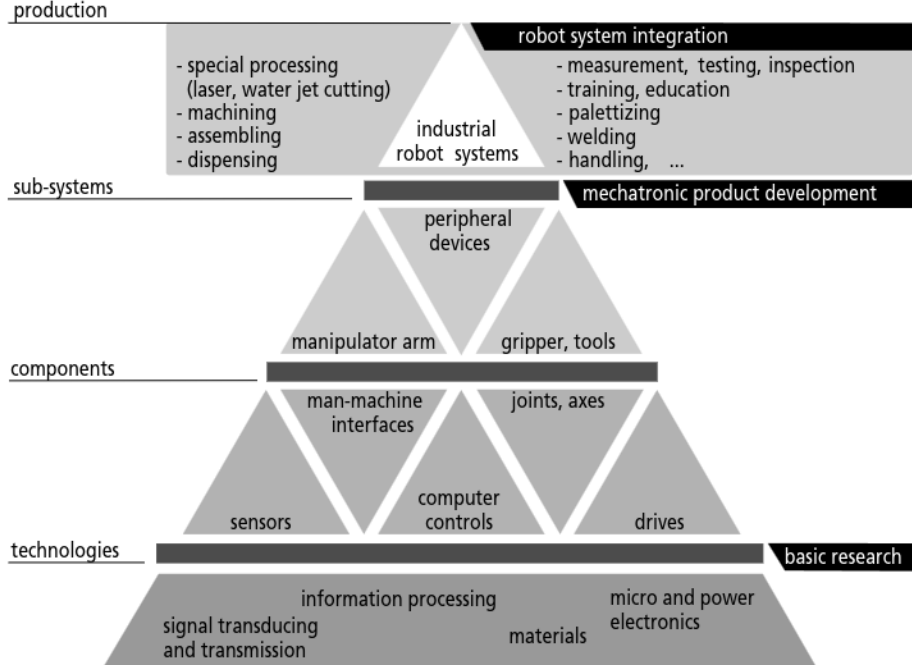


Figure 2 Robotics and mechatronics.

formance of a system as in robot development and application. Robotics integrates the state of the art of many frontrunning technologies, as depicted in Figure 2.

A sound background in mechatronics and the use of adequate design methods forms the basis of creative, time-efficient, effective robot development. Sections 2 through 9 give an overview of the basics of robot technology and adequate methods with their tools for arriving at a functional and cost-effective design.

## 2 PRINCIPLES OF ROBOT SYSTEMS ENGINEERING

The planning and development of robots is, as for any other product, a stepwise process with typical tasks, methods, and tools for each phase (see Figure 3). *Product planning*

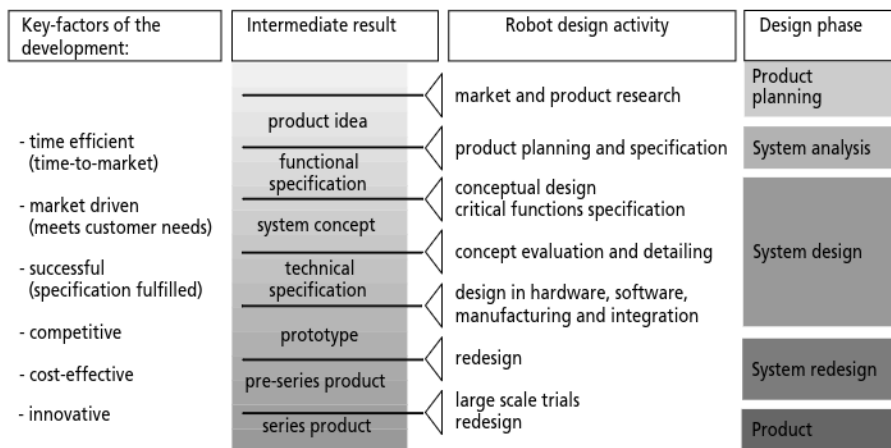
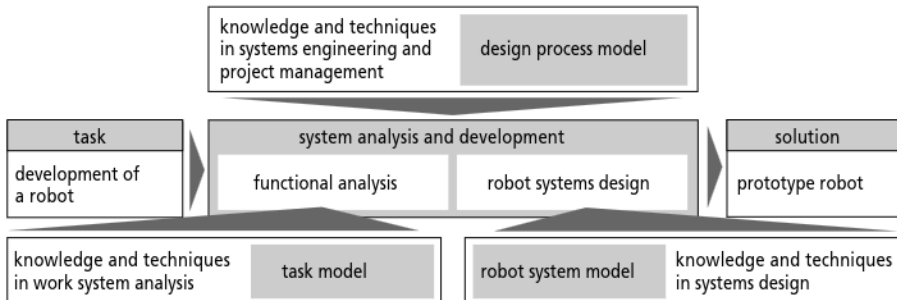


Figure 3 Industrial robot design process.



**Figure 4** General system engineering method for robot development.

includes all steps from an initial product idea to the specification of a product profile, covering all information on major performance data, anticipated product cost, quantities, distribution channels, and projected development time and cost.

The subsequent *systems analysis and design phase* includes the robot's functional specification, conceptual design, and detailing in hardware and software, as well as a complete documentation of all information relevant to manufacturing, assembly, operation, and maintenance of the robot. The design phase ends with the experimental verification of the robot prototype.

The *system redesign phase* covers all activities toward improving the robot system on the grounds of detected deficits, quality, performance and cost potentials, requested modifications, and planned product variants.

Figure 4 shows a general engineering model of the design phase in accordance to the systems engineering method by (Daenzer and Huber, 1994).

*Systems analysis and development* consists here of two methods and three models. It supports the engineer during both the functional analysis and the robot system design.

*Functional analysis* extracts from a task all functions and performance requirements that will be automated and specifies the environment of the task execution. All subsequent design work and the competitive posture of the robot rely on the functional analysis.

Due to their importance in the subsequent development process, the functional specifications of robots have been investigated in depth. Herrmann (1976) showed the functional relationship between manual tasks and basic performance data of a robot. Another approach is to review existing robots in terms of cost, performance, etc., so that a competitive market position for a new design can be determined (Furgaç, 1986).

Many *robot system design* methods and tools have been discussed in the past. Most stress the kinematic layout and its optimization as the central design property. Some methods represent an integrated approach resolving the interdependencies between design tasks such as kinematics and transmission (Klafter, Chmielewski, and Negin, 1989; Waner, 1988; Inoue et al., 1993; Nakamura, 1991).

## 2.1 Design Tasks

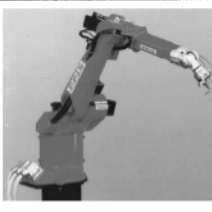
Specialization of robot design has a direct impact on the overall R&D goals and thus the robot's general appearance (see Figure 5).

In the past, the number of multipurpose or universal robot designs was overwhelming. However, many applications have occurred frequently enough that robot designs that take up specific process requirements could emerge. Examples of the different designs and their specific requirements are given in Figure 6.

## 2.2 Functional Analysis

Although many requirements may be obvious or are already defined, some central design parameters must be deduced from a work systems analysis. In order to arrive at the determination of geometric, kinematic, and mechanical performance data of a robot design, typical work systems that should be automated must be selected, observed, and described.

This analysis usually focuses on properties of objects that are handled, transported, machined, or worked on. In a "top-down" approach a given task can be broken down

Specialization of robots			
universal robot	application specific	specialist (modular design)	specialist (customized design)
			
Examples: Reis RV6	ABB Flex Palettizer	CMB Modular Robot	IPA Robot Refuelling
<ul style="list-style-type: none"> <li>• design fits standard applications</li> <li>• product variants according to payload, dexterity, working envelope</li> <li>• use of customized components</li> <li>• high manufacturing quantities</li> </ul>	<ul style="list-style-type: none"> <li>• application oriented designs</li> <li>• integrated process-control functions</li> <li>• preconfigured workcells available</li> <li>• medium manufacturing quantities</li> </ul>	<ul style="list-style-type: none"> <li>• task specific design</li> <li>• integration of standard modules (axis, control, sensors)</li> <li>• preferred applications: material handling</li> <li>• small manufacturing quantities</li> </ul>	<ul style="list-style-type: none"> <li>• task specific designs</li> <li>• primary applications: non-manufacturing fields (service robots)</li> <li>• task based kinematic structure</li> <li>• small to large manufacturing quantities</li> </ul>

**Figure 5** Specialization of robot designs, with examples (courtesy Reis Robotics, ABB Flexible Automation, CMB Automation).

			
palletizing	welding	assembly	coating, spray painting
<ul style="list-style-type: none"> <li>• large working envelope</li> <li>• high speeds</li> <li>• high accelerations</li> <li>• small footprint</li> <li>• 4 or 5 DOF</li> </ul>	<ul style="list-style-type: none"> <li>• interfaces to welding equipment</li> <li>• sensor integration (seam tracking)</li> <li>• low load capacity</li> <li>• 6 DOF</li> </ul>	<ul style="list-style-type: none"> <li>• fast horizontal/vertical motions</li> <li>• high precision</li> <li>• sensor integration (part detection, quality control)</li> <li>• 4-6 DOF</li> </ul>	<ul style="list-style-type: none"> <li>• fast spatial movements</li> <li>• high dexterity</li> <li>• explosion protected</li> <li>• 5,6 DOF</li> <li>• off-line programmable</li> <li>• process control functions</li> </ul>
			
measuring, quality control	laboratory automation	press-handling	machining
<ul style="list-style-type: none"> <li>• high precision</li> <li>• sensor integration (tactile, vision)</li> <li>• high dexterity</li> <li>• 5 or 6 DOF</li> </ul>	<ul style="list-style-type: none"> <li>• inexpensive</li> <li>• easy to program</li> <li>• desk top installation</li> <li>• 3-5 DOF</li> <li>• limited load capacity</li> </ul>	<ul style="list-style-type: none"> <li>• high payload</li> <li>• heavy duty</li> <li>• fast</li> <li>• 4-6 DOF</li> <li>• weight balanced</li> </ul>	<ul style="list-style-type: none"> <li>• high stiffness</li> <li>• positioning accuracy</li> <li>• sensor integration (tactile, vision)</li> <li>• 6 DOF</li> </ul>

**Figure 6** Application-specific designs of robots and their major functional requirements (courtesy FANUC Robotics, CLOOS, Adept Technology, ABB Flexible Automation, Fenoptik, CRS Robotics, Motoman Robotec).

into task elements, as in classic work analysis methods such as methods time measurements (MTM) or work factor (WF). However, the focus of the functional description of the considered tasks is on the analysis of geometries, motions, and exerted forces of object, tools or peripheral devices and with their possible dependence upon observation and supervision by sensors. Object or tool motions are divided into elementary motions without sensor guidance and control and sensorimotor primitives, defined as an encapsulation of perception and motion (Morrow and Khoshla, 1997; Canny and Goldberg, 1995).

Quantification of these motion elements led to the definition of the geometric, kinematic, and dynamic properties that play a central role in the subsequent robot design. Figure 7 gives a model of the breakdown of the tasks into motion and perceptive elements.

Typical performance and functional criteria are given in Table 1. The parameter with the strongest impact on the robot's complexity, cost, and appearance is its number of independent axis, i.e., degrees of freedom (d.o.f.). These are given by predefined goal frames and spatial trajectories that the robot endeffector must meet.

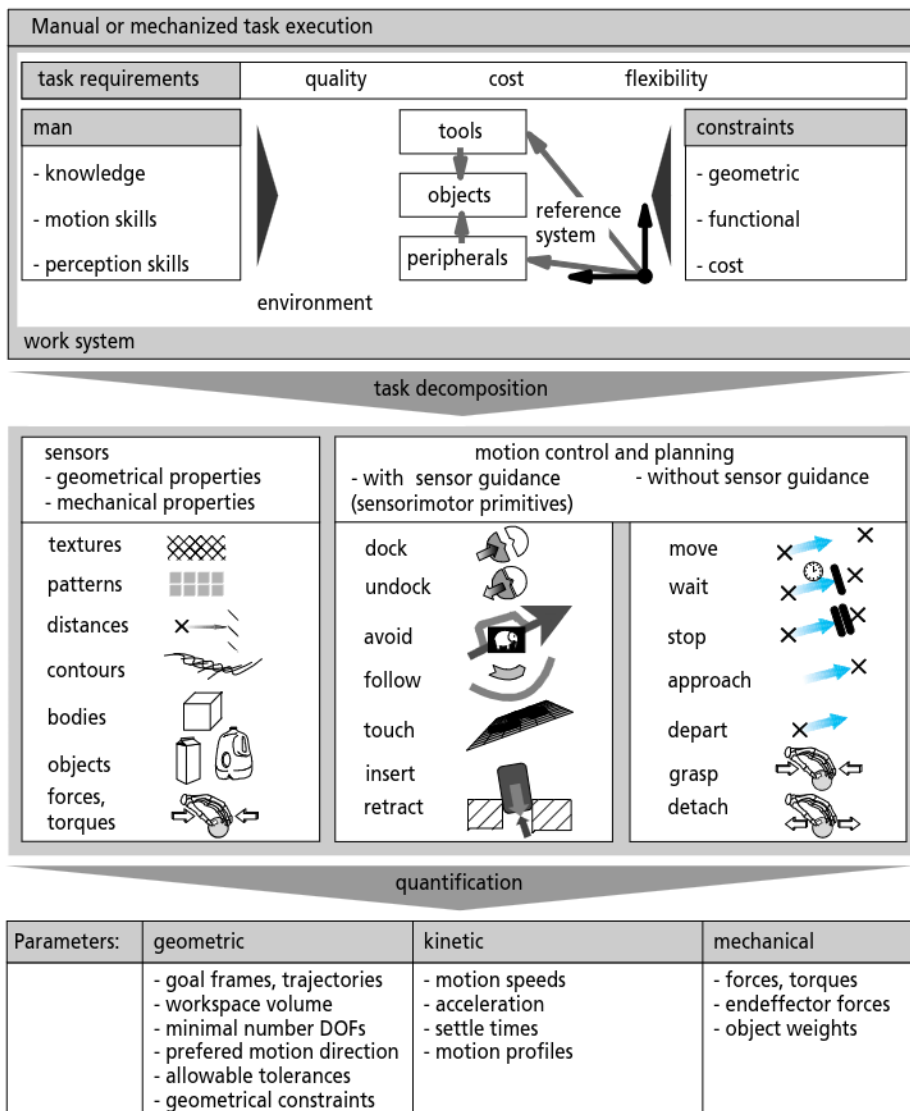


**Figure 7** Task model for the functional analysis of robots.

**Table 1 Basic Performance and Functional Criteria of a Robot**

Criteria	Characterization
Load capacity	<ul style="list-style-type: none"> <li>● Weight, inertia of handled object and endeffector</li> <li>● External movements/forces on endeffector or axes</li> <li>● Load history (RMS): static, periodic, stochastic, etc.</li> </ul>
Degrees of freedom	<ul style="list-style-type: none"> <li>● Required dexterity of endeffector</li> <li>● Number of degrees of freedom of peripherals (turn table etc.)</li> </ul>
Handled object, tools	<ul style="list-style-type: none"> <li>● Dimensions, size of objects/parts,</li> <li>● Kind of tools (torch, gripper, grinder, etc.)</li> <li>● Interfaces to robot</li> </ul>
Task characteristics	<ul style="list-style-type: none"> <li>● Changes from gripping to machining</li> <li>● Object/part presentation</li> <li>● Accessibility of objects/parts</li> <li>● Tolerances (parts, part presentation)</li> <li>● Fixing and positioning</li> <li>● Speed, acceleration</li> </ul>
Accuracy	<ul style="list-style-type: none"> <li>● Positioning accuracy</li> <li>● Repeatability</li> <li>● Path accuracy</li> </ul>
Path control	<ul style="list-style-type: none"> <li>● Point-to-point (PTP)</li> <li>● Continuous path (CP), motion profile</li> <li>● Rounding</li> </ul>
Environmental conditions	<ul style="list-style-type: none"> <li>● Quantifiable parameters (noise, vibration, temperature, etc.)</li> <li>● Not quantifiable parameters</li> </ul>
Economical criteria	<ul style="list-style-type: none"> <li>● Manufacturing cost, development cost</li> <li>● Break-even point, tradeoffs</li> <li>● Delivery time</li> <li>● Quality</li> <li>● Capacity (typical cycle times, throughput, etc.)</li> <li>● Point of sales (robot; workcell; production line)</li> </ul>
Repair, maintenance	<ul style="list-style-type: none"> <li>● Installation</li> <li>● Programming (on-line, off-line)</li> <li>● Remote servicing</li> <li>● Maintenance tasks and maintenance cycles</li> <li>● Changeability of modules and parts</li> </ul>
Flexibility	<ul style="list-style-type: none"> <li>● Workcell, CIM integration (logical and geometric interfaces)</li> <li>● Error handling, diagnosis</li> <li>● Cooperation with peripheral devices such as turntables, material handling equipment, other robots</li> </ul>

The result of the functional analysis is a requirement list that quantifies the robot's functionality and performance data according to:

- Fixed criteria that must be met
- Target criteria that should be meet
- Wishes ("nice to have" criteria)

### 2.3 Robot Systems Design

In the robot design, solutions have to be developed on the basis of the robot's functional specifications. Finding solutions for given functional and performance requirements is both an intuitive and a systematic process (Pahl and Beitz, 1995). A stepwise process helps in gradually approaching optimal solutions. The subdivision of the robot system into subsystems or modules supports a systematic and complete search for solution principles. Often so-called morphological tables are used, which list solution principles for each subsystem or module. Compatible solution principles can be combined with system solutions that are evaluated against each other.

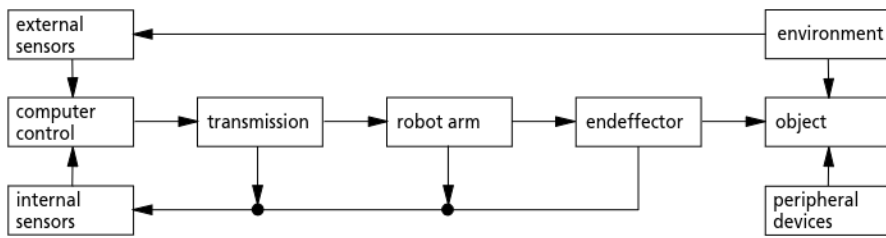


Figure 8 Robot system model.

The modular structure of a robot is obvious (Stadler, 1995; see Figure 8). For each subsystem possible solution principles are given in catalogues. Some of these are discussed in Sections 4 to 8.

The robot design process can be subdivided into three phases (Table 2, Figure 3), with increasing levels of detail:

1. The robot concept phase follows a top-down approach—a gradual development from the system's outer structure (kinematics) to its inner structure (transmissions).

**Table 2** Robot Design Process

I Robot Concept	
Process Step	Result
Selection of kinematic structure	Kinematic structure
Estimate of link, joint parameters	Kinematic model (DH-Parameters), joint travels
Selection of transmission principle	Structure of joint driving system
Selection of transmission components	Geometrical, performance data, and interfaces of selected components
II Robot Structural Design and Optimization	
Process Step	Optimization Criteria
Optimization of robot link and joint parameters (DH parameters)	Minimum number d.o.f., kinematic dexterity, footprint Maximum workspace
Optimization of kinetic performance	Minimum motion times Minimum joint accelerations
Selection of motors, gears, bearings, couplings	Maximum torques Minimum torque peaks (uniform torque profiles) Maximum heat dissipation
Cabling	Minimum test and bend, space occupancy
Selection of materials	Minimum weight, machining, corrosion Maximum stiffness
Dimensioning of axes, housing, base, tool flange	Minimum machining, weight, part numbers, assembly
III Robot Detail Design	
Process Step	Result
Part design	Part drawings
Robot system assembly	Bill of materials, assembly, calibration instructions
Electrical, electronical design (switching cabinet)	Electric circuit layout bill of materials
Documentation	Operation manual, servicing instructions

**Table 3 Categories of Tools for Robot Design**

Tool Category	Purpose
Symbolic equation solver	Generation of mathematical robot models, analysis, optimization of robot kinematic, kinetic, and dynamic parameters
Multibody simulation packages	Modeling, analysis, and synthesis of dynamic multibody structures
Finite element packages (FEM)	Structural, modal and vibration analysis of bodies and multibody system
Computer-aided design (CAD) packages	Representation, dimensioning, documentation of parts, structures, and systems
Computer-aided engineering (CAE) packages	Versatile tools covering all steps in the product development process from product specification to manufacturing

2. The robot structural design and optimization phase refines the chosen concept.
3. The robot detail design further details the optimized design to produce all documents for manufacturing, assembly, operation and maintenance of the robot.

Suitable tools for robot design help the engineer to find successful solutions quickly at the various levels of the design process. Design variations can easily be carried out and evaluated, as well as complex computations for robot kinematic, kinetic, dynamic and structural analysis and optimization. For this purpose many program packages are available, as listed in Table 3.

Special computer-aided engineering (CAE) tools for design simulation, optimization, and off-line programming for robots are widely used for their kinematic and transmission design. These tools offer both computer-aided design (CAD) and multibody simulation features. Various robot CAE packages have been presented, of which IGRIP (DENEB Robotics) and ROBCAD (Tecnomatix) have found wide acceptance. An example of their use in robot design is given in Figure 9.

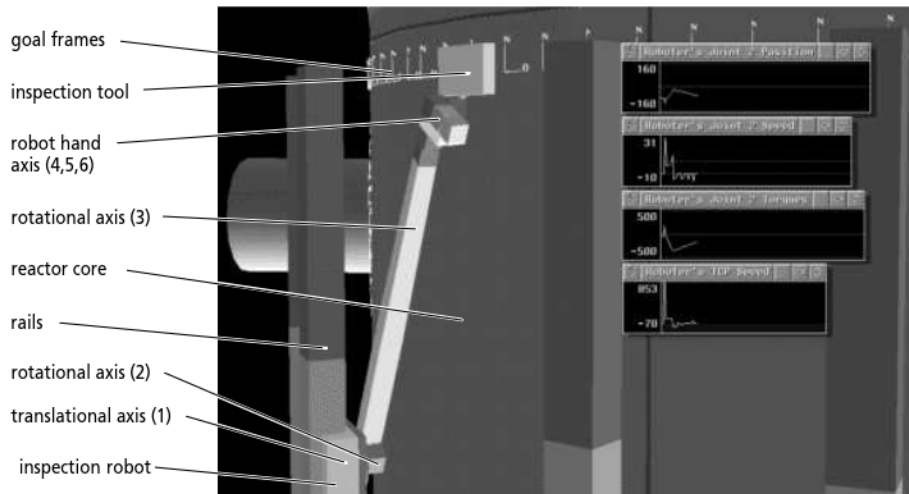


**Figure 9** Application of IGRIP in the design of a reactor outer core inspection robot. In this example the robot's joint 2 position, speed, torque, and tool center point Cartesian speed are displayed given a specific motion.

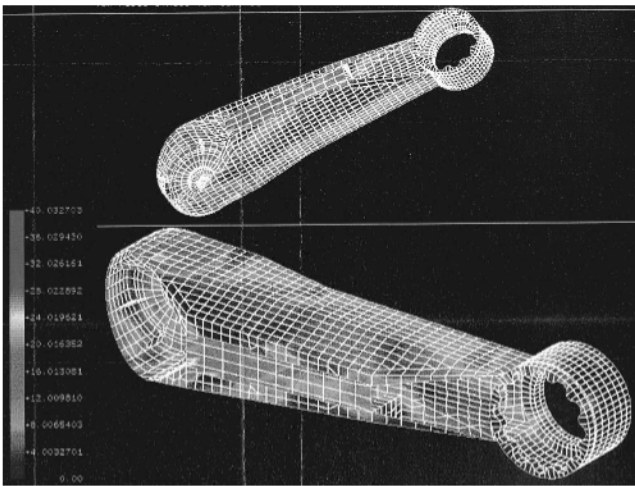


**Figure 10** Finite element model of the Reis RV6 robot arm (axis 2) with stress pattern (courtesy Reis Robotics), see also Fig. 5 for the robot's structure.

Finite element methods (FEMs) are widely used in robot mechanical design. A large number of well-established FEM programs offer valuable support in the robot's structural analysis and optimization (Burnett, 1987):

- Structural deflections and failure due to external loads
- Vibration models of both forced and unforced vibrations
- Structural stress patterns
- Structural heat flow (i.e., from servo-motors or gears).

FEMs represent complex 3D objects as a finite assembly of continuous geometric primitives with appropriate constraints (Figure 10). Today most packages interactively guide the user through the three major steps of a finite element calculation (Roy and Whitcomb, 1997):

1. *Preprocessing:* the 3D shape of the candidate structure is discretized into a finite number of primitive continuous geometric shapes with common vertices. Many programs perform automatic mesh generation.
2. *Solution generation:* the model response for given loads, material data, boundary conditions, etc. is computed. Many packages offer optimization features, i.e., the variation of shapes within specified boundaries for homogeneous stress distribution.
3. *Postprocessing:* besides tabulated data, results are usually displayed graphically.

#### 2.4 Design Evaluation and Quality Control

World-class manufacturers are better able than competitors to align their products and services with customer requirements and needs. Achieving this goal requires an ongoing interchange between customer and manufacturer, designer and supplier. Quality function deployment (QFD) is a suitable method for managing functional and performance inputs through the entire development process (Clausing, 1994).

The “house of quality” is a tool that records and communicates product information to all groups involved in the robot design process. It contains all relevant requirements for evaluating the design (Akao and Asaka, 1990; Ragsdell, 1994). The first task to be completed in any QFD undertaking is to clarify interdependencies in the design process that would otherwise be hidden or neglected:

- Systematic listing and evaluation of requirements
- Identification of critical functions and performance requirements
- Quality and cost-oriented requirements
- Evaluation of critical parts and production processes

In order to trace requirements from the beginning of product planning to the most detailed instructions at the operating level, QFD uses an interlocking structure to link ends and means at each development stage (Figures 11, 12).

Numerous QFD tools, such as QFD/CAPTURE and HyperQFD, support the engineer in the specification process and the quality control of the system development and its production.

### 3 ROBOT KINEMATIC DESIGN

The task of an industrial robot in general is to move a body (workpiece or tool) with a maximal of six degrees of freedom (three translations, three rotations) into another point and orientation within the workspace. The complexity of the task determines the robot's required kinematic configuration.

Industrial robots, according to ISO 8373, are kinematic chains with at least three links and joints. The number of degrees of freedom of the system determines how many independently driven and controlled axes are needed to move a body in a defined way in space. In the kinematic description of a robot we distinguish between:

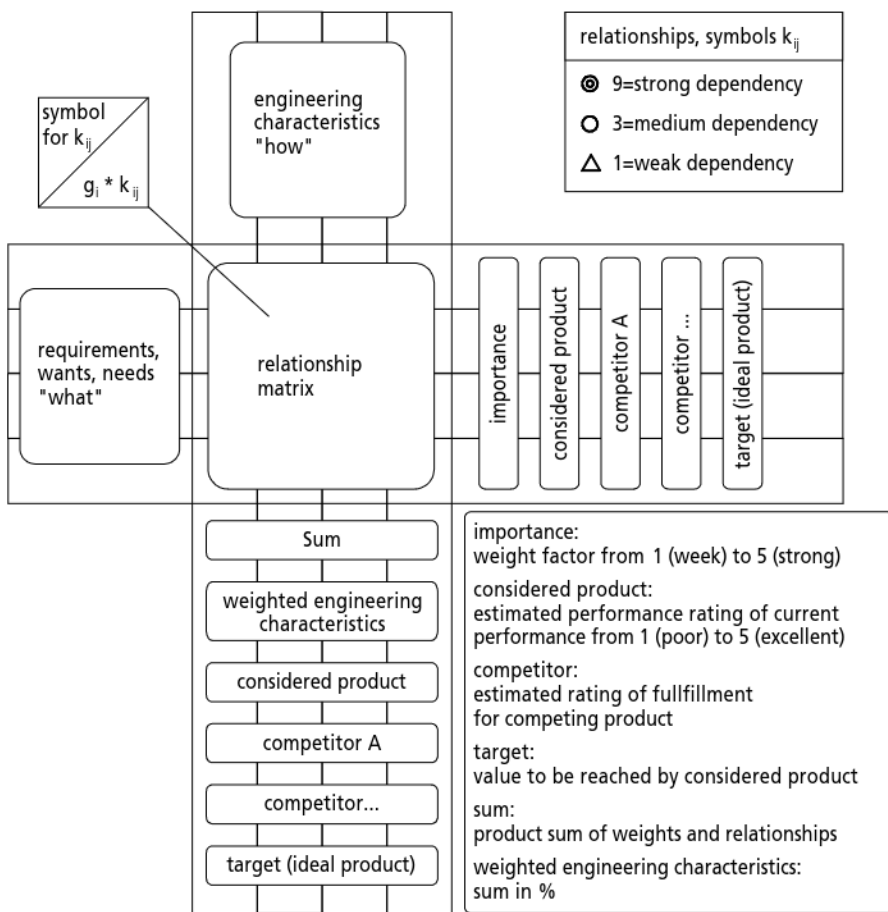
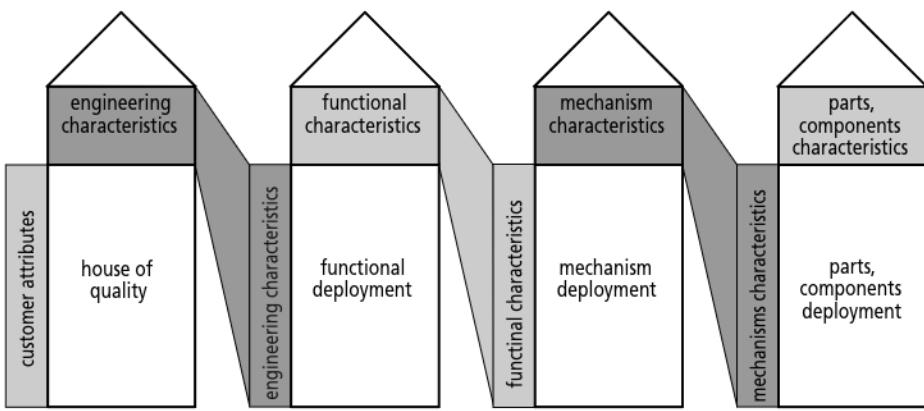


Figure 11 House of quality: QFD evaluation model for product design.



**Figure 12** Deployment of function and performance requirements in the robot design process.

**Arm:** an interconnected set of links and powered joints that support or move a wrist and hand or endeffector.

**Wrist:** A set of joints between the arm and the hand that allows the hand to be oriented to the workpiece. The wrist is for orientation and small changes in position.

Figure 13 illustrates the following definitions:

- The *reference system* defines the base of the robot and also, in most cases, the zero position of the axes and the wrist.
- The *tool system* describes the position of a workpiece or tool with 6 d.o.f. ( $x_k$ ,  $y_k$ ,  $z_k$  and  $A$ ,  $B$ ,  $C$ )
- The robot (*arm* and *wrist*) is the link between the reference system and tool system.

### 3.1 Robot Kinematic Configuration

Axes are distinguished as follows:

**Rotary axis:** an assembly connecting two rigid members that enables one to rotate in relation to the other around a fixed axis

**Translatory axis:** an assembly between two rigid members enabling one to have linear motion in contact with the other

**Complex joint:** an assembly between two closely related rigid members enabling one to rotate in relation to the other about a mobile axis.

Figure 14 gives an overview of the symbols used in VDI guideline 2861 and in this chapter. The kinematic chain can be combined by translatory and rotatory axes.

The manifold of possible variations of an industrial robot structure can be determined as follows:

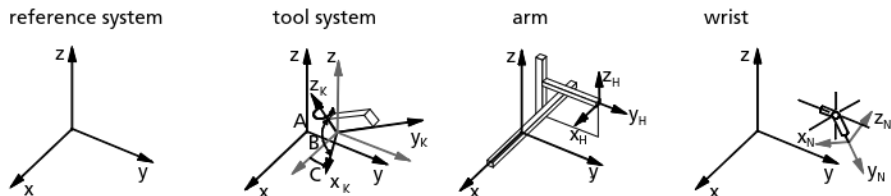


**Figure 13** Definition of coordinate systems for the handling task and the robot.

System	Translatory axis		Rotary axis		Gripper	Tool	Separation of arm and wrist
	telescopic	traverse	pivot	hinge			
Symbol							

**Figure 14** Symbols for the kinematic structure description of industrial robots according to VDI Guideline 2681.

$$V = 6^{\text{d.o.f.}}$$

where  $V$  = number of variations

d.o.f. = number of degrees of freedom

These considerations show that a very large number of different chains can be built; for example, for six axes 46,656 different chains are possible. However, a large number are inappropriate for kinematic reasons (Angeles, 1997):

- Positioning accuracy decreases with the number of axes.
- The kinetostatic performance depends directly on the choice of the robot kinematic configuration and its link and joint parameters.
- Power transmission becomes more difficult as the number of axes increases.

Industrial robots normally have up to four principal arm axes and three wrist axes. Figure 15 shows the most important kinematic chains of today. While many of the existing robot

Robot	Axes		Wrist (DOF)		
	Principle	Kinematic Chain	Workspace		
cartesian robot					
cylindrical robot					
spherical robot					
SCARA robot					
articulated robot					
parallel robot					

**Figure 15** Typical arm and wrist configurations of industrial robots.

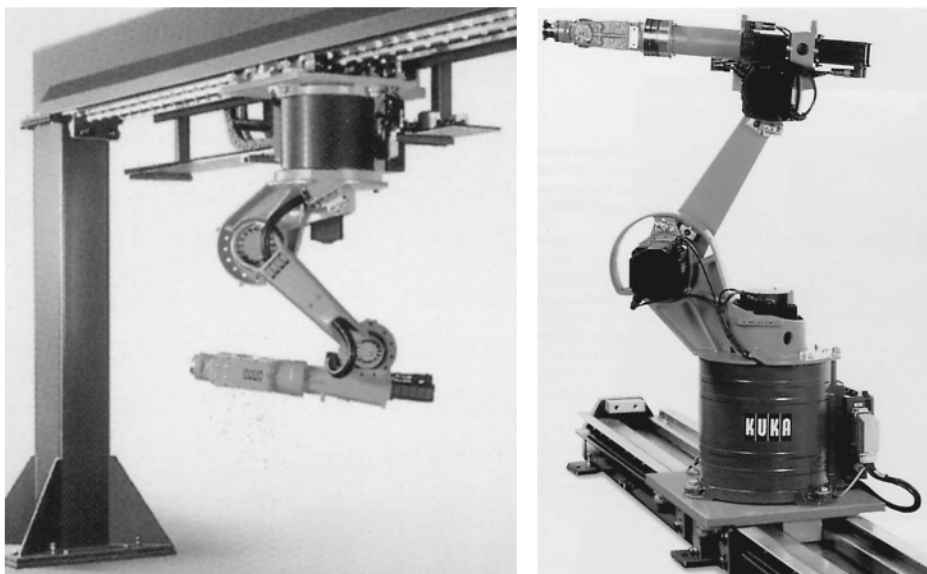


**Figure 16** Floor and overhead installations of a 6-d.o.f. industrial robot on a translational axis, representing a kinematically redundant robot system (courtesy KUKA).

structures use serial kinematic chains (with the exception of closed chains for weight compensation and motion transmission), some parallel kinematic structures have been adopted for a variety of tasks. Most closed-loop kinematics are based on the so-called hexapod principle (Steward platform), which represents a mechanically simple and efficient design. The structure is stiff and allows excellent positioning accuracy and high speeds, but shows only very limited working volume.

If the number of independent robot axes (arm and wrist) is greater than six, we speak of kinematically redundant arms. Because there are more joints than the minimum number required, internal motions may exist that allow the manipulator to move while keeping the position of the end-effector fixed (Murray, Li, and Gauthier, 1993). The improved kinematic dexterity may be useful for tasks taking place under severe kinematic constraints. Figure 27 shows a prominent example of an 11-degree-of-freedom redundant arm kinematics installed on a mobile base for aircraft cleaning. Other redundant configurations, such as a six-axis articulated robot installed on a linear axis (Figure 16) or even a mobile robot (automated guided vehicle), are quite common and are used as measures to increase the working volume of a robot.

### 3.1.1 Cartesian Robot

Cartesian robots have three prismatic joints, whose axes are coincident with a Cartesian coordinate system. Most Cartesian robots come as gantries, which are distinguished by a framed structure supporting the linear axes. Gantry robots are widely used for handling tasks such as palletizing, warehousing, and order picking or special machining tasks such as water jet or laser cutting where robot motions cover large surfaces.

Most gantry robot designs follow a modular system built up. Their principal axes can be arranged and dimensioned according to the given tasks. Wrists can be attached to the gantry's  $z$ -axis for end-effector orientation (Figure 17). Furthermore, a large variety of linear axes can be combined with gantry robots. Numerous component manufacturers offer complete programs of different-sized axes, drives, computer controls, cable carriers, grippers, etc.

### 3.1.2 Cylindrical and Spherical Robots

Cylindrical and spherical robots have an arm with two rotary joints and one prismatic joint. A cylindrical robot's arm forms a cylindrical coordinate system, and a spherical robot's arm forms a spherical coordinate system. Today these robot types play only a

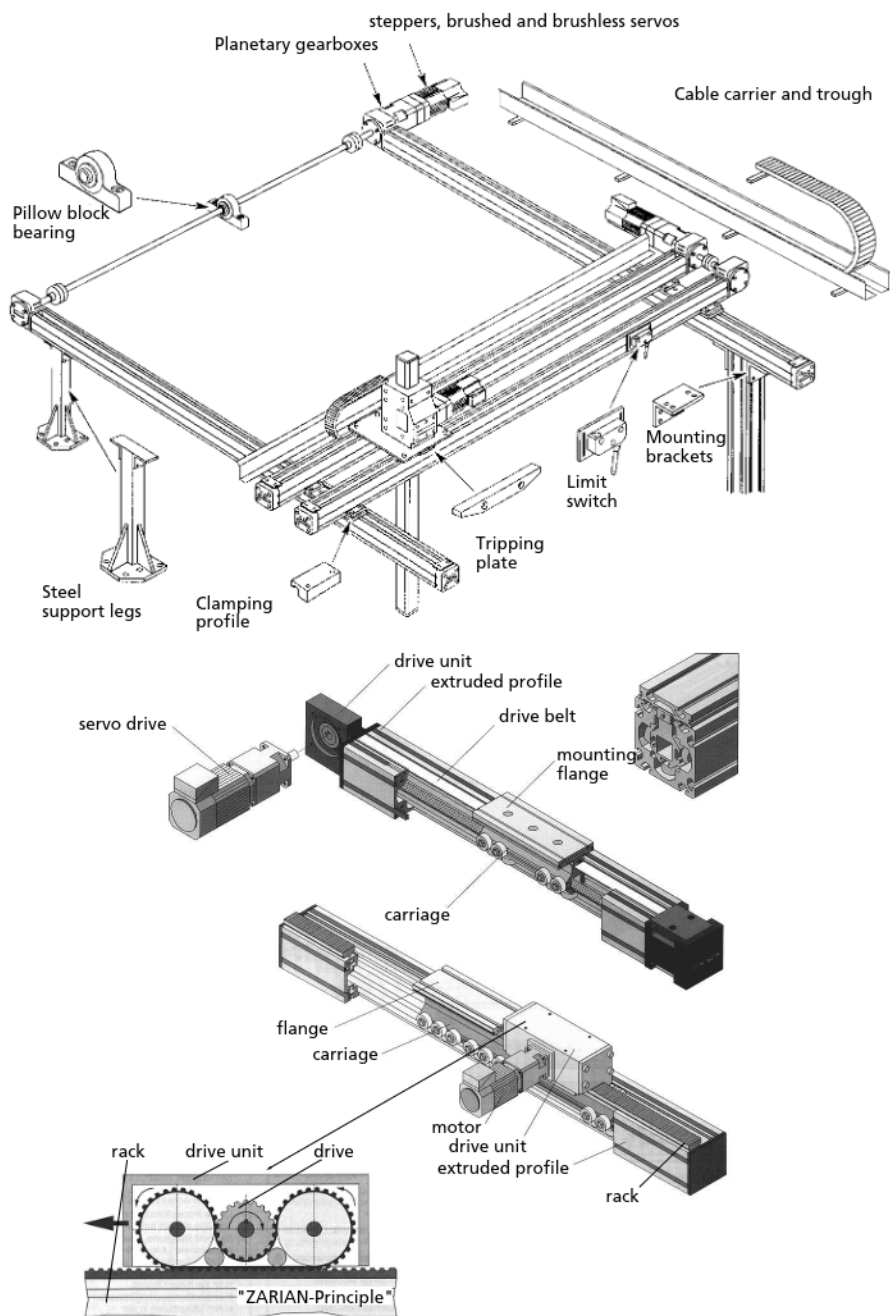


**Figure 17** Modular gantry robot program with two principles of toothed belt-driven linear axes (courtesy Parker Hannifin, Hauser Division).

minor role and are preferably used for palettizing, loading, and unloading of machines. See Figure 18.

### 3.1.3 SCARA-Type Robots

As a subclass of cylindrical robots, the Selective Compliant Articulated Robot for Assembly (SCARA) consists of two parallel rotary joints to provide selective compliance

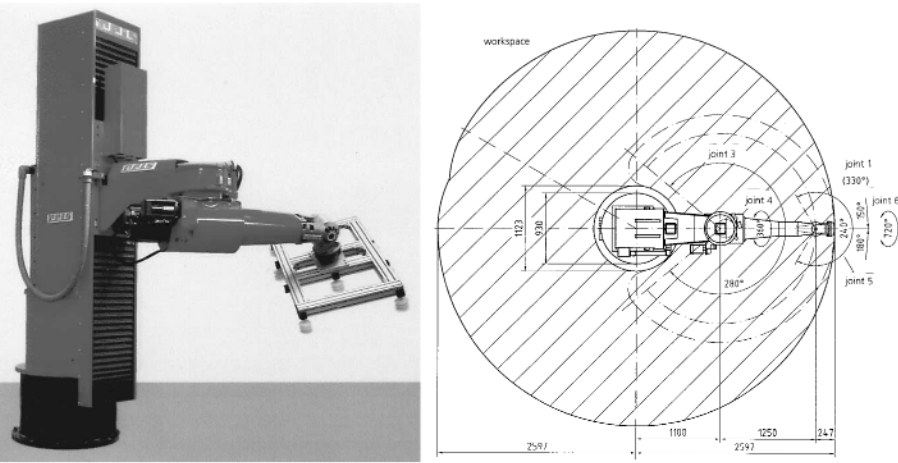


**Figure 18** Five-d.o.f. cylindrical robot with depiction of its workspace (in millimeters) (courtesy Reis Robotics).

in a plane, which is produced by its mechanical configuration. The SCARA was introduced in Japan in 1979 and has since been adopted by numerous manufacturers. The SCARA is stiff in its vertical direction but, due to its parallel arranged axes, shows compliance in its horizontal working plane, thus facilitating insertion processes typical in assembly tasks. Furthermore, the lateral compliance can be adjusted by setting appropriate force feedback gains. In SCARAs direct drive technology can bring in all potentials: high positioning accuracy for precise assembly, fast but vibration-free motion for short cycle times, and advanced control for path precision and controlled compliance. Figure 19 shows the principle of a direct-drive SCARA.

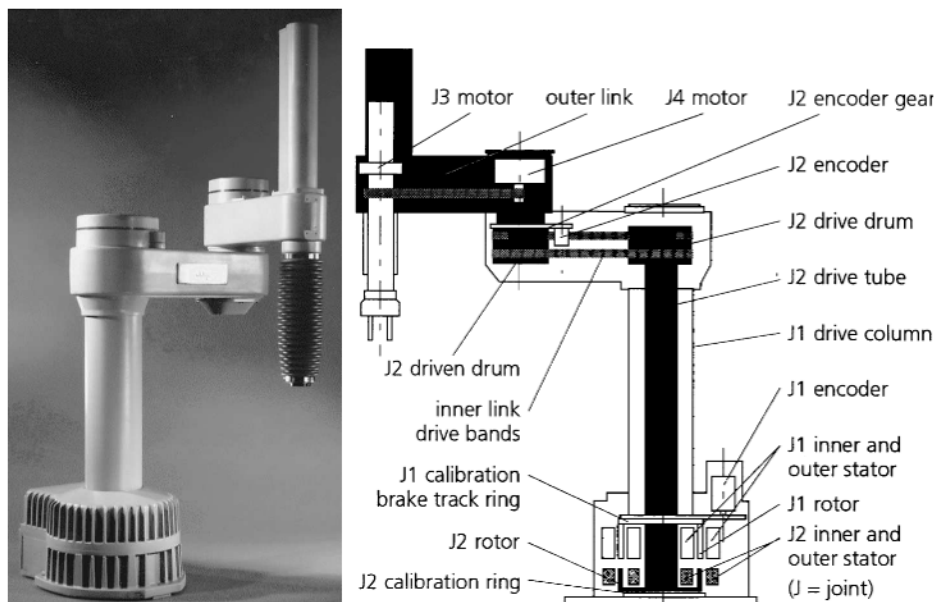


**Figure 19** View of a SCARA-type robot (left) and cross section of its direct-driven arm transmission for joint 2 (courtesy Adept Technology).

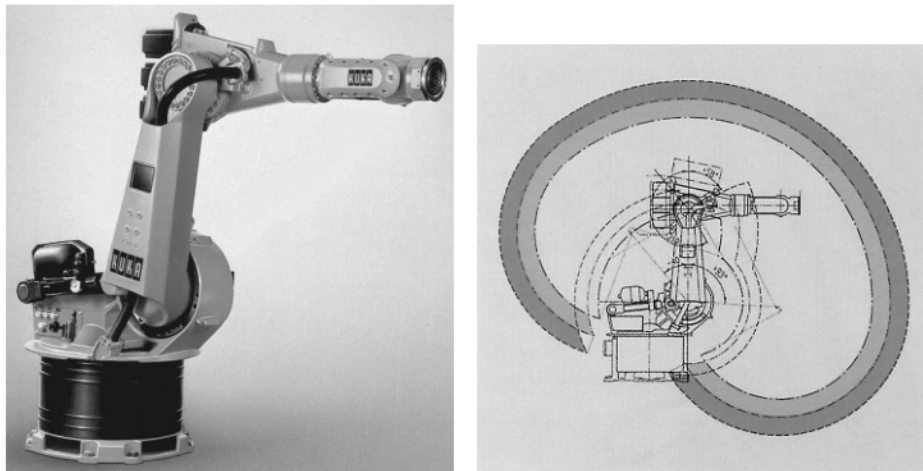


**Figure 20** Articulated robot (KUKA) and its workspace. Note the gas spring acting as a counterbalance to the weight produced by axis 2 (courtesy KUKA).

### 3.1.4 Articulated Robots

The articulated robot arm, the most common kinematic configuration, consists by definition of at least three rotary joints. High motor torques produced by the axes' own weight and relatively long reach can be counterbalanced by weights or springs. Figure 20 displays a typical robot design.

### 3.1.5 Modular Robots

For many applications the range of tasks that can be performed by commercially available robots may be limited by the robots' mechanical structure. It might therefore be advantageous to deploy a modular robotic system that can be reassembled for other applications. A vigorous modular concept has been proposed that allows universal kinematic configurations:

- Each module with common geometric interfaces houses power and control electronics, an AC servo-drive, and a harmonic drive reduction gear.
- Only one cable, which integrates DC power and field bus fibers, connects the modules.
- The control software is configured for the specific kinematic configuration using a development tool.
- A simple power supply and a PC with appropriate field bus interfaces replace a switching cabinet.

Figure 21 illustrates the philosophy of this system and gives an example.

### 3.1.6 Parallel Robots

Parallel robots are distinguished by concurrent prismatic or rotary joints. Of the many proposed parallel robot configurations, two kinematic designs have become popular:

1. The tripod with three translatory axes connecting end-effector, plate and base plate, and a 2 or 3-d.o.f. wrist
2. The hexapod with six translatory axes for full spatial motion

At the extremities of the link are a universal joint and a ball-and-socket joint. Due to the interconnected links, the kinematic structure generally has many advantages, such as high stiffness, accuracy, load capacity, and damping (Masory, Wang, and Zhuang, 1993; Wang and Masory, 1993). However, kinematic dexterity is usually limited.

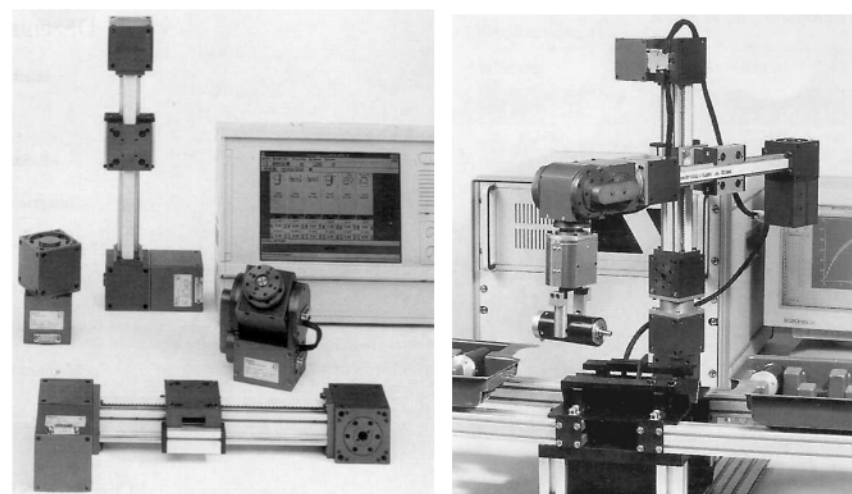


**Figure 21** Modular robot system consisting of rotary and translatory axis modules, grippers, and configurable control software (courtesy amtec).

Parallel robots have opened up many new applications where conventional serial chain robots have shown their limits, such as in machining, deburring, and parts joining, where high process forces at high motion accuracy are overwhelming.

Parallel robots can be quite simple in design and often rely on readily available precision translatory axes, either electrically or hydraulically powered (Merlet, 1995). Figure 22 gives examples of tripod and hexapod platforms.

Although parallel manipulators have been introduced quite recently and their design is quite different from that of most classical manipulators, their advantage for many

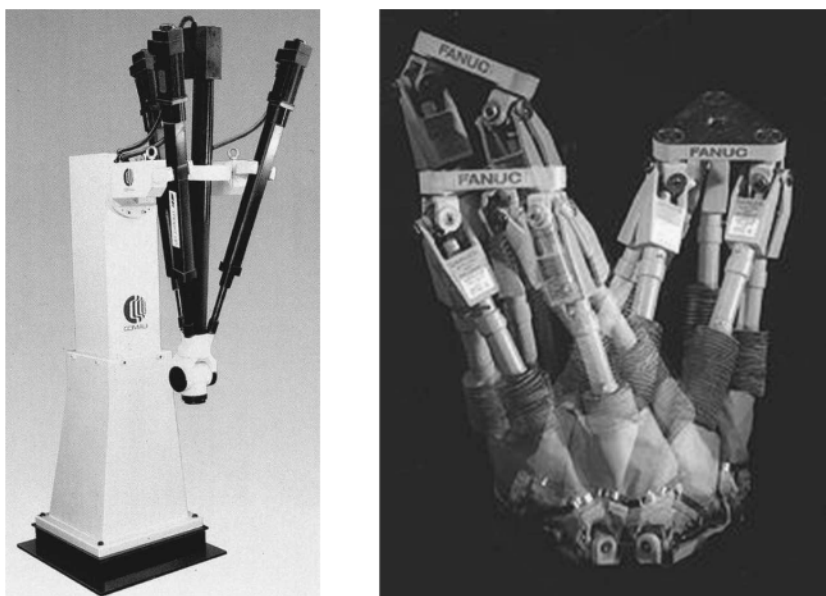


**Figure 22** The COMAU Tricept, a 6-d.o.f. tripod, and the FANUC FlexTool Steward platform with six servo-spindle modules connecting the bottom and moving plate (courtesy COMAU, FANUC Robotics).

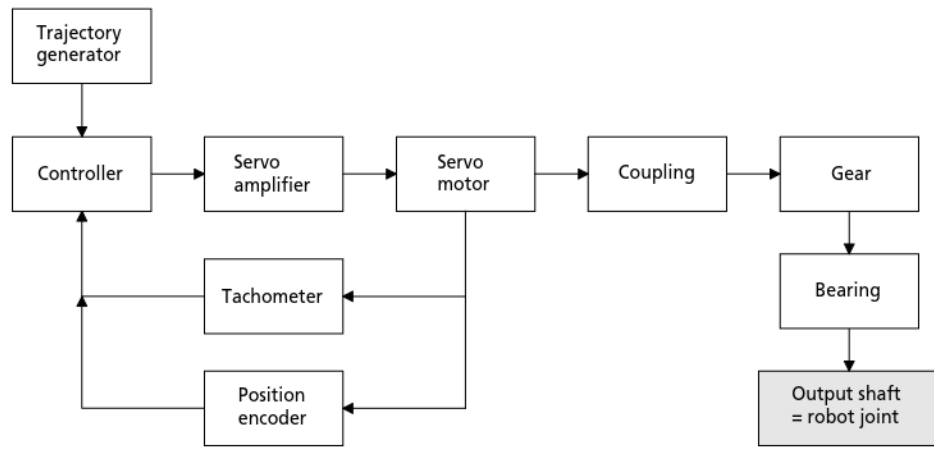


**Figure 23** Drive chain of industrial robots.

robotics tasks is obvious, so they will probably become indispensable in the near future. (See also Chapter 47.)

#### 4 DRIVE CHAIN

The drive chain of common industrial robots is shown in Figure 23. The control system is fed by the trajectory generator with desired joint values and delivers control commands to the servo-amplifier, which passes on the amplified control signal to the servo-motor. The tachometer and position encoder are typically located on the motor shaft and close the velocity and position loop. The torque produced by the servo-motor is transferred via coupling, gear, and bearing to the output shaft of the robot.

##### 4.1 Computation of Drive Chain

Computation of drive chain begins after kinematics, motor, and gear performance have been set (Figure 24). The desired performance of the manipulator is then defined in terms of working cycles. This leads to motion profiles for each joint, where position, velocity, and acceleration are defined. Transition to joint torques is done by the dynamic model of the manipulator which should include gravitational and frictional forces/momenta. In general, the equation system of joint torques and joint position, velocity, and acceleration is highly coupled, so special simulation software is used for this task. Peak torque and an equivalent torque number, calculated as a function of joint torque, time proportions of working cycle, and mean input speed, are typical numbers for gear validation, where motor validation is done by continuous and peak torque reduced by the gear. If the preselections of motor and gear performance do not match the desired manipulator performance, there are two ways of adaptation:

1. Increase motor and gear performance.
2. Decrease manipulator performance.

After this, calculation begins again until the deviation between required and available performance is within a tolerated error range.

#### 5 SERVO-DRIVES

Table 4 sets out the principles for servo-drives.

In general, servo-drives for robotics applications convert the command signal of the controller into movements of the robot arm. Working cycles of industrial robots are characterized by fast acceleration and deceleration and therefore by short cycle times in the application process. Thus, servo-motors for industrial robots have to fulfill a high standard concerning dynamics.

Because of their good controllability and large speed and power range, only electrical servo-drives find practical use in common industrial robots. Direct electrical drives are

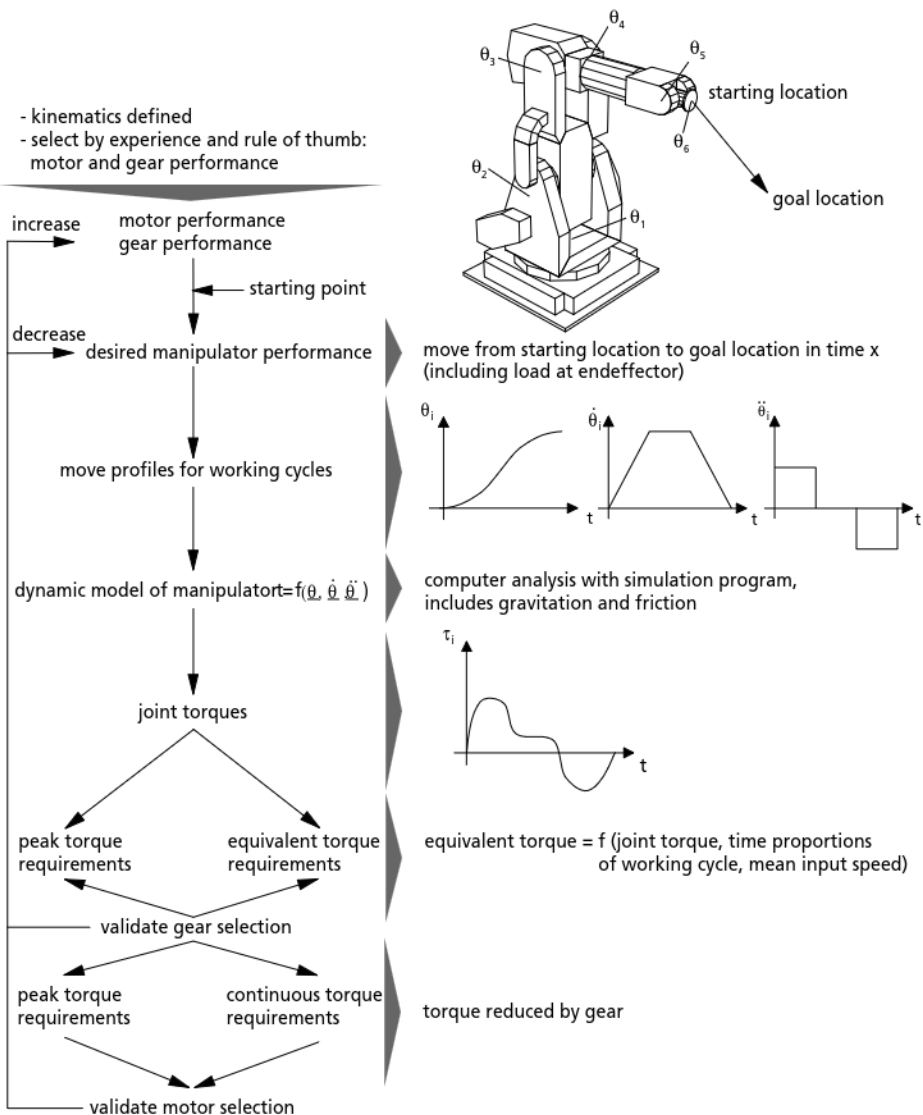


Figure 24 Computation of drive chain torques.

Table 4 Principles for Servo-drives

Driving Principle	Field of Application	Advantages	Disadvantages
Hydraulic	Manipulators with very high loads and/or large workspace	<ul style="list-style-type: none"> <li>High dynamics</li> <li>Very high power to weight ratio</li> </ul>	<ul style="list-style-type: none"> <li>Requires equipment: pumps, hoses, servo-valves</li> <li>“Dirty”</li> <li>Require maintenance</li> <li>Low efficiency</li> </ul>
Electric	Standard for industrial robotics	<ul style="list-style-type: none"> <li>High dynamics</li> <li>Very good controllability</li> <li>Large power range</li> <li>Large speed range</li> </ul>	<ul style="list-style-type: none"> <li>Reduction gear necessary</li> <li>Heating</li> </ul>

found only in a few SCARA-type robots (Figure 19). In all others the high rated speed of 1000 rpm is lowered by reduction gears. Hydraulic drives are used only at very high loads and/or in large workspaces because of their high power-to-weight ratio.

## 5.1 Electrical Motor Drives

A wide variety of electrical motors are available, each with its own special features.

### 5.1.1 Stepper Motors

Stepper motors usually provide open loop position and velocity control. They are relatively low in cost and interface easily with electronic drive circuits. Developments in control systems have permitted each stepper motor step to be divided into many incremental microsteps. As many as 10,000 or more microsteps per revolution can be obtained. Motor magnetic stiffness, however, is lower at these microstepping positions. Typically, stepper motors are run in an open-loop configuration. In this mode they are underdamped systems and are prone to vibration, which can be damped either mechanically or through application of closed-loop control algorithms. Power-to-weight ratios are generally lower for stepper motors than for any other types of electric motors.

### 5.1.2 DC Motor Drives

DC motor drives are characterized by nearly constant speed under varying load and easy control of speed via armature current. Consequently, the direct current drive had a dominant role at the beginning of electric servo-driving technique for robot systems. A disadvantage, however, is wear-ridden mechanic commutation by brushes and commutators, which also limits the maximally transferring current. DC motor drives are more and more replaced by drives with electronic commutation, although recent developments in commutator technique have raised service life of the brushes to up to 30,000 hours.

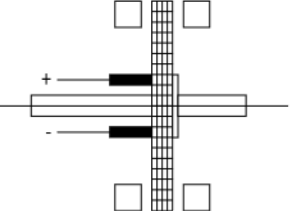
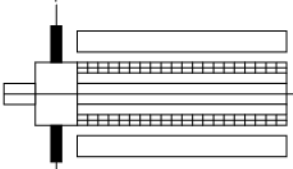
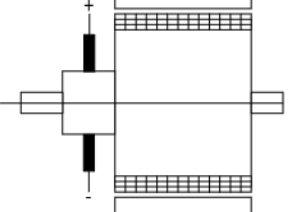
### 5.1.3 Alternating Current Drives

#### Synchronous Motors

Synchronous alternating current drives have been made more powerful by the replacement of conventional oxide ceramic magnets by rare earth magnets (samarium cobalt, neodymium ferrite boron), which have much higher power density. Newly developed power semiconductor technology (e.g., IGBT, insulated gate bipolar transistor) has improved dynamics and controllability. Synchronous motors are used with power up to 10–20 kW and rotational speeds up to 3000 rpm. Because the rotating field is commutated contactless, the drive is nearly maintenance-free.

**Table 5 Types of Servomotors**

Type of Servomotor	Maximum Output Power	Specific Properties
Stepper motor	1 kW	<ul style="list-style-type: none"> <li>• Running in open servo-loop</li> <li>• Heating in stalling</li> <li>• Poor dynamics</li> </ul>
DC-brush motor	5 kW	<ul style="list-style-type: none"> <li>• Good controllability via armature current</li> <li>• High starting torque</li> <li>• Brushes subject to wear</li> </ul>
DC-brushless motor	10 kW	<ul style="list-style-type: none"> <li>• Maintenance-free</li> <li>• Commutation by resolver or Hall-effect or optical sensor</li> <li>• High power density with rare earth magnets</li> </ul>
AC-synchronous motor	20 kW	
AC-asynchronous motor	80 kW	<ul style="list-style-type: none"> <li>• Maintenance-free</li> <li>• Very robust motor</li> <li>• High speed range</li> <li>• Expensive to control</li> </ul>

disk armature	- very small moment of inertia - large speed range - high positioning accuracy - flat type of construction	
squirrel-cage motor	- robust drive - small moment of inertia - high number of revolutions up to 10,000 U/min - secondary transmission required	
torque-drive	- high torque at low number of revolutions - suited for direct drive, free of backlash - large motor diameter	

**Figure 25** Construction types of direct current drives.

### Asynchronous Motors

Asynchronous drives are more robust than synchronous drives and have a higher density of power. They are used with power up to 80 kW and rotational speeds up to 10,000 rpm. By weakening the magnetic field, asynchronous drives can operate in a large field of constant power output beyond the nominal number of revolutions, which offers a great advantage over synchronous motors.

#### 5.1.4 Linear Drives

If a rotary electric drive is cut open at the circumference and evenly unrolled, the result, in principle, is a linear drive (see Figure 26). For Cartesian robot transmissions, linear drives, for example, can be used for highly dynamic pick-and-place tasks. Compared with spindle drives, the most important advantages of the linear drives, which are mostly realized as synchronous and asynchronous drives for high loads, are high velocities (up to 3 m/s) and high accelerations (up to 10 g). Linear drives will probably replace some spindle drives in high-speed applications in the near future.

#### 5.2 Electrohydraulic Servo-drives

Electrohydraulic servo-drives consist of a hydromotor or a hydrocylinder and a servovalve for controlling the motor. Combined with a positional encoder, electrohydraulic servo-drives exhibit very good dynamics in closed loop control. Disadvantages are the need for much equipment, need for maintenance, and low efficiency. Figure 27 shows a hydraulic-driven manipulator.

## 6 GEARS

### 6.1 Introduction

Electric servomotors generate acceptable efficiency (up to 95%) only at relatively high numbers of revolutions (1000 rpm). For this reason they have not to this point been

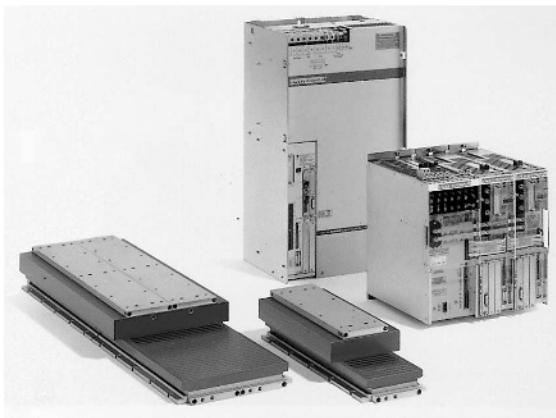


**Figure 26** Linear electrical drive (courtesy Indramat).

well suited for direct drives, with the exception of some high-performance SCARA-type robots.

Robot gears convert high input numbers of revolutions and low torque into lower output numbers of revolutions and high torque (see Figure 28). At the same time they reduce the moment of inertia of the robot arm for the servo-drive.

Besides the conversion of torque and number of revolutions, robot gears induce some disadvantages in the drive chain:

- No gear is backlash-free. This is a problem in position accuracy and control.
- Gears can induce torsional oscillation because they act as elastic elements in the drive chain.

The requirements in Table 6 cannot be fulfilled separately. For example, the minimization of backlash requires pretensioned gear teeth, which on the other hand leads to an extension of friction and as a consequence to reduced efficiency.



**Figure 27** Manipulator "Skywash" with hydraulic drives (courtesy Putzmeister).



**Figure 28** Conversion of speed and torque by robot gear.

## 6.2 Gears for Linear Movements

Linear robot axes can be found in

- Cartesian robots for pick-and-place tasks
- Vertical axes for SCARA-type robots
- Gantry robots
- Peripheral axes, mostly under the base of an articulated robot in order to enlarge workspace

Different gears are used according to the dimension of joint range, demanded accuracy, and load, as shown in Table 7.

Figures 29 and 30 show a rack-and-pinion and a ball bearing spindle.

The maximum length of toothed belt and ball bearing spindle is limited by bending and torsional resonance frequencies.

**Table 6 Quality Requirements for Robot Gears**

Requirements	Typical Values
Very small backlash	Few arcmin
High efficiency	80–95%
Large reduction in few steps	100–320
Low inertia, low friction	Dependent on gear size
High torsional stiffness	Dependent on gear size
High power density, low weight	

**Table 7**

Naming	Common Joint Ranges	Accuracy	Load
Toothed belt	<10 m	Max. 0.1 mm	Small to medium
Ball bearing spindle	<5 m	Max. 0.001 mm	Small to medium
Rack-and-pinion	Theoretically unlimited	Max. 0.01 mm	Medium to high

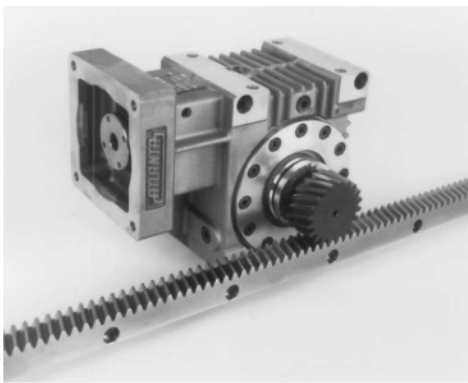


**Figure 29** Worm gear and rack-and-pinion (courtesy Atlanta).

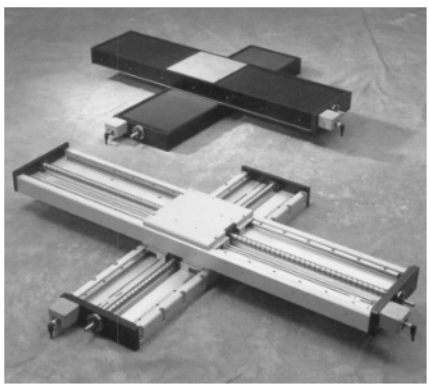


**Figure 30** x, y-axis with ball bearing spindle.

Usually the servo-motor is not joined directly with the linear gear but with an intermediate gear (transmission, bevel, or worm gear).

### 6.3 Gears for Rotary Movements

Gears for rotary movements can be found in all articulated robots and SCARA-type robots. They are usually offered as compact, pot-shaped kits. Depending on the gear type, output bearings up to the main axes are integrated.

Table 8 shows different types of common rotary drive gears.

Figure 31 gives a survey of construction schemes.

Examples of robot gears for rotary joints are shown in Figures 32 to 35.

## 7 COUPLINGS

Couplings are installed between servo-motor and gear and servo-motor and encoder to balance alignment faults between shafts. They also transfer torque and rotating movements. The coupling influences the performance of the whole drive chain. To apply couplings the following quantities must be considered:

- Torsional stiffness of coupling
- Damping of coupling

Figure 36 shows some typical couplings for robotic systems.

Following recent developments in articulated robots, the servo-motor–gear connection is executed without coupling. Instead, the servo-motor is directly flanged to the solid-constructed gear aggregate.

**Table 8 Properties of Different Rotor Gears**

Type of Gear	Typical Properties	Application
Planetary gear	Very high efficiency	Base axes
Harmonic drive gear	Very compact Very high reduction in one-gear stage Small to medium torques	Wrist axes
Cycloid gear	High efficiency High torque	Base axes
Involute gear	Very compact Very high reduction in one-gear stage Small to medium torques	Wrist axes

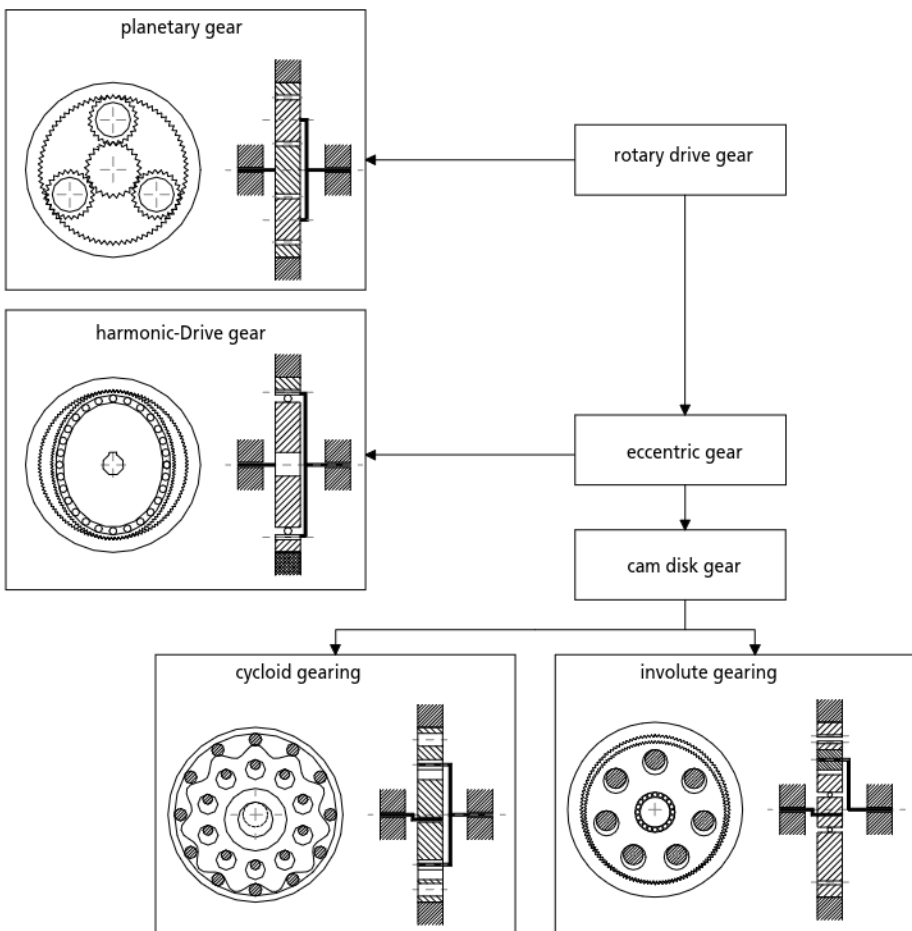


Figure 31 Survey of rotary drive gears.

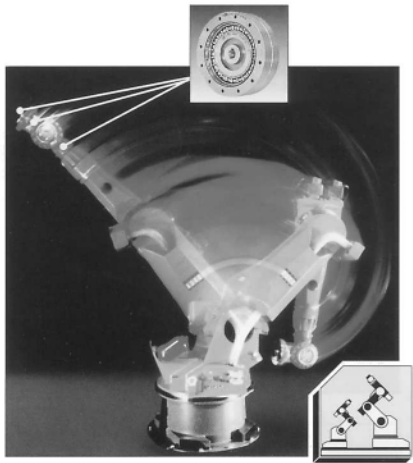


Figure 32 KUKA robot with Harmonic Drive gears (courtesy Harmonic Drive).

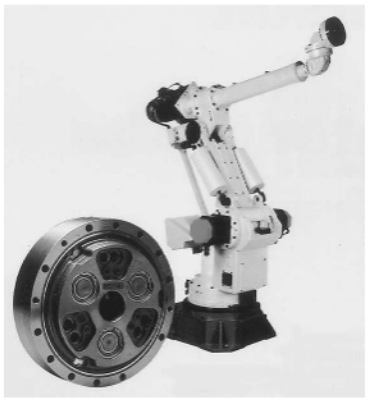


Figure 33 Fanuc robot with cycloid gears (courtesy Teijin Seiki).

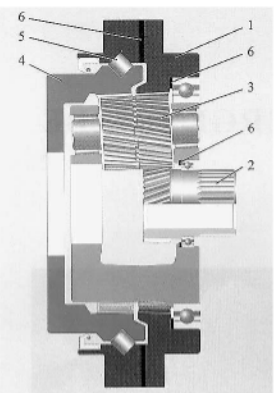


Figure 34 Planetary gear (courtesy ZF Friedrichshafen).

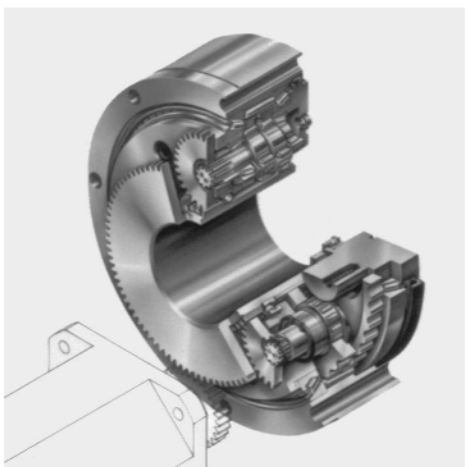


Figure 35 Cycloid gear (courtesy Teijin-Seiki).

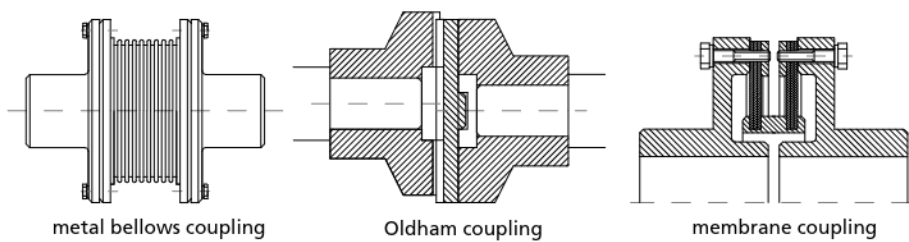


Figure 36 Different types of couplings used in robotics.

## 8 MEASURING SYSTEMS

Measuring systems feed back the positional signal from the robot joint to the controller. The resolution of the position sensor is a limiting factor for the precision of the robot system. Three types of encoders are commonly used in industrial robotics:

### 8.1 Optical Absolute Encoder

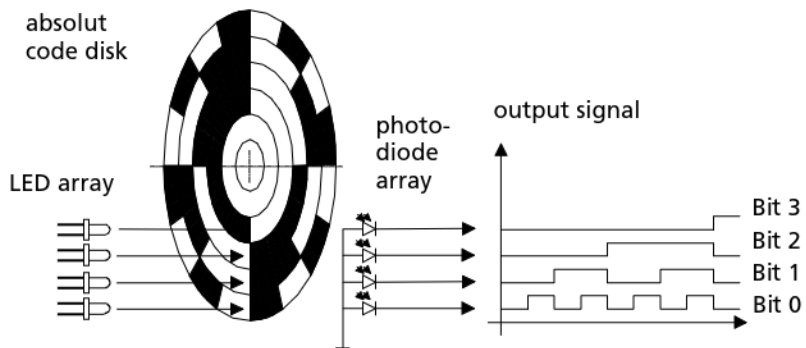
The electrical output signal of an optical absolute encoder provides a continuous digital signal that holds the information about the absolute position of the robot joint (see Figure



Figure 37 Optical measuring systems.

Table 9

Measuring System	Principle	Output Signal	Common Resolutions	Typical Properties
Optical absolute encoder	Linear/rotary	Digital absolute	12–16 bit	<ul style="list-style-type: none"> <li>• No position loss during power down</li> <li>• Multiturn possible</li> </ul>
Optical incremental encoder	Linear/rotary	Digital relative	5,000–100,000 pulses/rev	<ul style="list-style-type: none"> <li>• Position loss during power down</li> <li>• High resolution</li> </ul>
Resolver	Rotary	Analog absolute	12–16 bit	<ul style="list-style-type: none"> <li>• No position loss during power down</li> <li>• Robust</li> <li>• Inexpensive</li> </ul>



**Figure 38** Functional diagram of an optical absolute encoder.

38). Sampling of joint position works contact-free using optical devices. Light from an LED array passes through a code disk fixed to the robot joint, which carries parallel tracks of binary code patterns of black and transparent segments. The optical signal is transformed into an electrical signal by an ASIC chip, which consists of a photovoltaic diode array, comparator, memory, code inverter, and driver. Typical resolutions of optical absolute encoders are 12–16 bits.

The most common code used to represent a numerical value in absolute encoders is the Graycode. When there is a transition from one numerical value to the next, only one bit changes. Imaging binary code, transition from 2 to 3 will change bit numbers 1, 2, and 3 at the same time. If there are only small tolerances on the code disk between dark and transparent segments of different bit-tracks, these bits will not change at exactly the same time and the output signal will not be well defined at this moment.

## 8.2 Incremental Optical Encoders

Compared to optical absolute encoders, incremental encoders provide only a relative signal, which means that pulses are counted in relation to a fixed reference point (see Figure 39). Loss of the reference point, as when the power supply is switched off for a short time, means that the position is lost and must be referenced again by searching the reference point. This is a big disadvantage in robotic systems, because up to six axes have to be referenced again, which is possible only in a special joint position configuration.

The direction of movement of the code disk is evaluated by comparing the signal of two photovoltaic diodes arranged so that they receive the signal from the LED 90° degree phase-shifted. Signal conditioning is done afterwards by a Schmitt trigger and an up/down counter.

As opposed to absolute encoders, typical incremental encoder design has a resolution of up to 5,000 pulses per revolution. By evaluation of the signal edges (or transitions),

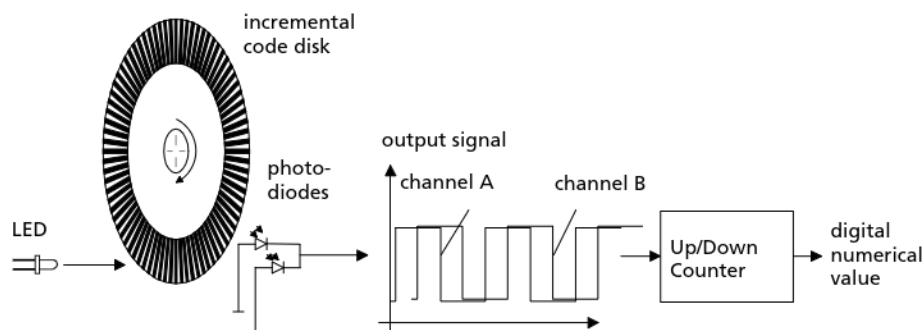


**Figure 39** Functional diagram of an incremental optical encoder.

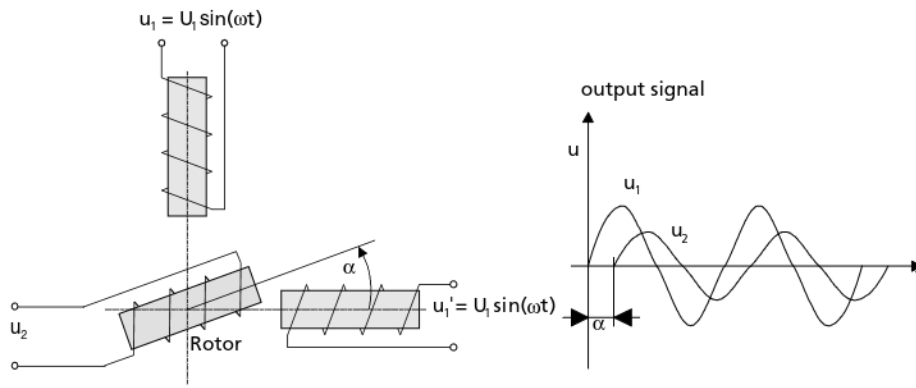


**Figure 40** Functional principle of the resolver.

the resolution is increased by factor 4. If the encoder provides a sine output signal, by interpolation of the signal the resolution can be increased by factor 10.

Thus, in ultra-precision linear applications where resolution of some  $\mu\text{m}$  or better is required, only incremental encoders can be used. These applications usually occur in linear Cartesian systems for measurement or precision assembly.

### 8.3 Resolver

A resolver is an analogous measuring system giving out an absolute angular signal via one rotation (see Figure 40). Multiturn resolvers incorporate a reduction gear with a counter of revolutions to give out a continuous signal for more than one revolution.

Immediately after starting, the resolver indicates the exact position. The axis does not have to be moved to make new references, which provides a decisive advantage. Via a rotary transformer (brushless version), alternating voltage is fed into the rotor. The stator is composed of two windings into which this signal is induced. Both stator windings are mechanically arranged to distribute their signals by  $90^\circ$ . The computation of the combined output signals is done by an ASIC. Common resolutions of resolvers are 12–16 bits.

Resolvers are high-resolution, robust, and inexpensive position sensors that can easily be designed with a hollow shaft. For that reason, resolvers increasingly replace optical sensor systems in rotational robot joints.

## 9 ROBOT CALIBRATION

### 9.1 Introduction

A general task for a robot is to move its TCP coordinate system to a specific orientation and a certain point within its workspace. In this context, accuracy is the ability of the robot to move its end-effector to this pose and repeatability is the robot's ability to return to a previously achieved pose. In other words, in considering repeatability, the desired pose has been previously attained and therefore the necessary joint values are known. In considering accuracy, however, the pose is specified in task space and the desired set of joint displacements that corresponds to this pose must be determined. Typically, industrial robots have much better repeatability than accuracy.

For the robot's end-effector to be moved into desired pose in task space for the first time, the predefined coordinates of the desired pose must be translated into the robot's joint values. This conversion from the robot's task space to the robot's joint space is accomplished using a mathematical model that represents the manipulator's kinematics. This model relates the joint displacements to the TCP pose and vice versa and is used by the robot controller. If the mathematical model is incorrect, the manipulator will not have sufficient accuracy. However, the repeatability is not affected by this error. Additionally, the repeatability of a manipulator is relatively constant across the workspace, while the accuracy can vary significantly and is normally much worse than the repeatability. The mathematical model therefore contains a certain amount of parameters that, if correctly identified, allow the model to match the actual robot and enhance the robot's

accuracy within its workspace. Equation (1) shows the relationship between the robot's task space and joint space:

$$P = f(\theta, c) \quad (1)$$

$P$  is the  $(6 \times 1)$  vector that describes the pose in task space (see Figure 41). Its six components represent three translational and three rotational degrees of freedom.  $\theta$  is the  $(n \times 1)$  vector that describes the pose in joint space where  $n$  is equivalent to the amount of robot axes.  $c$  represents the set of parameters used in the model, and  $f$  is the function that transforms the joint space coordinates  $\theta$  into task space coordinates  $P$  with respect to the set of parameters  $c$ .

Robot calibration requires a process of defining an appropriate mathematical model and then determining and implementing the various model parameters that make the model match the robot as closely as possible (Mooring, Roth, and Driels, 1991). For costs for calibration to be reduced, the mathematical model must be as complex as necessary but as simple as possible. (See also Chapter 39.)

## 9.2 Steps in Robot Calibration

Figure 42 depicts the steps in robot calibration.

### 9.2.1 Modeling

A detailed discussion of fundamentals of kinematic modeling may be found in the literature (Asada and Slotine, 1986; Craig, 1986; Fu, Gonzalez, and Lee, 1987; Payonnet, Aldon, and Liegeois, 1985; Nikravesh, 1988).

Depending on the complexity and scope of the calibration task, Mooring, Roth, and Driels (1991) suggest three different levels of calibration procedures:

*Level 1* (joint level) calibration has as its goal the determination of the relationship between the actual joint displacement and the signal generated by the joint displacement transducer. See Figure 42.

*Level 2* calibration covers the entire robot model calibration. In addition to the correct joint angle relationships, the basic kinematic geometry of the robot must be identified.

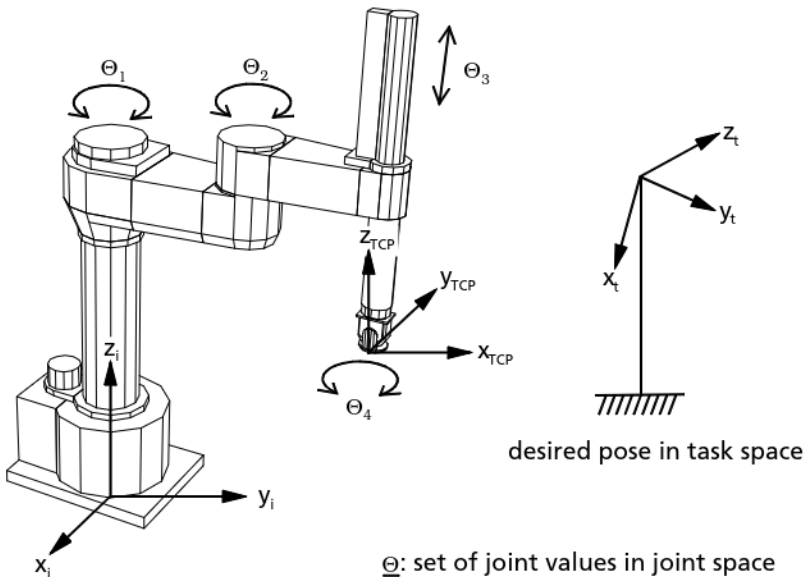


Figure 41 Task space and joint space.

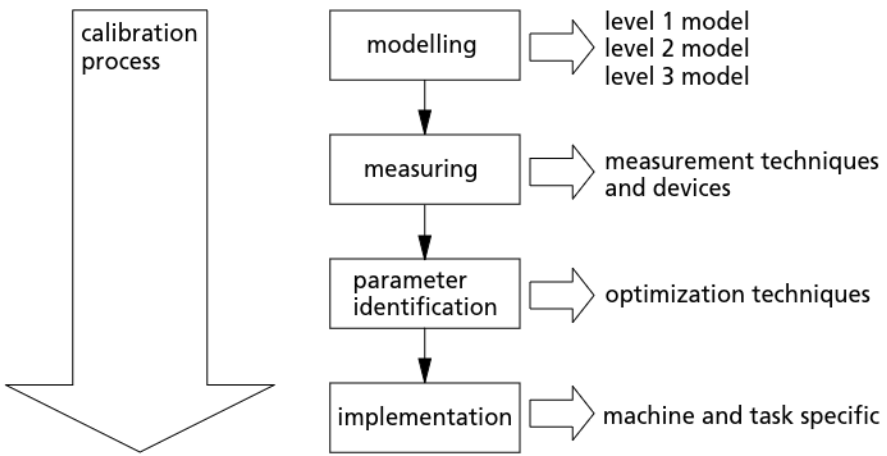


Figure 42 Calibration process and problems to be solved.

**Level 3** (nonkinematic) calibration deals with nonkinematic errors in positioning of the robot's TCP that are due to effects such as joint compliance, friction, and clearance.

Each level implies a different mathematical model, and that means a different functional form for Equation (1) of the considered robotic system. While level 1 and 2 models correspond to practical needs, level 3 models are to be examined by scientists and have less practical relevance. Figure 43 shows a very simple kinematic model of a robotic device for a level 1 (= joint level) calibration.

Simulation systems such as IGRIP (Deneb Robotics Inc.) or ROBCAD (Tecnomatics) provide calibration tools that contain standard kinematics of industrial robots and algorithms that compute the forward kinematics and solve the inverse kinematics numerically.

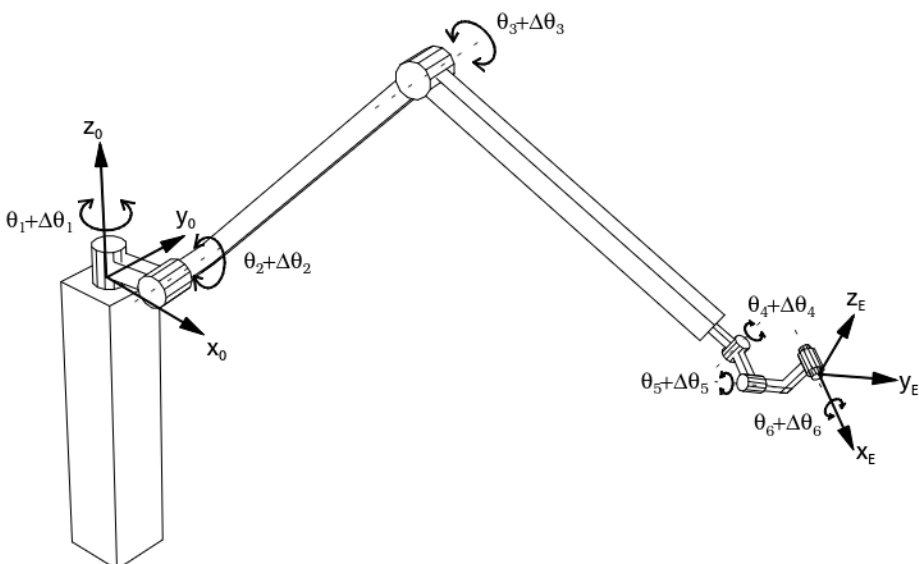


Figure 43 Kinematic schema of a six-d.o.f. industrial robot.

The following paragraphs will explain the next steps in manipulator calibration for a level 1 mathematical model. More complex procedures can be found in Mooring, Roth, and Driels (1991).

### 9.2.2 Measurement Devices and Techniques

Measurement devices and techniques differ depending on the mathematical model's set of parameters that have to be identified. Measurement devices can be divided into two groups:

*Internal* measurement devices are sensors that belong to the robotic system and are attached to the robot permanently: the joint displacement transducers. The most commonly used joint displacement transducers can be listed as follows:

- The *encoder* is a device for measuring linear or angular displacement. It produces a digital signal that can be easily interfaced to the robot control. The achievable accuracy depends on the encoder's resolution and can be high.
- The *resolver* is a device for measuring displacement of a revolute joint. Its output is a digital signal representing the error between the desired and the actual shaft angle. Its accuracy is high, but it is significantly more expensive than an encoder package with comparable resolution.

Internal measurement devices, such as encoders, are discussed above in Section 8. A more detailed introduction to internal measurement devices can be found in Doebelin (1983). (See also Chapters 12, 13.)

*External* measurement devices are sensors that belong to the measurement setup needed for the actual calibration procedure and are either attached to the robotic system temporarily or installed close to the robot. External sensors are used for such applications as measuring the pose of the robot's end-effector. See Figures 44 and 45.

The goal of the measurement process for a level 1 (= joint level) mathematical model is to accurately determine the robot's end-effector pose with a set of external measurement devices for a given set of joint displacements recorded by internal measurement devices.

This task can be completed with a 3D laser tracking system. An example of such a system is the LEICA LT/LTD 500 system from LEICA AG, Switzerland. It contains a freely movable target reflector, which must be attached to the robot's end-effector, and a laser tracker, which consists of a mirror system with two motors and two encoders, a laser interferometer, and a precision distance sensor.

A PC is used as a control computer for the measurement system. The system is capable of recording the target reflector with end-effector velocities of more than 4 m/s and end-effector accelerations of more than 2 g. To receive position information, one target reflector is sufficient. In order to measure the complete end-effector pose, at least three targets at the end-effector have to be recorded simultaneously.

### 9.2.3 Parameter Identification

Parameter identification is the mathematical process of using the data internally and externally measured to identify the coefficients of the mathematical model. Parameter identification describes the process of finding the optimal set of parameters for given sets of internal and corresponding external measurements. In other words, for a level 1 mathe-

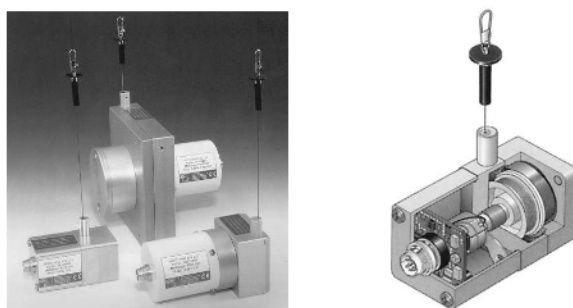


Figure 44 External 1D rope sensors for long-distance measurements (courtesy ASM, Germany).



**Figure 45** LEICA LTD 500 Laser Tracking System (courtesy Leica AG, Switzerland).

mathematical model of a manipulator, the internal joint displacement transducers' readings plus the identified joint offset parameters should form the correct input for the forward kinematics, so that the computed end-effector pose and the externally measured end-effector pose match as closely as possible.

The identification techniques therefore attempt to determine the parameter set that will optimize some performance index. Various approaches to achieve this task relate to such fields as control theory and dynamic systems modeling. The difference in these approaches comes, for example, in the type of model that is used or in the assumptions that are made about noise. Mooring, Roth, and Driels (1991) suggest the following classification:

1. *Deterministic vs. stochastic*: depending on whether or not probabilistic models for process and measurement noise are utilized.
2. *Recursive vs. nonrecursive*: depending on whether the whole set of observed data is saved and processed in its entirety or used sequentially.
3. *Linear vs. nonlinear*: depending on the type of mathematical model that is used.

Linear and nonlinear least square fittings are the most straightforward approaches for estimating the unknown model parameters from measured data. For very complex nonlinear target functions, genetic algorithms can serve as optimization techniques.

Gerald and Wheatley (1990) give an overview of applied numerical analysis.

#### 9.2.4 Implementation

The implementation procedure is the process of incorporating the improved version of the robot's mathematical model—in other words, the mathematical model plus the identified parameters of this model—into the controller so that the correct relationship between workspace coordinates and joint transducer values is achieved. This is seldom a simple process; the forward kinematic model and the inverse kinematic model have to be implemented in the controller. For simple kinematic models the inverse equations can be solved explicitly. For more complex models iterative methods have to be established.

The theory and examples of inverse kinematics can be found in the literature. See, e.g., Raghavan and Roth (1993); Zhiming and Leu (1990). (See also Chapter 6.)

## 10 PERFORMANCE TESTING

ISO 9283 is the International Standard that describes methods of specifying and testing the following performance characteristics of manipulating industrial robots:

- Unidirectional pose accuracy and pose repeatability
- Multidirectional pose accuracy variation
- Distance accuracy and distance repeatability
- Pose stabilization time
- Pose overshoot
- Drift of pose characteristics
- Path accuracy and path repeatability
- Cornering deviations

Criteria to be tested	Clause in ISO 9283	Applications									
		Spot welding 1	Handling/ loading/ unloading 1	Assembly		Inspection		Machining deburring 2	Spray painting 2	Arc welding 2	Adhesive sealing 2
		1	2	1	2	1	2				
Unidirectional pose accuracy	7.2.1	✓	✓	✓	✓	✓	✓		✓		
Unidirectional pose repeatability	7.2.2	✓	✓	✓	✓	✓	✓		✓		
Multi-directional pose accuracy variation	7.2.2		✓		✓	✓	✓				
Distance accuracy	7.3.2	✓ 3	✓ 3	✓ 3	✓ 3	✓ 3	✓ 3				
Distance repeatability	7.3.3	✓ 3	✓ 3	✓ 3	✓ 3	✓ 3	✓ 3				
Pose stabilization time	7.4	✓	✓	✓	✓	✓	✓				
Pose overshoot	7.5	✓	✓	✓	✓	✓	✓		✓		
Drift of pose characteristics	7.6	✓	✓	✓	✓	✓	✓		✓		
Path accuracy	8.2			✓		✓	✓	✓	✓	✓	✓
Path repeatability	8.3			✓		✓	✓	✓	✓	✓	✓
Corner deviations	8.4			✓		✓	✓	✓	✓	✓	✓
Stabilization path length	8.4.2			✓		✓	✓	✓	✓	✓	✓
Path velocity accuracy	8.5.2					✓		✓	✓	✓	✓
Path velocity repeatability	8.5.3					✓		✓	✓	✓	✓
Path velocity fluctuation	8.5.4					✓		✓	✓	✓	✓
Minimum positioning time	9	✓	✓	✓	✓				✓		
Static compliance	10	✓	✓	✓	✓		✓				

Notes: 1 Application where pose-to-pose control is normally used  
 2 Application where continuous path control is normally used  
 3 Only in case of explicit programming

**Figure 46** Performance testing methods versus applications according to ISO 9283.

- Path velocity characteristics
- Minimum positioning time
- Static compliance

Figure 46 is a guide to selecting performance criteria for typical applications.

Many manufacturers that use industrial robots, such as General Motors and Mercedes Benz, have also developed their own standards (Schröer, 1998). Copies of these performance testing criteria can be obtained from the companies.

## REFERENCES

- Akao, Y., and T. Asaka. 1990. *Quality Function Deployment: Integrating Customer Requirements into Product Design*. Cambridge and Norwalk: Productivity Press.
- Angeles, J. 1997. *Fundamentals of Robotic Mechanical Systems—Theory, Methods and Algorithms*. New York: Springer-Verlag.
- Asada, H., and J.-J. Slotine. 1986. *Robot Analysis and Control*. New York: John Wiley & Sons.
- Burnett, D. S. 1987. *Finite Element Analysis*. Reading: Addison-Wesley.
- Canny, J. F., and K. Y. Goldberg. 1995. "A RISC-Based Approach to Sensing and Manipulation." *Journal of Robotic Systems* 6, 351–363.
- Clausing, D. P. 1994. "Total Quality Development." *Manufacturing Review* 7(2), 108–119.
- Craig, John J. 1986. *Introduction to Robotics Mechanics and Control*. Reading: Addison-Wesley.
- Daenzer, W. F., and F. Huber, eds. 1994. *Systems Engineering: Methodik und Praxis*. 8. verbesserte Auflage. Zürich: Verlag Industrielle Organisation.
- Doebelin, E. 1983. *Measurement Systems: Application and Design*. New York: McGraw-Hill.
- DRAFT AMENDMENT ISO 9283: 1990/DAM 1. 1990. Manipulating Industrial Robots—Performance Criteria and Related Test Methods. Amendment 1: Guide for Selection of Performance Criteria for Typical Applications. Geneva: International Organization for Standardization.
- Fu, K. S., R. C. Gonzalez, and C. S. G. Lee. 1987. *Robotics: Control, Vision, and Sensing*. New York: McGraw-Hill.
- Furgaç, I. 1986. "Aufgabenbezogene Auslegung von Robotersystemen." Dissertation, Universität Berlin.
- Gerald, C. F., and P. O. Wheatley. 1990. *Applied Numerical Analysis*. 4th ed. Reading: Addison-Wesley.
- Hayward, V., and R. Kurtz. 1989. "Preliminary Study of Serial-Parallel Redundant Manipulator." In *NASA Conference on Space Telerobotics*, Pasadena, January 31. 39–48.
- Herrmann, G. 1976. "Analyse von Handhabungsvorgängen im Hinblick auf deren Anforderungen an programmierbare Handhabungsgeräte in der Teilefertigung." Dissertation, Universität Stuttgart.
- Inoue et al. 1993. "Study on Total Computer-Aided Design System for Robot Manipulators." In *24th ISIR*, November 4–6, Tokyo. 729–736.
- International Federation of Robotics (IFR). 1997. *World Industrial Robots 1997—Statistics, Analysis and Forecasts to 2000*.
- ISO 9283 First Edition 1990-12-15. 1990. Manipulating Industrial Robots—Performance Criteria and Related Test Methods. Reference number ISO 9283: 1990(E). Geneva: International Organization for Standardization.
- Klafter, R. D., T. A. Chmielewski, and M. Negin. 1989. *Robot Engineering: An Integrated Approach*. Englewood Cliffs: Prentice-Hall International.
- Masory, O., J. Wang, and H. Zhang. 1993. "On the Accuracy of a Stewart Platform. Part II: Kinematic Calibration and Compensation." In *Proceedings of the IEEE International Conference on Robotics and Automation*, Atlanta, May 2–6.
- Merlet, J.-P. 1995. "Designing a Parallel Robot for a Specific Workspace." Research Report 2527 INRIA, April.
- Mooring, B. W., Z. S. Roth, and M. R. Driels. 1991. *Fundamentals of Manipulator Calibration*. New York: John Wiley & Sons.
- Morrow, J. D., and P. K. Khoshla. 1997. "Manipulation Task Primitives for Composing Robot Skills." In *Proceedings of the 1997 IEEE International Conference on Robotics and Automation*, Albuquerque, April. 3454–3459.
- Murray, R. M., Z. Li, and S. S. Sastry. 1993. *A Mathematical Introduction to Robotic Manipulation*. Boca Raton: CRC Press.
- Nakamura, Y. 1991. *Advanced Robotics Redundancy and Optimization*. Reading: Addison-Wesley.
- Nikravesh, Parviz E. 1988. *Computer-Aided Analysis of Mechanical Systems*. Englewood Cliffs: Prentice-Hall.
- Pahl, G., and W. Beitz. 1995. *Engineering Design: A Systematic Approach*. 2nd ed. Trans. K. Wallace and L. Blessing. New York: Springer-Verlag.

- Paredis, C., and P. Khoshla. 1997. "Agent-Based Design of Fault Tolerant Manipulators for Satellite Docking." In *Proceedings of the 1997 IEEE International Conference on Robotics and Automation*, Albuquerque, April. 3473–3480.
- Payannet, D., M. J. Aldon, and A. Liegeois. 1985. "Identification and Compensation of Mechanical Errors for Industrial Robots." In *Proceedings of the 15th International Symposium on Industrial Robots*, Tokyo.
- Raghavan, M., and B. Roth. 1993. "Inverse Kinematics of the General 6R Manipulator and Related Linkages." *Transactions of the ASME* **115**(3), 502–508.
- Ragsdell, K. M. 1994. "Total Quality Management." *Manufacturing Review* **3**, 194–204.
- Roy, J., and L. Whitcomb. 1997. "Structural Design Optimization and Comparative Analysis of a New High-Performance Robot Arm via Finite Element Analysis." In *Proceedings of the 1997 IEEE International Conference on Robotics and Automation*, Albuquerque, April. 2190–2197.
- Schröer, Klaus (Editor); Commission of the European Communities, Directorate-General XII: Programme on Standards, Measurements and Testing: Handbook on Robot Performance Testing and Calibration: Improvement of Robot Industrial Standardisation IRIS. Stuttgart: Fraunhofer IRB Verlag, 1998.
- Stadler, W. 1995. *Analytical Robotics and Mechatronics*. McGraw-Hill Series in Electrical and Computer Engineering. New York: McGraw-Hill.
- Wang, J., and O. Masory. 1993. "On the Accuracy of a Stewart Platform. Part I: The Effect of Manufacturing Tolerances." In *Proceedings of the IEEE International Conference on Robotics and Automation*, Atlanta, May 2–6. 114–120.
- Wanner, M. C. 1988. "Rechengestützte Verfahren zur Auslegung der Mechanik von Industrierobotern." Dissertation, Universität Stuttgart.
- Zhiming, Z., and M. C. Leu. 1990. "Inverse Kinematics of Calibrated Robots." *Journal of Robotic Systems* **7**(5), 675–687.

# CHAPTER 6

## KINEMATICS AND DYNAMICS OF ROBOT MANIPULATORS

**Andrew A. Goldenberg**

**Mohammad R. Emami**

University of Toronto

Toronto, Ontario

### 1 INTRODUCTION

This chapter reviews current practical methodologies for kinematics and dynamics modeling and calculations. A kinematics model is a representation of the motion of the robot manipulator without considering masses and moments of inertia; a dynamics model is a representation of the balancing of external and internal loads acting on the manipulator whether it is stationary or moving. Both models are used widely in design, simulation, and, more recently, real-time control.

These topics are considered fundamental to the study and use of robotics. In the early development of this branch of science and engineering, kinematics and dynamics modeling were the main topics treated in the literature. Over the years, kinematics and dynamics modeling have generated the greatest number of publications related to robotics. This chapter attempts to extract some of the most relevant issues, but does not provide a summary of all the published work. Its aim is to present the standard tools for kinematics and dynamics modeling without prerequisites. The reader is also referred to the corresponding chapter in the first edition of this handbook (Walker, 1985).

### TERMINOLOGY

$n$	number of degrees of freedom of the manipulator
$\mathbf{q}$	vector of joint variable displacements
$\dot{\mathbf{q}}$	vector of joint variable velocities
$\ddot{\mathbf{q}}$	vector of joint variable accelerations
$Q$	joint space
$T$	task space
$\mathbf{F}_i$	coordinate frame attached to link $i$
$R_{i-1,i}$	$3 \times 3$ rotation matrix between frames $(i - 1)$ and $i$
$\mathbf{p}_{i-1,i}$	position vector of the origin of frame $i$ with respect to frame $(i - 1)$ expressed in frame $(i - 1)$
$H_{i-1,i}$	$4 \times 4$ homogeneous transformation matrix between frames $(i - 1)$ and $i$
$\boldsymbol{\epsilon}$	axis of general rigid body rotation
$\boldsymbol{v}$	axis of general rigid body translation
$\Psi$	$4 \times 4$ twist matrix
$W(P_w)$	wrist workspace
$W(P_e)$	end-effector workspace
$\boldsymbol{\omega}_i$	angular velocity vector of frame $i$
$\dot{\boldsymbol{\omega}}_i$	angular acceleration vector of frame $i$
$\boldsymbol{v}_i$	linear velocity vector of the origin of frame $i$
$\dot{\boldsymbol{v}}_i$	linear acceleration vector of the origin of frame $i$
$\mathbf{v}_{ci}$	linear velocity vector of the center of mass of link $i$
$\dot{\mathbf{v}}_{ci}$	linear acceleration vector of the center of mass of link $i$
$\mathbf{p}_{ci}$	position vector of the center of mass of link $i$ with respect to frame $i$

$I_{ci}$	$3 \times 3$ moment of inertia matrix of link $i$ about its center of mass expressed in frame $i$
$m_i$	mass of link $i$
$J$	$6 \times n$ Jacobian matrix
$\tau$	vector of joint torques and forces
$\mathbf{f}_e$	vector of resulting reaction forces at the end-effector
$\mathbf{g}_e$	vector of resulting reaction moments at the end-effector
$\mathbf{f}_{ext}$	vector of external forces acting at the end-effector
$\mathbf{g}_{ext}$	vector of external moments acting at the end-effector
$\mathbf{G}_e$	wrench vector
$M$	$n \times n$ manipulator inertia matrix
$g$	gravity acceleration vector

## 2 KINEMATICS

This section considers the motion of the robot manipulator irrespective of inertial and external forces. A study of the geometry of motion is essential in manipulator design and control in order to obtain the mapping between the end-effector location (position and orientation) and the movement of manipulator links, as well as the mapping between the end-effector velocity and the speed of manipulator links. The final goal is to use these mappings to relate the end-effector (or gripper, or tool mounted on the end-effector) motion to joint displacements (generalized coordinates) and velocities.

### 2.1 Forward Kinematics

The objective of forward kinematics is to determine the location of the end-effector with respect to a reference coordinate frame as a result of the relative motion of each pair of adjacent links. Attention is restricted to the case of an *open-chain* manipulator, a serial link of rigid bodies connected in pairs by *revolute* and/or *prismatic* joints, for relative rotation and relative translation, respectively.

#### 2.1.1 Different Configuration Spaces for Robot Manipulators

The configuration of a robot manipulator can be specified using either of the following algebraic spaces:

1. The *joint space*  $\mathcal{Q}$  is the set of all possible vectors of joint variables. The dimension of the joint vector is equal to the number of joints (or degrees of freedom), i.e.,  $\mathcal{Q} \subset \mathbb{R}^n$ . Each joint variable is defined as an angle  $\theta \in \mathcal{S} = [0, 2\pi)$  for a revolute joint, or a linear translation  $d \in \mathbb{R}$  for a prismatic joint. Let  $\mathbf{q} \in \mathcal{Q}$  denote the vector of generalized coordinates.
2. The *task space*  $T$  is the set of pairs  $(\mathbf{p}, R)$ , where  $\mathbf{p} \in \mathbb{R}^3$  is the position vector of the origin of link coordinate frame and  $R \in SO(3)$  represents the orientation of the link frame, both with respect to a general reference frame. Here,  $SO(3)$  denotes the group of  $3 \times 3$  proper rotation matrices. Thus, the task space is a *Special Euclidean group*  $SE(3)$ , defined as follows:

$$SE(3) = \{(\mathbf{p}, R) : \mathbf{p} \in \mathbb{R}^3, R \in SO(3)\} = \mathbb{R}^3 \times SO(3). \quad (1)$$

Using the above notation, the forward kinematics is a mapping  $H$ , defined as follows:

$$H: \mathcal{Q} \rightarrow SE(3). \quad (2)$$

This mapping can be represented by a  $4 \times 4$  *homogeneous transformation* matrix, defined as

$$\begin{bmatrix} R & | & \mathbf{p} \\ \hline - & | & - \\ [0] & | & 1 \end{bmatrix}.$$

#### 2.1.2 The End-Effector Position and Orientation

In order to obtain the forward kinematics mapping  $H$ , suitable coordinate frames should be assigned to the manipulator base, end-effector, and intermediate links. One standard method attributed to Denavit and Hartenberg (1965) is based on the homogeneous transformation  $H$ . The Denavit–Hartenberg (DH) convention uses the minimum number of parameters to completely describe the geometric relationship between adjacent robot links.

Each link and joint of the manipulator is numbered, as illustrated in Figure 1. The frame  $\mathbf{F}_i$  attached to link  $i$  is defined with the  $\mathbf{z}_i$  along the axis of joint  $(i + 1)$ ; the origin is located at the intersection of  $\mathbf{z}_i$  and the common normal to  $\mathbf{z}_{i-1}$  and  $\mathbf{z}_i$ , and  $\mathbf{x}_i$  is along the common normal, as illustrated in Figure 1. The homogeneous transformation matrix between links  $i$  and  $(i - 1)$  is then expressed as (Walker, 1985):

$$H_{i-1,i} = \begin{bmatrix} R_{i-1,i} & \mathbf{p}_{i-1,i} \\ [0] & 1 \end{bmatrix} = \begin{bmatrix} \cos \theta_i & -\sin \theta_i \cos \alpha_i & \sin \theta_i \sin \alpha_i & a_i \cos \theta_i \\ \sin \theta_i & \cos \theta_i \cos \alpha_i & -\cos \theta_i \sin \alpha_i & a_i \sin \theta_i \\ 0 & \sin \alpha_i & \cos \alpha_i & d_i \\ 0 & 0 & 0 & 1 \end{bmatrix} \quad (3)$$

where

$R_{i-1,i}$  = relative rotation of frame  $\mathbf{F}_i$  with respect to  $\mathbf{F}_{i-1}$ ;

$\mathbf{p}_{i-1,i}$  = position vector of the origin of  $\mathbf{F}_i$  with respect to  $\mathbf{F}_{i-1}$ , expressed in  $\mathbf{F}_{i-1}$ ;

$[0]$  =  $1 \times 3$  null matrix.

The three link parameters  $a_i$ ,  $\alpha_i$ ,  $d_i$  and one joint variable  $\theta_i$  required to specify the transformation (3) are defined as follows:

$a_i$  = the length of the common normal between  $\mathbf{z}_{i-1}$  and  $\mathbf{z}_i$  (link length)

$\alpha_i$  = the angle between  $\mathbf{z}_{i-1}$  and  $\mathbf{z}_i$  measured about  $\mathbf{x}_i$  (twist angle)

$d_i$  = the distance from  $\mathbf{x}_{i-1}$  to  $\mathbf{x}_i$  measured along  $\mathbf{z}_{i-1}$  (link offset or distance)

$\theta_i$  = the angle between  $\mathbf{x}_{i-1}$  and  $\mathbf{x}_i$  measured about  $\mathbf{z}_{i-1}$ .

The homogeneous transformation between the base frame  $\mathbf{F}_0$  and the end-effector frame  $\mathbf{F}_n$  (for an  $n$ -d.o.f. manipulator) can then be systematically determined by successive multiplication of the intermediate transformations, namely:

$$H_{0n} = H_{01}H_{12} \cdots H_{i-1,i} \cdots H_{n-2,n-1}H_{n-1,n} \quad (4)$$

The matrix  $H_{0n}$  contains the rotation matrix between frames  $\mathbf{F}_0$  and  $\mathbf{F}_n$  ( $R_{0n}$ ), and the location of the origin of  $\mathbf{F}_n$  with respect to  $\mathbf{F}_0$ , expressed in  $\mathbf{F}_0$ :

$$H_{0n} = \begin{bmatrix} R_{0n} & \mathbf{p}_{0n} \\ [0] & 1 \end{bmatrix} = \begin{bmatrix} n_{0n}^x & o_{0n}^x & a_{0n}^x & p_{0n}^x \\ n_{0n}^y & o_{0n}^y & a_{0n}^y & p_{0n}^y \\ n_{0n}^z & o_{0n}^z & a_{0n}^z & p_{0n}^z \\ 0 & 0 & 0 & 1 \end{bmatrix} \quad (5)$$

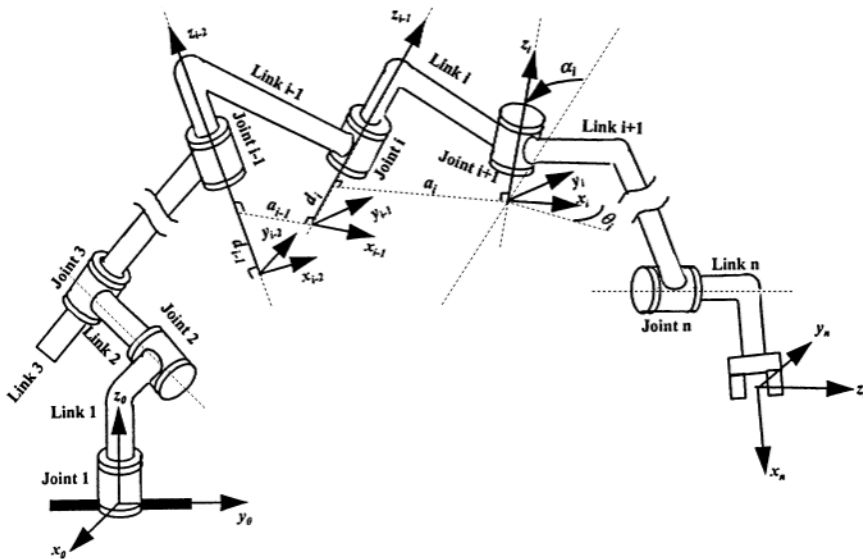


Figure 1 DH link frames and parameters.

where vectors  $\mathbf{n}_{0n}$ ,  $\mathbf{o}_{0n}$  and  $\mathbf{a}_{0n}$  specify the orientation of the  $\mathbf{x}_n$ ,  $\mathbf{y}_n$  and  $\mathbf{z}_n$  axes, respectively, of frame  $\mathbf{F}_n$  with respect to frame  $\mathbf{F}_0$ .

### 2.1.3 Standard Coordinate Frames

Figure 2 shows some of the standard frames commonly used in industrial applications. The position of the origin and the orientation of each frame with respect to the base frame is obtained by successive multiplications of the intermediate homogeneous transformation matrices. For example, the representation of the tool frame with respect to the base frame is determined by

$$H_{0t} = H_{0n}H_{nt} \quad (6)$$

where  $H_{nt}$  and  $H_{0n}$  are the homogeneous transformation matrices between the end-effector and the tool frames and between the end-effector and the base frames, respectively.

### 2.1.4 Computational Considerations and Symbolic Formulation

In practical applications it is always effective to minimize the computational time required to perform the kinematic calculations. The calculations can be performed recursively because the open-chain manipulator can be seen as being constructed by adding a link to the previous links. This reduces the number of multiplications and additions at the cost of creating local variables in order to avoid the use of common terms throughout the computation. Algorithm 1 illustrates a backward recursive formulation for calculating the forward kinematics (Hoy and Sriwattanathamma, 1989).

Symbolic kinematic equations that describe the end-effector (or tool) position and orientation as explicit functions of joint coordinates can be derived in advance of real-time computation. If suitable trigonometric simplifications are implemented, symbolic representation helps to reduce the number of arithmetic operations. Either general-purpose (such as MATHEMATICA and MAPLE) or special-purpose (such as SD/FAST (Westmacott, 1993)) symbolic modeling software can replace manual derivation to generate symbolic kinematic relationships automatically (Vukobratovic, 1986).

Transcendental functions are a major computational expense in forward kinematics calculations when standard software is used. Instead, lookup table implementations of these functions may reduce the required calculation time by a factor of two to three, or more (Ruoff, 1981). Moreover, using fixed-point instead of floating-point representation can speed up the operations. A 24-bit representation of joint variables is adequate due to the typically small dynamic range of these variables (Turner, Craig, and Gruver, 1984).

### 2.1.5 Manipulator Workspace

Evaluation of the manipulator workspace is a subject of interest for purposes of both analysis and synthesis. The workspace of a manipulator is defined as the set of all end-effector locations (positions and orientations of the end-effector frame) that can be reached by arbitrary choices of joint variables within the corresponding ranges. If both end-effector

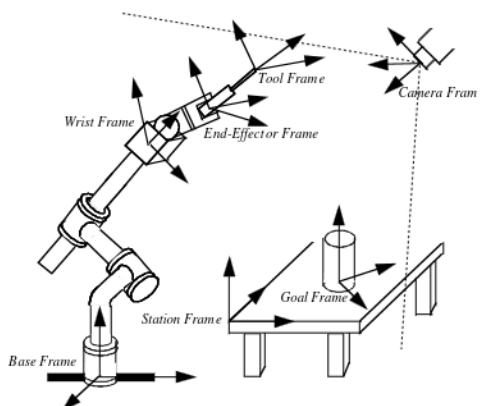


**Figure 2** Standard coordinate frames.

LOOP: FOR  $i = n - 1$  to 1

$$\begin{aligned}
 1. \text{ SET: } R_{i,n} &= \begin{bmatrix} n_{i,n}^x & o_{i,n}^x & a_{i,n}^x \\ \hline n_{i,n}^y & o_{i,n}^y & a_{i,n}^y \\ \hline n_{i,n}^z & o_{i,n}^z & a_{i,n}^z \end{bmatrix} = \begin{bmatrix} [R_{i,n}^x] \\ [R_{i,n}^y] \\ [R_{i,n}^z] \end{bmatrix} \\
 2. \text{ CALCULATE: } &\begin{cases} [M_{i,n}] = \cos \alpha_i [R_{i,n}^y] - \sin \alpha_i [R_{i,n}^z] \\ r_{i,n} = \cos \alpha_i p_{i,n}^y - \sin \alpha_i p_{i,n}^z \\ s_{i,n} = \begin{cases} p_{i,n}^x + a_i & \text{if joint } i \text{ is revolute} \\ p_{i,n}^x & \text{if joint } i \text{ is prismatic} \end{cases} \end{cases} \\
 3. \text{ CALCULATE: } &\begin{cases} [R_{i-1,n}^x] = \cos \theta_i [R_{i,n}^x] - \sin \theta_i [M_{i,n}] \\ [R_{i-1,n}^y] = \sin \theta_i [R_{i,n}^x] + \cos \theta_i [M_{i,n}] \\ [R_{i-1,n}^z] = \sin \alpha_i [R_{i,n}^y] + \cos \alpha_i [R_{i,n}^z] \\ p_{i-1,n}^x = \cos \theta_i s_{i,n} - \sin \theta_i r_{i,n} \\ p_{i-1,n}^y = \sin \theta_i s_{i,n} + \cos \theta_i r_{i,n} \\ p_{i-1,n}^z = \sin \alpha_i p_{i,n}^y + \cos \alpha_i p_{i,n}^z + d_i \end{cases}
 \end{aligned}$$

NEXT  $i$

Algorithm 1 Backward recursive formulation of the forward kinematics problem.

position and orientation are considered, the workspace is the *complete workspace*; disregarding the orientation of the end-effector gives the *reachable workspace*. The subset of the reachable workspace that can be attained with arbitrary orientations of the end-effector is the *dexterous workspace*. Most industrial manipulators have spherical wrists; therefore, for a 6-d.o.f. manipulator, the wrist is positioned using the first three joints. If the wrist point  $P_w$  and the end-effector point of interest  $P_e$  are different, then, after the workspace of the wrist point  $W(P_w)$  is determined, a sphere of radius  $\overline{P_w P_e}$  is moved so that its center is on the boundary of the wrist workspace  $W(P_w)$ . The inner and outer envelopes are the boundaries of the dexterous and reachable workspaces, respectively. Nevertheless, due to machining tolerances, assembly errors, and other limitations, it is impossible to build a perfect wrist with three orthogonal revolute axes intersecting at one point. Thus a general methodology is required for determining the manipulator workspace (Ceccarelli, 1994).

## 2.1.6 The Product of Exponentials (PE) Formula

A geometric description of the robot kinematics can be obtained based on classical *screw theory* (Yuan, 1971). The fundamental fact is that any arbitrary rigid body motion is equivalent to a rotation  $\theta$  about a certain line  $\epsilon$  ( $\|\epsilon\| = 1$ ) combined with a translation  $l$  parallel to that line. The homogeneous transformation of the rigid body motion with respect to a reference frame can then be represented as

$$H(\theta, l) = e^{\Psi\theta} H(0, 0) \quad (7)$$

where  $H(0, 0)$  is the initial homogeneous representation of the rigid body with respect to the same reference frame when  $\theta = 0$  and  $l = 0$ . In Equation (7),  $\Psi$  is a  $4 \times 4$  matrix called the *twist* and is defined as

$$\Psi = \begin{bmatrix} E & -E\mathbf{p} + (l/\theta)\epsilon \\ \hline 0 & 0 \end{bmatrix} \quad (8)$$

where  $E$  is a  $3 \times 3$  skew-symmetric matrix of the rotation axis  $\epsilon = [\epsilon_x \ \epsilon_y \ \epsilon_z]^T$  such that

$$E = \begin{bmatrix} 0 & -\epsilon_z & \epsilon_y \\ \epsilon_z & 0 & -\epsilon_x \\ -\epsilon_y & \epsilon_x & 0 \end{bmatrix} \quad (9)$$

and  $\mathbf{p} = [p_x \ p_y \ p_z]^T \in \mathbb{R}^3$  is the position vector of an arbitrary point located on the

rotation axis  $\epsilon$  and expressed in the same reference frame. The matrix exponential mapping  $e^{\Psi\theta}$  is based on the following formulation (Park and Okamura, 1994).

$$e^{\Psi\theta} = \begin{bmatrix} e^{E\theta} & A(-E\mathbf{p} + (l/\theta)\epsilon) \\ [0] & 1 \end{bmatrix} \quad (10)$$

where

$$e^{E\theta} = [I] + E \sin \theta + E^2(1 - \cos \theta) \quad (11)$$

and

$$A = [I]\theta + E(1 - \cos \theta) + E^2(\theta - \sin \theta) \quad (12)$$

For a pure rigid body translation ( $\theta = 0$ ) along some axis  $v$  ( $\|v\| = 1$ ), the twist is defined as

$$\Psi_{\text{trans}} = \begin{bmatrix} [[0]] & lv \\ [0] & 0 \end{bmatrix} \quad (13)$$

where  $[[0]]$  and  $[0]$  are  $3 \times 3$  and  $1 \times 3$  null matrices, respectively. In this case the matrix exponential mapping becomes

$$e^{\Psi_{\text{trans}}\theta} = \begin{bmatrix} [I] & lv \\ [0] & 1 \end{bmatrix} \quad (14)$$

with  $[I]$  as the  $3 \times 3$  identity matrix.

Based on the above formulation of rigid body motion, for an open-chain manipulator, the homogeneous transformation of each link  $i$  with respect to the base frame is obtained by an exponential mapping

$$H_{0i}(q_i) = e^{\Psi_i q_i} H_{0i}(0) \quad (15)$$

where

$q_i$  = joint variable;  
 $\Psi_i$  = twist of link  $i$ .

The homogeneous representation of the end-effector with respect to the base frame is obtained by combining a sequence of mappings into the so-called *product of exponentials* (PE) formula (Brockett, 1983).

$$H_{0n}(q_1, q_2, \dots, q_n) = e^{\Psi_1 q_1} e^{\Psi_2 q_2} \cdots e^{\Psi_n q_n} H_{0n}(0, 0, \dots, 0). \quad (16)$$

The matrix  $H_{0n}(0, 0, \dots, 0)$  represents the homogeneous transformation of the end-effector frame with respect to the base frame when the manipulator is in its *reference configuration*, i.e., all joint variables are zero. The twist  $\Psi_i$  corresponds to the screw motion of the  $i^{\text{th}}$  link as a result of moving joint  $i$  with all other joint variables held fixed at  $q_j = 0$  ( $j \neq i$ ).

One of the features of the PE formula is that, in contrast to the DH representation, there is no need to attach a frame to each link: once the base, end-effector, and a reference configuration frame have been chosen, a unique set of link twists is obtained that describes the forward kinematics of the robot. This property and the geometric representation make the PE formula a superior alternative to the DH convention.

## 2.2 Inverse Kinematics

Inverse kinematics is used to find the values of the joint variables that will place the end-effector at a desired location, i.e., desired position and orientation relative to the base, given the manipulator geometry (link lengths, offsets, twist angles, and the location of the base). Formally, for an  $n$ -d.o.f. manipulator, given the homogeneous matrix  $H_{0n}$  (5), the values of  $q_1, q_2, \dots, q_n$  are calculated. In general, the matrix equation (4) corresponds to 12 scalar equations; because the rotation matrix  $R_{0n}$  is orthonormal, only 6 of the 12 equations are independent. Therefore, the problem of inverse kinematics of a general 6-d.o.f. manipulator corresponds to solving a set of six nonlinear, transcendental equations with six unknowns (joint variables). There may be no solution, a unique solution, or multiple solutions to the inverse kinematics problem.

### 2.2.1 Solvability and Number of Solutions

A general approach for systematically solving the inverse kinematics problem (Lee and Liang, 1988) is to consider the set of nonlinear equations as a set of multivariate polynomials in  $s_i = \sin \theta_i$  and  $c_i = \cos \theta_i$  for  $i = 1, 2, \dots, n$ . This is possible since the entries of each homogeneous transformation matrix (3) are unary (i.e., of degree one or less) in  $s_i$  and  $c_i$ . Then, by elimination of variables in a systematic way (Salmon, 1964),  $n - 1$  variables are eliminated in a system of  $n$  polynomials in  $n$  variables, and a single polynomial in one variable is obtained. This method is called *dyalitic elimination*, and the resultant polynomial is called the *characteristic polynomial*. Once the roots of this polynomial are found, the eliminated variables can be determined from a set of linear equations. This general algorithm is presented in the next subsection, which addresses the existence and number of solutions of the inverse kinematics problem.

Generally, at least six joints are required to attain arbitrary three-dimensional task positions and orientations. The necessary condition for the existence of a solution is that the desired end-effector location lie in the reachable workspace. If the desired location is inside the workspace, then the existence of at least one solution is guaranteed. The existence of an analytical, closed-form solution to the inverse kinematics problem depends on the order of the characteristic polynomial. If the characteristic polynomial is of order 4 or less, since the roots can be obtained as algebraic functions of the polynomial coefficients, the corresponding inverse kinematics problem can be solved analytically. Otherwise, iterative numerical methods must be relied upon to obtain the roots of the polynomial. In this case, the problem is considered numerically solvable when: 1) an upper bound on the number of solutions exists. 2) an efficient algorithm for computing all solutions is available. Based on recent results in kinematics (Selfridge, 1989), all 6-d.o.f. open-chain manipulators with revolute and prismatic joints are solvable. The number of solutions depends on the number of prismatic joints and kinematic parameters. For the general case of six revolute joints (6R manipulator) or one prismatic and five revolute joints (5R1P manipulator), there are at most 16 different configurations for each end-effector location. For 4R2P manipulators the number of possible configurations drops to 8, and for the 3R3P the number is 2. These numbers are independent of the physical order of revolute and prismatic joints in the chain. In all of the above cases, the number of *real* roots of the characteristic polynomials (and hence the number of real configurations) may be less than the numbers cited above by any multiple of 2. Certain values of the kinematic parameters may also reduce the number of possible configurations. A detailed investigation can be found in Mavroidis and Roth (1994). As an example, a 6R manipulator with three consecutive joint axes intersecting in a common point (Pieper and Roth, 1969) or with three parallel joint axes (Duffy, 1980) has at most 8 configurations, and the characteristic polynomial is of order 4 with repeated roots; therefore analytical solutions exist. A 6R manipulator with a spherical wrist is very common in industry. The analytical technique for this case is first to solve for the first three joint variables to satisfy the desired wrist point location and then to find the last three joint variables to achieve the required hand orientation (Pieper and Roth, 1969).

### 2.2.2 A General Solution for Six-Degree-of-Freedom Manipulators

A systematic method of solving the inverse kinematics of 6-d.o.f. manipulators is to arrange the set of nonlinear equations as a set of multivariate polynomials in  $s_i$  and  $c_i$  and then eliminate all variables except  $\theta_3$ , thus obtaining a polynomial of order 16 in  $\tan(\theta_3/2)$  such that the joint angle  $\theta_3$  can be computed as its roots. The remaining joint variables are obtained by substituting and solving for some intermediate equations. In this section, the procedure is presented for general 6R manipulators. The extension to manipulators with prismatic joints is also discussed. The following algorithm is a summary of the algorithm presented in Raghavan and Roth (1993).

#### Step 1

Determine the DH parameters and homogeneous transformation matrices  $H_{i-1,i}$  and then rewrite the forward kinematics matrix equation in the following form:

$$H_{23}H_{34}H_{45} = H_{12}^{-1}H_{01}^{-1}H_{06}H_{56}^{-1} \quad (17)$$

#### Step 2

Equate each of the first three elements of the third and fourth columns of both sides of Equation (17). This gives two sets of three scalar equations, from which all the other

equations are formed. These sets are written as two three-dimensional vector equations, denoted  $P$  (corresponding to the third column) and  $Q$  (corresponding to the fourth column):

$$P \equiv \begin{bmatrix} P_{1l} = P_{1r} \\ P_{2l} = P_{2r} \\ P_{3l} = P_{3r} \end{bmatrix}; \quad Q \equiv \begin{bmatrix} Q_{1l} = Q_{1r} \\ Q_{2l} = Q_{2r} \\ Q_{3l} = Q_{3r} \end{bmatrix} \quad (18)$$

where  $P_{il}$  and  $Q_{il}$  refer to the left-hand side and  $P_{ir}$  and  $Q_{ir}$  refer to the right-hand side of the equations.

The set of all six equations can be written in the following matrix form:

$$A\mathbf{X}_1 = B\mathbf{Y} \quad (19)$$

For a 6R manipulator,  $A$  is a  $6 \times 9$  matrix whose elements are linear combinations of  $s_3$ ,  $c_3$ ,  $B$  is a  $6 \times 8$  matrix with constant elements, and  $\mathbf{X}_1$  and  $\mathbf{Y}$  are  $9 \times 1$  and  $8 \times 1$  matrices, respectively, defined as

$$\mathbf{X}_1 = [s_4s_5 \quad s_4c_5 \quad c_4s_5 \quad c_4c_5 \quad s_4 \quad c_4 \quad s_5 \quad c_5 \quad 1]^T \quad (20)$$

$$\mathbf{Y} = [s_1s_2 \quad s_1c_2 \quad c_1s_2 \quad c_1c_2 \quad s_1 \quad c_1 \quad s_2 \quad c_2]^T \quad (21)$$

### Step 3

Construct the following scalar and vector equations to obtain eight new scalar equations:

$$Q \cdot Q \equiv [Q_{1l}^2 + Q_{2l}^2 + Q_{3l}^2 = Q_{1r}^2 + Q_{2r}^2 + Q_{3r}^2] \quad (22)$$

$$P \cdot Q \equiv [P_{1l}Q_{1l} + P_{2l}Q_{2l} + P_{3l}Q_{3l} = P_{1r}Q_{1r} + P_{2r}Q_{2r} + P_{3r}Q_{3r}] \quad (23)$$

$$P \times Q \equiv \begin{bmatrix} P_{2l}Q_{3l} - P_{3l}Q_{2l} = P_{2r}Q_{3r} - P_{3r}Q_{2r} \\ P_{3l}Q_{1l} - P_{1l}Q_{3l} = P_{3r}Q_{1r} - P_{1r}Q_{3r} \\ P_{1l}Q_{2l} - P_{2l}Q_{1l} = P_{1r}Q_{2r} - P_{2r}Q_{1r} \end{bmatrix} \quad (24)$$

$$P(Q \cdot Q) - 2Q(P \cdot Q) \equiv \begin{bmatrix} P_{1l} \sum_{i=1}^3 Q_{il}^2 - 2Q_{1l} \sum_{i=1}^3 P_{il}Q_{il} = P_{1r} \sum_{i=1}^3 Q_{ir}^2 - 2Q_{1r} \sum_{i=1}^3 P_{ir}Q_{ir} \\ P_{2l} \sum_{i=1}^3 Q_{il}^2 - 2Q_{2l} \sum_{i=1}^3 P_{il}Q_{il} = P_{2r} \sum_{i=1}^3 Q_{ir}^2 - 2Q_{2r} \sum_{i=1}^3 P_{ir}Q_{ir} \\ P_{3l} \sum_{i=1}^3 Q_{il}^2 - 2Q_{3l} \sum_{i=1}^3 P_{il}Q_{il} = P_{3r} \sum_{i=1}^3 Q_{ir}^2 - 2Q_{3r} \sum_{i=1}^3 P_{ir}Q_{ir} \end{bmatrix} \quad (25)$$

These eight equations have the same functional form as  $P$  and  $Q$ . Therefore, combining all the equations generates a set of 14 nonlinear equations of the form

$$\bar{A}\mathbf{X}_1 = \bar{B}\mathbf{Y} \quad (26)$$

where  $\bar{A}$  is a  $14 \times 9$  matrix whose elements are linear combinations of  $s_3$ ,  $c_3$ , and  $\bar{B}$  is a  $14 \times 8$  constant matrix.

### Step 4

Use any 8 of the 14 equations in (26) to solve for  $\mathbf{Y}$  in terms of  $\mathbf{X}_1$ . The resulting system of 6 equations takes the form

$$\Gamma_1 \mathbf{X}_1 = 0 \quad (27)$$

where  $\Gamma_1$  is a  $6 \times 9$  matrix. As a result, joint variables  $\theta_1$  and  $\theta_2$  are eliminated from the set of equations.

### Step 5

Change Equation (27) into polynomial form by the following substitutions:

$$s_i = \frac{2x_i}{1+x_i^2}, \quad c_i = \frac{1-x_i^2}{1+x_i^2} \quad \text{for } i = 3, 4, 5 \quad (28)$$

where  $x_i = \tan(\theta_i/2)$ . Then multiply each equation by  $(1 + x_4^2)$  and  $(1 + x_5^2)$  to clear the denominators, and multiply the first four equations by  $(1 + x_3^2)$  to obtain the following form:

$$\Gamma_2 \mathbf{X}_2 = 0 \quad (29)$$

where  $\Gamma_2$  is a  $6 \times 9$  matrix whose entries are linear combinations of  $s_3$ ,  $c_3$ . For a general 6R manipulator, the vector  $\mathbf{X}_2$  is

$$\mathbf{X}_2 = [x_4^2 x_5^2 \quad x_4^2 x_5 \quad x_4^2 \quad x_4 x_5^2 \quad x_4 x_5 \quad x_5^2 \quad x_5 \quad 1]^T \quad (30)$$

### Step 6

Multiply the 6 equations in Equation (29) by  $x_4$  to obtain 6 more equations. The set of all 12 equations forms the following homogeneous system:

$$\Gamma \mathbf{X} = \begin{bmatrix} \Gamma_2 & [0] \\ [0] & \Gamma_2 \end{bmatrix} \mathbf{X} = 0 \quad (31)$$

where  $[0]$  is the  $6 \times 9$  null matrix and  $\mathbf{X}$  is the vector of power products, which for a 6R manipulator is obtained as follows:

$$\mathbf{X} = [x_4^3 x_5^2 \quad x_4^3 x_5 \quad x_4^3 \quad x_4^2 x_5^2 \quad x_4^2 x_5 \quad x_4^2 \quad x_4 x_5^2 \quad x_4 x_5 \quad x_4 \quad x_5^2 \quad x_5 \quad 1]^T \quad (32)$$

### Step 7

Apply the condition of having nontrivial solutions to the homogeneous system in order to obtain the characteristic equation in  $x_3$ , i.e.,

$$\det(\Gamma) = 0 \quad (33)$$

which is a polynomial of order 16 in the case of a general 6R manipulator.

### Step 8

Obtain the roots of the characteristic polynomial by numerical methods. The real roots correspond to the real configurations of the inverse kinematics problem. For each value of  $x_3$  thus obtained, the corresponding joint variable  $\theta_3$  may be computed from the formula  $\theta_3 = 2 \tan^{-1}(x_3)$ .

### Step 9

Substitute each real value of  $x_3$  into the coefficient matrix of Equation (31), and then solve for  $X$  to obtain unique values for  $x_4$  and  $x_5$ , and hence  $\theta_4$  and  $\theta_5$ , using  $\theta_i = 2 \tan^{-1}(x_i)$ .

### Step 10

Substitute the values of  $\theta_3$ ,  $\theta_4$ , and  $\theta_5$  into Equation (26) and use a subset of 8 equations to solve for  $\mathbf{Y}$ ; then use the numerical values of  $s_1$ ,  $c_1$  and  $s_2$ ,  $c_2$  to obtain  $\theta_1$  and  $\theta_2$ , respectively.

### Step 11

Substitute values of  $\theta_1$ ,  $\theta_2$ ,  $\theta_3$ ,  $\theta_4$ , and  $\theta_5$  into the first and second entries of the first column of the following kinematics relationship:

$$H_{56} = H_{45}^{-1} H_{34}^{-1} H_{23}^{-1} H_{12}^{-1} H_{01}^{-1} H_{06} \quad (34)$$

to obtain two linear equations in  $s_6$  and  $c_6$  from which a unique value for  $\theta_6$  is obtained.

For 5R1P manipulators, the above algorithm remains unchanged. However for a prismatic joint  $k$ ,  $\sin \theta_k$  is replaced by  $d_k$ , and  $\cos \theta_k$  is replaced by  $(d_k)^2$ . For 4R2P manipulators, there are fewer power products and therefore fewer equations are required, leading to a characteristic polynomial of order 8. However, the procedure is essentially the same as above (Kohli and Osvatic, 1992). For 3R3P manipulators, the procedure simplifies considerably, leading to a characteristic polynomial of order 2 (Kohli and Osvatic, 1992).

### 2.2.3 Repeatability, Accuracy, and Computational Considerations

Industrial robots are rated on the basis of their ability to return to the same location when repetitive motion is required. The locations attained for any number of repeated motions

may not be identical. The *repeatability* of the manipulator is the expected maximum error at any attained location with respect to an *average* attained location of repeated motions. Manipulators with low joint backlash, friction, and flexibility usually have high repeatability.

Another robot rating criterion is the precision with which a desired location can be attained. This is called the *accuracy* of the manipulator, and it is the error between the desired and attained locations. The accuracy can be enhanced if two major obstacles are overcome. First, due to manufacturing errors in the machining and assembly of manipulators, the physical kinematics parameters may differ from the design parameters, which can produce significant errors between the actual and predicted locations of the end-effector. To solve this problem, calibration techniques are devised to improve accuracy through estimation of the individual kinematics parameters (Hollerbach, 1989). The second difficulty is that the numerical algorithms for solving the inverse kinematics problem are not efficient for practical implementations. For instance, for a general 6R manipulator the algorithm illustrated in Section 2.2.2 takes on average 10 seconds of CPU on an IBM 370-3090 using double precision arithmetic (Wampler and Morgan, 1991), while a speed on the order of milliseconds would be required in real-time applications. Furthermore, the problem of computing the roots of a characteristic polynomial of degree 16 can be ill-conditioned (Wilkinson, 1959). Closed-form solutions are quite efficient, but they exist only for a few special manipulators. This is one reason most industrial manipulators are limited to simple configurations and inverse kinematics calculations are not performed on-line. Recently some efficient algorithms have been suggested for the general solution of the inverse kinematics problem for 6-d.o.f. manipulators (Manocha and Canny, 1994). These algorithms require that the following operations be performed.

#### **Off-line Symbolic Formulation and Numeric Substitution**

For any class of manipulators, symbolic preprocessing can be performed to obtain the entries of matrices  $A$ ,  $B$ , and  $\Gamma$  in Equations (26) and (31) as functions of kinematic parameters and elements of the end-effector homogeneous matrix  $H_{06}$ . The symbolic derivation and simplification can be performed using MATHEMATICA or MAPLE. Then, the numerical values of the kinematic parameters of a particular manipulator can be substituted in advance into the functions representing the elements of matrices  $\bar{A}$ ,  $\bar{B}$ , and  $\Gamma$ . Given the desired location of the end-effector, the remaining numerical substitutions are performed on-line.

#### **Changing the Problem of Finding the Roots of the Characteristic Polynomial to an Eigenvalue Problem**

A more efficient method of finding nontrivial solutions for the matrix Equation (31) is to set up an equivalent eigenvalue problem (Ghasvini, 1993), rather than expanding the determinant of the coefficient matrix. The matrix  $\Gamma$  in Equation (31) can be expressed as (Ghasvini, 1993)

$$\Gamma = Lx_3^2 + Nx_3 + K \quad (35)$$

where  $L$ ,  $N$ , and  $K$  are  $12 \times 12$  matrices. For a nonsingular matrix  $L$ , the following  $24 \times 24$  matrix is constructed:

$$\Pi = \begin{bmatrix} [0] & | & [I] \\ -L^{-1}K & | & -L^{-1}N \end{bmatrix} \quad (36)$$

where  $[0]$  and  $[I]$  are  $12 \times 12$  null and identity matrices, respectively. The eigenvalues of  $\Pi$  are equal to the roots of Equation (33). Moreover, the eigenvector of  $\Pi$  corresponding to the eigenvalue  $x_3$  has the structure

$$\mathbf{V} = \begin{bmatrix} \mathbf{X} \\ x_3 \mathbf{X} \end{bmatrix} \quad (37)$$

which can be used to compute the solutions of Equation (27). If the matrix  $L$  is singular, then the following two matrices are constructed:

$$\Pi_1 = \begin{bmatrix} [I] & [0] \\ [0] & L \end{bmatrix}; \quad \Pi_2 = \begin{bmatrix} [0] & [I] \\ -K & -N \end{bmatrix} \quad (38)$$

The roots of Equation (33) are equal to the eigenvalues of the generalized eigenvalue problem  $(\Pi_1 - x_3\Pi_2)$ , which has the same eigenvalues as Equation (36).

## 2.3 Velocity Kinematics

### 2.3.1 Link Velocity, Jacobian

In addition to the kinematic relationship between joint displacements and the end-effector location, the relationship between the joint velocity vector and end-effector linear and angular velocities is also useful. The absolute velocities (i.e., relative to the base coordinate frame) of the link  $i$  coordinate frame are computed from the absolute velocities of the link  $i - 1$  frame as follows:

If the  $i^{\text{th}}$  joint is revolute, i.e.,  $\dot{q}_i = \dot{\theta}_i$ ,

$$\begin{aligned}\mathbf{v}_i &= \mathbf{v}_{i-1} + \boldsymbol{\omega}_i \times \mathbf{p}_{i-1,i} \\ \boldsymbol{\omega}_i &= \boldsymbol{\omega}_{i-1} + \mathbf{z}_{i-1}\dot{q}_i\end{aligned}\quad (39)$$

and if the  $i^{\text{th}}$  joint is prismatic, i.e.,  $\dot{q}_i = \dot{d}_i$ ,

$$\begin{aligned}\mathbf{v}_i &= \mathbf{v}_{i-1} + \boldsymbol{\omega}_i \times \mathbf{p}_{i-1,i} + \mathbf{z}_{i-1}\dot{q}_i \\ \boldsymbol{\omega}_i &= \boldsymbol{\omega}_{i-1}\end{aligned}\quad (40)$$

where  $\boldsymbol{\omega}_i$  is the angular velocity vector of frame  $F_i$  (attached to link  $i$ ),  $\mathbf{v}_i$  is the linear velocity vector of its origin, and  $\mathbf{z}_i$  is the unit vector along the axis of joint  $i$ .

Combining Equations (39) and (40), the relationship between the link frame and joint velocities is obtained as follows (Whitney, 1969):

$$\mathbf{V}_i = \begin{bmatrix} \mathbf{v}_i \\ \boldsymbol{\omega}_i \end{bmatrix} = J_i(q_1, q_2, \dots, q_{i-1})\dot{\mathbf{q}} \quad (41)$$

The  $n \times 1$  matrix  $\dot{\mathbf{q}} = [\dot{q}_1 \ \dot{q}_2 \ \dots \ \dot{q}_n]^T$  consists of joint velocities, and  $J_i$  is a  $6 \times n$  “Jacobian” of link  $i$  defined as follows:

$$J_i(q_1, q_2, \dots, q_{i-1}) = \left[ \begin{array}{c|ccc} \mathbf{t}_0 \ \mathbf{t}_1 \ \cdots \ \mathbf{t}_{i-1} & [0] & [0] & \cdots & [0] \\ \hline & (n-i) \text{ columns} \end{array} \right] \quad (42)$$

where  $[0]$  is the  $6 \times 1$  null matrix and other columns of the Jacobian are of the form

$$\begin{cases} \mathbf{t}_j = \begin{bmatrix} \mathbf{z}_j \times \mathbf{p}_{j,i} \\ \mathbf{z}_j \end{bmatrix} & \text{for joint } j \text{ revolute} \\ \mathbf{t}_j = \begin{bmatrix} \mathbf{z}_j \\ [0] \end{bmatrix} & \text{for joint } j \text{ prismatic} \end{cases}; \quad j = 0, 1, 2, \dots, i-1 \quad (43)$$

with  $[0]$  as the  $3 \times 1$  null matrix.

The robot Jacobian  $J_n$  (or simply the Jacobian  $J$ ) is obtained from Equations (42) and (43) with  $i$  equal to  $n$  (the total number of joints):

$$J(\mathbf{q}) = [\mathbf{t}_0 \ \mathbf{t}_1 \ \cdots \ \mathbf{t}_{n-2} \ \mathbf{t}_{n-1}] \quad (44)$$

and therefore the end-effector linear and angular velocities are obtained from the linear mapping

$$\mathbf{V} = J(\mathbf{q})\dot{\mathbf{q}} \quad (45)$$

Numerical computation of the Jacobian depends on the frame in which the vectors in Equation (43) are expressed. If all vectors are taken in the base frame, the resulting Jacobian matrix denoted by  $J^0$  is represented in the base frame, and so are the absolute velocities of the end-effector from Equation (45). A recursive formulation of  $J^0$  is readily obtained from the recursive formulation of the forward kinematics by adding the following step to the backward loop of Algorithm 1:

$$4. \text{ CALCULATE: } \mathbf{t}_{i-1} = \begin{cases} \begin{bmatrix} a_{i-1,n}^y p_{i-1,n}^z - a_{i-1,n}^z p_{i-1,n}^y \\ a_{i-1,n}^z p_{i-1,n}^x - a_{i-1,n}^x p_{i-1,n}^z \\ a_{i-1,n}^x p_{i-1,n}^y - a_{i-1,n}^y p_{i-1,n}^x \\ a_{i-1,n}^x \\ a_{i-1,n}^y \\ a_{i-1,n}^z \end{bmatrix} & \text{if joint } i-1 \text{ is revolute} \\ \begin{bmatrix} a_{i-1,n}^x \\ a_{i-1,n}^y \\ a_{i-1,n}^z \\ 0 \\ 0 \\ 0 \end{bmatrix} & \text{if joint } i-1 \text{ is prismatic} \end{cases} \quad (46)$$

The absolute velocities of the end-effector can also be expressed in its own frame, with the Jacobian being computed in this frame (denoted by  $J^n$ ). The Jacobian matrix  $J^n$  can be directly obtained from the following formulation:

$$J^n = \begin{bmatrix} R_{0n}^T [0] \\ [0] \\ [0] \end{bmatrix} J^0 \quad (47)$$

As in the forward kinematics problem, a symbolic formulation is recommended for real-time tasks.

### 2.3.2 Link Acceleration

Link accelerations are computed the same way as link velocities. The absolute linear and angular accelerations (i.e., relative to the base coordinate frame) of the link  $i$  coordinate frame are obtained from the absolute accelerations of the link  $i-1$  frame as follows:

for joint  $i$  revolute, i.e.,  $\dot{q}_i = \dot{\theta}_i$  and  $\ddot{q}_i = \ddot{\theta}_i$ ,

$$\begin{aligned} \dot{\mathbf{v}}_i &= \dot{\mathbf{v}}_{i-1} + \dot{\boldsymbol{\omega}}_i \times \mathbf{p}_{i-1,i} + \boldsymbol{\omega}_i \times (\boldsymbol{\omega}_i \times \mathbf{p}_{i-1,i}) \\ \dot{\boldsymbol{\omega}}_i &= \dot{\boldsymbol{\omega}}_{i-1} + \mathbf{z}_{i-1} \dot{q}_i + \boldsymbol{\omega}_i \times (\mathbf{z}_{i-1} \dot{q}_i) \end{aligned} \quad (48)$$

and for joint  $i$  prismatic, i.e.,  $\dot{q}_i = \dot{d}_i$  and  $\ddot{q}_i = \ddot{d}_i$ ,

$$\begin{aligned} \dot{\mathbf{v}}_i &= \dot{\mathbf{v}}_{i-1} + \dot{\boldsymbol{\omega}}_i \times \mathbf{p}_{i-1,i} + \boldsymbol{\omega}_i \times (\boldsymbol{\omega}_i \times \mathbf{p}_{i-1,i}) + \mathbf{z}_{i-1} \ddot{q}_i + 2\boldsymbol{\omega}_i \times (\mathbf{z}_{i-1} \dot{q}_i) \\ \dot{\boldsymbol{\omega}}_i &= \dot{\boldsymbol{\omega}}_{i-1} \end{aligned} \quad (49)$$

The above equations can be written in compact form as

$$\dot{\mathbf{V}}_i = \begin{bmatrix} \dot{\mathbf{v}}_i \\ \dot{\boldsymbol{\omega}}_i \end{bmatrix} = J_i(q_1, q_2, \dots, q_{i-1}) \ddot{\mathbf{q}} + J_i(q_1, \dots, q_{i-1}, \dot{q}_1, \dots, \dot{q}_{i-1}) \dot{\mathbf{q}} \quad (50)$$

### 2.3.3 Singularity

Generally, the link frames velocities corresponding to a particular set of end-effector linear and angular velocities can be obtained from the inverse of the linear mapping (45) as

$$\dot{\mathbf{q}} = J^{-1}(\mathbf{V}) \quad (51)$$

The linear mapping (51) exists only for configurations at which the inverse of the Jacobian matrix exists, i.e., *nonsingular* configurations. In a *singular configuration*, the end-effector cannot move in certain direction(s); thus the manipulator loses one or more degrees of freedom. In a singular configuration, the Jacobian rank decreases, i.e., two or more columns of  $J$  become linearly dependent; thus the determinant of the Jacobian becomes zero. This is a computational test for the existence of singular configurations. Singular configurations should usually be avoided because most of the manipulators are designed for tasks in which all degrees of freedom are required. Furthermore, near sin-

gular configurations the joint velocities required to maintain the desired end-effector velocity in certain directions may become extremely large. The most common singular configurations for 6-d.o.f. manipulators are listed below (Murray, Li, and Sastry, 1994):

1. *Two collinear revolute joint axes* occur in spherical wrist assemblies that have three mutually perpendicular axes intersecting at one point. Rotating the second joint may align the first and third joints, and then the Jacobian will have two linearly dependent columns. Mechanical restrictions are usually imposed on the wrist design to prevent the wrist axes from generating a singularity of the wrist.
2. *Three parallel coplanar revolute joint axes* occur, for instance, in an elbow manipulator (Murray, Li, and Sastry, 1994, p. 90) that consists of a 3-d.o.f. manipulator with a spherical wrist when it is fully extended or fully retracted.
3. *Four revolute joint axes intersecting in one point.*
4. *Four coplanar revolute joints.*
5. *Six revolute joints intersecting along a line.*
6. *A prismatic joint axis perpendicular to two parallel coplanar revolute joints.*

In addition to the Jacobian singularities, the motion of the manipulator is restricted if the joint variables are constrained to a certain interval. In this case, a reduction in the number of degrees of freedom may occur when one or more joints reach the limit of their allowed motion.

#### 2.3.4 Redundant Manipulators and Multiarm Robots

A *kinematically redundant* manipulator is one that has more than the minimum number of degrees of freedom required to attain a desired location. In this case, an infinite number of configurations can be obtained for a desired end-effector location. Multi-arm robots are a special class of redundant manipulators. When two or more robot arms are used to perform a certain task cooperatively, an increased load-carrying capacity and manipulation capability are achieved. For a general redundant manipulator with  $n$  degrees of freedom ( $n > 6$ ), the Jacobian is not square, and there are only  $(n - 6)$  arbitrary variables in the general solution of mapping (51), assuming that the Jacobian is full rank. Additional constraints are needed to limit the solution to a unique one. Therefore, redundancy provides the opportunity for choice or decision. It is typically used to optimize some secondary criteria while achieving the primary goal of following a specified end-effector trajectory. The secondary criteria considered so far in the literature are robot singularity and obstacle avoidance, minimization of joint velocity and torque, increasing the system precision by an optimal distribution of arm compliance, and improving the load-carrying capacity by optimizing the transmission ratio between the input torque and output forces. Hayward (1988) gives a review of the different criteria. As an example, one common approach is to choose the minimum (in the least squares sense) joint velocities that provide the desired end-effector motion. This is achieved by choosing (Hollerbach, 1984)

$$\dot{\mathbf{q}} = J^*(\mathbf{q})\mathbf{V} \quad (52)$$

where

$$J^*(\mathbf{q}) = J^T(JJ^T)^{-1} \quad (53)$$

is the *pseudo-inverse* of the Jacobian matrix.

#### 2.4 Parallel Manipulators

Parallel manipulators are mechanisms that contain two or more serial chains connecting the end-effector to the base. Generally, parallel manipulators can offer more accuracy in positioning and orienting objects than open-chain manipulators. They can also possess a high payload/weight ratio, and they are easily adaptable to position and force control. On the other hand, the workspace of parallel manipulators is usually smaller than that of serial manipulators. A typical configuration of parallel manipulators is the so-called *in-parallel* manipulators, in which each serial chain has the same structure and one joint is actuated in each chain (Duffy, 1996). A popular example of this type is the Stewart platform, shown in Figure 3. The mechanism consists of a rigid plate connected to the base by a set of prismatic joints, each of which is connected to the plate and the base by spherical joints, allowing complete rotational motion. Only the prismatic joints are actuated.

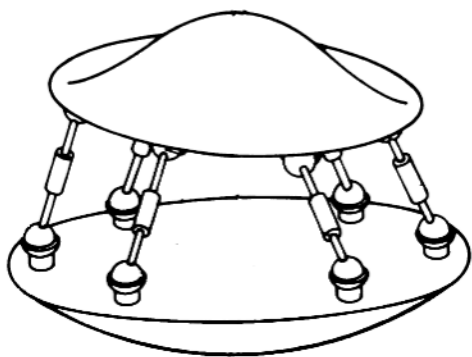


**Figure 3** A general form of the Stewart platform.

The forward kinematics of a parallel manipulator can be expressed by equating the end-effector location to each individual chain. Consider a parallel manipulator with  $m$  chains so that each chain contains  $n_i$  ( $i = 1, 2, \dots, m$ ) joints. The forward kinematics model can then be described as

$$H_{0e} = H_{01}H_{12}^1 \cdots H_{n1,n1}^1 = H_{01}^2H_{12}^2 \cdots H_{n2-1,n2}^2 = \cdots = H_{01}^mH_{12}^m \cdots H_{nm-1,nm}^m \quad (54)$$

where  $H_{ij}^k$  is the homogeneous transformation matrix between joints  $i$  and  $j$  in the chain  $k$ . All quantities are specified with respect to a unique base and end-effector coordinate frame. Equation (54), called the *structure equation*, introduces constraints between the joint displacements of the manipulator. As a result, unlike for serial manipulators, the joint space for a parallel manipulator is not the Cartesian product of the individual joint spaces but a subset of it that satisfies Equation (54). In a parallel manipulator, if  $N$  and  $L$  are the number of joints and links, respectively, and  $l_i$  is the number of degrees of freedom of the  $i^{\text{th}}$  joint, then the number of degrees of freedom of the manipulator can be obtained by taking the total number of degrees of freedom for all links and subtracting the number of constraints imposed by the joints attached to the links. For the specific case where all joints apply independent constraints, the number of degrees of freedom  $F$  can be calculated as

$$F = 6L - \sum_{i=1}^N (6 - l_i) = 6(L - N) + \sum_{i=1}^N l_i \quad (55)$$

The inverse kinematics problem is no more difficult for a parallel manipulator than for the open-chain case, as each chain can be analyzed separately.

The end-effector velocity of a parallel manipulator can be obtained from each chain equivalently:

$$\mathbf{V} = J_1\dot{\mathbf{q}}_1 = J_2\dot{\mathbf{q}}_2 = \cdots = J_m\dot{\mathbf{q}}_m \quad (56)$$

Obviously not all joint velocities can be specified independently. The relationship between joint torques and end-effector forces is more complex in a parallel manipulator than in a serial manipulator, as there are internal interactions between forces produced by the different chains in a parallel manipulator. The reader is referred to more detailed sources, such as Duffy (1996), and open-chain manipulators will be considered in the sequel.

### 3 STATICS

This section discusses the relationship between the forces and moments that act on the manipulator when it is at rest. In open-chain manipulators, each joint is usually driven by an individual actuator. The corresponding input joint torque (for revolute joints) or force (for prismatic joints) is transmitted through the manipulator arm linkages to the end-effector, where the resultant force and moment balance an external load. The relationship between the actuator drive torques (or forces) and the end-effector resultant force and moment is determined using the manipulator Jacobian (Asada and Slotine, 1986):

$$\tau = (J^e)^T \begin{bmatrix} \mathbf{f}_e \\ \mathbf{g}_e \end{bmatrix} = (J^e)^T \mathbf{G}_e \quad (57)$$

where  $\tau \in \mathbb{R}^n$  is the vector of joint torques (and forces) and  $\mathbf{f}_e \in \mathbb{R}^3$  and  $\mathbf{g}_e \in \mathbb{R}^3$  are vectors of the resulting reaction force and moment, respectively, of the external loads acting on the end-effector and expressed in the end-effector frame:

$$\mathbf{f}_e = -\mathbf{f}_{ext}; \quad \mathbf{g}_e = -\mathbf{g}_{ext} \quad (58)$$

The *generalized force*  $\mathbf{G}_e \in \mathbb{R}^6$ , which consists of the force/moment pair, is called the wrench vector.

### 3.1 Duality Between the Velocity Kinematics and Statics

The statics (57) is closely related to the velocity kinematics (45) because the manipulator Jacobian is being used for both mappings. In a specific configuration, the kinematics and statics linear mappings can be represented by the diagram shown in Figure 4 (Asada and Slotine, 1986). For the velocity kinematics, the Jacobian is a linear mapping from the  $n$ -dimensional vector space  $\mathbb{R}^n$  to the six-dimensional space  $\mathbb{R}^6$ . Note that  $n$  (number of joints) can be more than six in the case of redundant manipulators. The range subspace  $R(J)$  represents all possible end-effector velocities that can be generated by the  $n$  joint velocities in the present configuration. If  $n > 6$ , there exists a null space  $N(J)$  of the Jacobian mapping that corresponds to all joint velocity vectors  $\dot{\mathbf{q}}$  that produce no net velocity at the end-effector. In a singular configuration,  $J$  is not full rank, and the subspace  $R(J)$  does not cover the entire vector space  $\mathbb{R}^6$ , i.e., there exists at least one direction in which the end-effector can not be moved.

The statics relationship is also a linear mapping from  $\mathbb{R}^6$  to  $\mathbb{R}^n$  provided by the transpose of the Jacobian. The range subspace  $R(J^T)$  and null subspace  $N(J^T)$  can be identified from the Jacobian mapping. The null subspace  $N(J^T)$  corresponds to the end-effector wrenches that can be balanced without input torques or forces at the joints, as the load is borne entirely by the structure of the arm linkages. For a redundant manipulator, the range subspace  $R(J^T)$  does not cover the entire space  $\mathbb{R}^n$ , and there are some sets of input joint torques or forces that cannot be balanced by any end-effector wrench. These configurations correspond to the null space of the kinematics mapping  $N(J)$  that contains the joint velocity vectors that produce no end-effector motion.

The velocity kinematics and statics are dual concepts that can be stated as follows:

1. In a singular configuration, there exists at least one direction in which the end-effector can not be moved. In this direction, the end-effector wrench is entirely balanced by the manipulator structure and does not require any input joint torque or force.

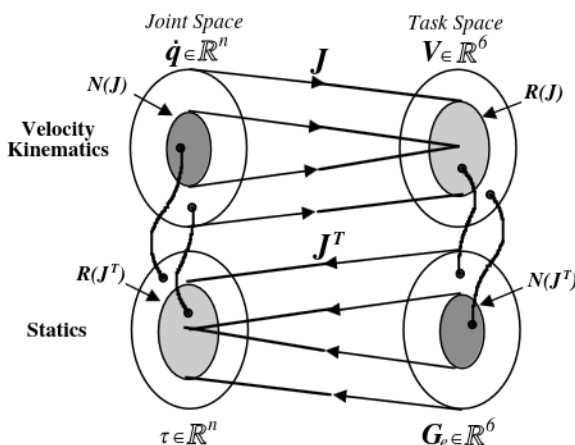


**Figure 4** The duality relation between statics and velocity kinematics linear mappings (from H. Asada and J. J. E. Slotine, *Robot Analysis and Control*. New York: John Wiley & Sons, Inc., 1986).

2. In each configuration of a redundant manipulator, there is at least one direction in which joint velocities produce no end-effector velocity. In this direction, the joint torques and forces cannot be balanced by any end-effector wrench. Therefore, in order to maintain a stationary arm configuration, no input joint torque or force that generates end-effector wrench should be applied.
3. For a general manipulator, in each configuration the directions of possible motion of the end-effector also define the directions in which wrenches that are applied to the end-effector can be entirely balanced by the joint torques and forces.

#### 4 DYNAMICS

The dynamics model describes the balance between internal and external loads applied to the manipulator. The input joint torques and forces generated by the actuators balance the other external forces and moments and the internal loads of the manipulator. The dynamics model is fundamental in mechanical and control system design and simulation of motion and also for real-time control (model-based control). The dynamics of a manipulator with  $n$  degrees of freedom can be expressed using the following equation of motion of each link  $i$  (Spong and Vidyasagar, 1989):

$$\tau_i + [J^T \mathbf{G}_{ext}]_i - N_i(\mathbf{q}, \dot{\mathbf{q}}) = \sum_{j=1}^n M_{ij}(\mathbf{q})\ddot{q}_j + \sum_{k=1}^n \sum_{j=1}^n h_{ijk}(\mathbf{q})\dot{q}_j\dot{q}_k; \quad i = 1, 2, \dots, n \quad (59)$$

The left-hand side of Equation (59) consists of all external forces and moments applied to the  $i^{\text{th}}$  link, which are decomposed into three parts. The first part  $\tau_i$  is the input torque (or force) applied by the actuator of joint  $i$ . The second part  $[J^T \mathbf{G}_{ext}]_i$  is the mapping of the external wrench  $\mathbf{G}_{ext}$  to the joint space, in particular the effect of the external wrench on link  $i$ . The third part  $-N_i(\mathbf{q}, \dot{\mathbf{q}})$  represents any other external force and moment that act on the  $i^{\text{th}}$  link, including gravity torque, friction, etc.

The right-hand side of (59) contains the reaction (internal) loads of the manipulator. The first term represents the inertial load on the  $i^{\text{th}}$  link, while the second term accounts for the Coriolis effect (for  $j \neq k$ ) and centrifugal effect (for  $j = k$ ). The entries  $[M_{ij}]$  of the manipulator inertia matrix are configuration-dependent, and the off-diagonal elements ( $i \neq j$ ) generate the coupling inertial loads. Coriolis and centrifugal terms  $h_{ijk}(\mathbf{q})$  also depend on configuration and introduce further interaction effects in the manipulator dynamics. The components of  $h_{ijk}(\mathbf{q})$  are defined as follows (Spong and Vidyasagar, 1989):

$$h_{ijk} = \frac{\partial M_{ij}}{\partial q_k} - \frac{1}{2} \frac{\partial M_{jk}}{\partial q_i}. \quad (60)$$

Equation (59) can be rewritten in compact form as

$$\tau + J^T \mathbf{G}_{ext} = M(\mathbf{q})\ddot{\mathbf{q}} + C(\mathbf{q}, \dot{\mathbf{q}})\dot{\mathbf{q}} + N(\mathbf{q}, \dot{\mathbf{q}}) \quad (61)$$

where the elements of matrix  $C$  are defined as

$$C_{ij}(\mathbf{q}, \dot{\mathbf{q}}) = \sum_{k=1}^n h_{ijk}\dot{q}_k \quad i, j = 1, 2, \dots, n \quad (62)$$

The matrices  $M$  and  $C$  express the inertial characteristics of the manipulator and have the following important properties (Spong and Vidyasagar, 1989):

1.  $M(\mathbf{q})$  is symmetric and bounded positive definite.
2.  $(M - 2C) \in \mathbb{R}^{n \times n}$  is a skew-symmetric matrix.

These properties are useful in reducing the number of operations in the calculation of the dynamics model, and they are also used in proofs of stability of many control laws for robot manipulators.

The manipulator dynamics model can be used in two modes:

1. To simulate the motion of the manipulator (joint displacements, velocities, and accelerations) for given input joint torques and forces; this is referred to as the *forward dynamics* problem

2. To calculate the joint torques and forces required to attain specific joint displacements, with given velocities and accelerations; this is called the *inverse dynamics* problem.

The computational algorithms of the above dynamics problems and related considerations are discussed in the sequel.

## 4.1 Inverse Dynamics

### 4.1.1 The Recursive Algorithm and Computational Considerations

Given the joint displacements, velocities, and accelerations, the joint torques can be directly computed from Equation (61). However, since at each trajectory point the configuration-dependent coefficients  $M$ ,  $C$ , and  $N$  must be computed, the amount of computation required is extremely high, and it increases very rapidly as the number of degrees of freedom  $n$  increases. Calculating Equation (61) requires  $(32n^4 + 86n^3 + 171n^2 + 53n - 128)$  multiplications and  $(25n^4 + 66n^3 + 129n^2 + 42n - 96)$  additions, or more than 100,000 arithmetic operations for a 6-d.o.f. manipulator. This heavy computational load is a bottleneck for the use of the inverse dynamics model in real-time control, especially since the calculation would have to be repeated at the rate of 60 Hz or higher.

If the dynamics equations are formulated in a *recursive* form, the computational complexity can be significantly reduced from  $O(n^4)$  to  $O(n)$  so that the required number of operations would vary linearly with the number of degrees of freedom. Most of the fast algorithms for the inverse dynamics problem are based on the Newton–Euler approach, and consist of two main steps. In the first step, the angular velocity and acceleration of each link of the manipulator and the linear velocity and acceleration of its center of mass are calculated starting with the first link and continuing through the last. In the second step, the force and moment exerted on each link are calculated backward starting from the last link. Furthermore, if the dynamic equations are expressed in a tensor form and tensor properties are used, the computational complexity of the inverse dynamics algorithm can be further reduced. Algorithm 2 presents an efficient inverse dynamics formulation that requires  $(104n - 77)$  multiplications and  $(92n - 70)$  additions for computing the joint torques or forces for each trajectory point. The basic formulation of this algorithm was originally developed in Balafoutis, Patel, and Misra (1988). Although this algorithm is not the fastest available formulation, it is simple and effective for real-time implementations. See He and Goldenberg (1990) for more details on computational considerations.

While the current recursive formulations are quite efficient, symbolic closed-form equations derived for a particular manipulator are likely to be the most efficient formulation (Burdick, 1986). If symbolic operations are used simplified formulations can easily be obtained for real-time applications.

## 4.2 Forward Dynamics

In forward dynamics, joint displacements and velocities are obtained as a result of applied joint torques (forces) and other external forces and moments. From Equation (61), given the current joint positions and velocities and the current external wrenches, the vector of joint accelerations can be calculated. From this calculation the corresponding joint velocities and positions are computed by subsequent integrations. In this way, the problem of forward dynamics is divided into two phases:

**Phase 1** Obtain joint accelerations from Equation (61).

**Phase 2** Integrate the joint accelerations and obtain the new joint velocities; then integrate again and obtain the new joint displacements.

In Phase 2 any suitable numerical integration method can be used. In Phase 1 the following form of Equation (61) is used:

$$M(\mathbf{q})\ddot{\mathbf{q}} = [C(\mathbf{q}, \dot{\mathbf{q}})\dot{\mathbf{q}} + N(\mathbf{q}, \dot{\mathbf{q}}) - J^T \mathbf{G}_{ext}] - \boldsymbol{\tau} \quad (63)$$

Phase 1 can be performed by completing the following three steps:

**Step 1.1.** Calculate the elements of  $[C(\mathbf{q}, \dot{\mathbf{q}})\dot{\mathbf{q}} + N(\mathbf{q}, \dot{\mathbf{q}}) - J^T \mathbf{G}_{ext}]$

**Step 1.2.** Calculate the elements of the inertia matrix  $M(\mathbf{q})$ .

**Step 1: Forward Kinematics**

OBTAİN link rotation matrices  $R_{i-1,i}$  for  $i = 1, 2, \dots, n$   
SET  $R_{n,n+1} = [I]_{3 \times 3}$

**Step 2: Initialization**

SET  $\begin{cases} \omega_0 = \dot{\omega}_0 = \mathbf{v}_0 = [0 \ 0 \ 0]^T; \ \dot{\mathbf{v}}_0 = -\mathbf{g}_e; \ \ddot{\omega}_0 = [0]_{3 \times 3} \\ \mathbf{f}_{n+1} = -\mathbf{f}_{ext}; \ \mathbf{g}_{n+1} = -\mathbf{g}_{ext}; \ m_i; \ I_{ci}; \ \mathbf{p}_{ci} \end{cases}$

**Step 3: Forward Loop**

FOR  $i = 1$  to  $n$

CALCULATE:  $\begin{cases} \begin{cases} \omega_i = R_{i-1,i}^T(\omega_{i-1} + [0 \ 0 \ \dot{q}]^T) \\ \dot{\omega}_i = R_{i-1,i}^T(\dot{\omega}_{i-1}[0 \ 0 \ \dot{q}]^T + [0 \ 0 \ \ddot{q}]^T) \end{cases} & \text{if joint } i \text{ is revolute} \\ \begin{cases} \omega_i = R_{i-1,i}^T \omega_{i-1} \\ \dot{\omega}_i = R_{i-1,i}^T \dot{\omega}_{i-1} \end{cases} & \text{if joint } i \text{ is prismatic} \end{cases}$

SET:  $\tilde{\omega}_i = \begin{bmatrix} 0 & -\omega_i^x & \omega_i^y \\ \omega_i^x & 0 & -\omega_i^z \\ -\omega_i^y & \omega_i^z & 0 \end{bmatrix}; \ \tilde{\dot{\omega}}_i = \begin{bmatrix} 0 & -\dot{\omega}_i^x & \dot{\omega}_i^y \\ \dot{\omega}_i^x & 0 & -\dot{\omega}_i^z \\ -\dot{\omega}_i^y & \dot{\omega}_i^z & 0 \end{bmatrix}$

CALCULATE:  $\begin{cases} \begin{cases} \mathbf{v}_i = \tilde{\omega}_i + \tilde{\dot{\omega}}_i \tilde{\omega}_i \\ \dot{\mathbf{v}}_i = R_{i-1,i}^T(\dot{\mathbf{v}}_{i-1} + \Omega \mathbf{p}_{i-1}) \\ \ddot{\mathbf{v}}_i = R_{i-1,i}^T(\ddot{\mathbf{v}}_{i-1} + \Omega_i \mathbf{p}_{i-1,i} + 2\tilde{\omega}_i[0 \ 0 \ \dot{q}]^T + [0 \ 0 \ \ddot{q}]^T) \end{cases} & \text{if joint } i \text{ is revolute} \\ \begin{cases} \mathbf{v}_{ci} = \dot{\mathbf{v}}_i + \omega \mathbf{p}_{ci} \\ \tilde{g}_{ci} = -(\Omega_i \mathbf{f}_{ci}) + (\Omega_i \mathbf{f}_{ci})^T \\ \mathbf{f}_{ci} = m_i \ddot{\mathbf{v}}_{ci} \end{cases} & \text{if joint } i \text{ is prismatic} \end{cases}$

SET:  $\mathbf{g}_{ci} = [-\tilde{g}_{ci}(1, 2) \ \tilde{g}_{ci}(1, 3) \ -\tilde{g}_{ci}(2, 3)]^T$

NEXT  $i$

**Step 4: Backward Loop**

FOR  $i = n$  to  $1$

SET:  $\tilde{P}_{i-1,i} = \begin{bmatrix} 0 & -p_{i-1,i}^z & p_{i-1,i}^y \\ p_{i-1,i}^z & 0 & -p_{i-1,i}^x \\ -p_{i-1,i}^y & p_{i-1,i}^x & 0 \end{bmatrix}; \ \tilde{P}_{ci} = \begin{bmatrix} 0 & -p_{ci}^z - p_{i-1,i}^z & p_{ci}^y + p_{i-1,i}^y \\ p_{ci}^z + p_{i-1,i}^z & 0 & -p_{ci}^x - p_{i-1,i}^x \\ -p_{ci}^y - p_{i-1,i}^y & p_{ci}^x + p_{i-1,i}^x & 0 \end{bmatrix}$

CALCULATE:  $\begin{cases} \mathbf{f}_i = R_{i,i+1} \mathbf{f}_{i+1} + \mathbf{f}_{ci} \\ \mathbf{g}_i = R_{i,i+1} \mathbf{g}_{i+1} + \mathbf{g}_{ci} + \tilde{P}_{ci} \mathbf{f}_{ci} + \tilde{P}_{i+1,i} \mathbf{f}_{i+1} \end{cases}$

CALCULATE:  $\begin{cases} \tau_i = [0 \ 0 \ 1] R_{i-1,i} \mathbf{g}_i & \text{if joint } i \text{ is revolute} \\ \tau_i = [0 \ 0 \ 1] R_{i-1,i} \mathbf{f}_i & \text{if joint } i \text{ is prismatic} \end{cases}$

NEXT  $i$

**Algorithm 2** Tensor recursive formulation of the inverse dynamics problem.

**Step 1.3.** Solve the set of simultaneous linear equations (63) for  $\ddot{\mathbf{q}}$ .

Step 1.1 can be directly computed using an inverse dynamics algorithm with the joint accelerations set to zero. If the inverse dynamics algorithm is represented (Walker, 1985) as the function

$$\tau = INV DYN(\mathbf{q}, \dot{\mathbf{q}}, \ddot{\mathbf{q}}, \dot{\mathbf{v}}_0, \mathbf{G}_{ext}) \quad (64)$$

then Step 1.1 can be performed as

$$[C(\mathbf{q}, \dot{\mathbf{q}})\ddot{\mathbf{q}} + N(\mathbf{q}, \dot{\mathbf{q}}) - J^T \mathbf{G}_{ext}] = INV DYN(\mathbf{q}, \dot{\mathbf{q}}, 0, \dot{\mathbf{v}}_0, \mathbf{G}_{ext}) \quad (65)$$

Using the inverse dynamics algorithm, the complexity of this step is  $O(n)$ .

The computation of the matrix  $M$  can also be performed using the inverse dynamics formulation. First  $\dot{\mathbf{q}}$ ,  $\ddot{\mathbf{v}}_0$  and  $\mathbf{G}_{ext}$  are set to be zero. Then the  $i^{\text{th}}$  column of  $M$ , denoted by  $[M]_i$ , can be obtained by setting the joint acceleration in the inverse dynamics algorithm to be  $\ddot{\mathbf{d}}_i$  which is a vector with all elements equal to zero except for the  $i^{\text{th}}$  element being equal to one. Thus

$$[M]_i = \text{INV DYN}(\mathbf{q}, 0, \ddot{\mathbf{d}}_i, 0, 0) \quad i = 1, 2, \dots, n \quad (66)$$

By repeating this procedure for  $n$  columns of  $M$ , the entire inertia matrix is obtained. This step requires  $n$  applications of the inverse dynamics with the order of complexity  $O(n)$ .

$M$  and the right-hand side of Equation (63) having been computed, the final step is to solve the set of simultaneous linear equations for  $\ddot{\mathbf{q}}$ . The order of complexity of this step is  $O(n^3)$ , thus making the order of complexity of the overall forward dynamics algorithm  $O(n^3)$ . The symmetry and positive definiteness of  $M$  can be exploited in Step 1.2 to calculate only the lower triangle of the matrix and in Step 1.3 to use specialized factorization techniques in order to improve the computational efficiency of the algorithm (Featherstone, 1987). New and efficient algorithms have recently been suggested (Lilly, 1993).

## 5 CONCLUSIONS

This chapter presents basic kinematics, statics, and dynamics modeling algorithms. These questions have been addressed extensively in the literature, but the approach taken here attempts to extract only the fundamentals needed by a reader wishing to obtain a complete set of tools to generate models of robot manipulators. The tools suggested could be computerized without great effort, and they could be useful in the design of new manipulators or workcells, the analysis of existing manipulators, simulations, and real-time control. The procedures and algorithms suggested here are considered the most computationally effective for fulfilling the basic tasks of modeling.

Some of the issues discussed are not commonly encountered in the literature. For example, the use of screw theory and products of exponentials in kinematics modeling, and even symbolic formulations in kinematics and dynamics modeling, have limited applicability, but can be very effective.

Further study is needed to investigate the numerical accuracy and robustness of inverse kinematics and forward dynamics calculations. In particular, there are strong indications that model-based control is more effective; thus incorporation of kinematics and dynamics models into real-time control is recommended. The computational overhead resulting from this methodology requires extensive work to minimize the number of arithmetic operations and to exploit parallel processing. In addition, the accuracy of on-line calculations must be addressed. In a different direction, special-configuration manipulators not describable as standard open-loop kinematic chains must also be investigated and specific models generated for them.

## REFERENCES

- Asada, H., and J. J. E. Slotine. 1986. *Robot Analysis and Control*. New York: John Wiley & Sons.
- Balafoutis, C. A., R. V. Patel, and P. Misra. 1988. "Efficient Modeling and Computation of Manipulator Dynamics Using Orthogonal Cartesian Tensors." *IEEE Journal of Robotics and Automation* 4(6), 665–676.
- Brockett, R. W. 1983. "Robotic Manipulators and Product of Exponentials Formula." In *Proceedings of International Symposium of Mathematical Theory of Networks and Systems*, Beer Sheba, Israel.
- Burdick, J. W. 1986. "An Algorithm for Generation of Efficient Manipulator Dynamic Equations." In *Proceedings of the 1986 IEEE International Conference on Robotics and Automation*, San Francisco, 212–218.
- Ceccarelli, M. 1994. "Determination of the Workspace Boundary of a General n-Revolute Manipulator." In *Advances in Robot Kinematics and Computational Geometry*. Ed. A. J. Lenarcic and B. B. Ravani. Dordrecht: Kluwer Academic. 39–48.
- Denavit, J., and R. S. Hartenberg. 1965. "A Kinematic Notation for Low-Pair Mechanisms Based on Matrices." *ASME Journal of Applied Mechanics* (June), 215–221.
- Duffy, J. 1980. *Analysis of Mechanisms and Manipulators*. New York: John Wiley & Sons.
- . 1996. *Statics and Kinematics with Applications to Robotics*. Cambridge: Cambridge University Press.
- Featherstone, R. 1987. *Robot Dynamics Algorithms*. Dordrecht: Kluwer Academic.

- Ghasvini, M. 1993. "Reducing the Inverse Kinematics of Manipulators to the Solution of a Generalized Eigenproblem." In *Computational Kinematics*. Ed. J. Angeles, G. Hommel, and P. Kovacs. Dordrecht: Kluwer Academic. 15–26.
- Hayward, V. 1988. "An Analysis of Redundant Manipulators from Several Viewpoints." In *Proceedings of the NATO Advanced Research Workshop on Robots with Redundancy: Design Sensing and Control*, Salo, Italy, June 27–July 1.
- He, X., and A. A. Goldenberg. 1990. "An Algorithm for Efficient Manipulator Dynamic Equations." *Journal of Robotic Systems* 7, 689–702.
- Ho, C. Y., and J. Sriwattanathamma. 1989. "Symbolically Automated Direct Kinematics Equations Solver for Robotic Manipulators." *Robotica* 7, 243–254.
- Hollerbach, J. M. 1984. "Optimal Kinematic Design for a Seven Degree of Freedom Manipulator." Paper presented at International Symposium of Robotics Research, Kyoto.
- . 1989. "A Survey of Kinematic Calibration." In *The Robotics Review I*. Ed. I. Khatib, J. J. Craig, and T. Lozano-Pérez. Cambridge: MIT Press.
- Kohli, D., and M. Osvatic. 1992. "Inverse Kinetics of General 4R2P, 3R3P, 4R1c, 4R2C, and 3C Manipulators." *Proceedings of 22nd ASME Mechanisms Conference*, Scottsdale, DE. Vol. 45. 129–137.
- Lee, H. Y., and C. G. Liang. 1988. "Displacement Analysis of the General Spatial 7-link 7R Mechanism." *Mechanism and Machine Theory* 23, 219–226.
- Lilly, K. W. 1993. *Efficient Dynamic Simulation of Robotic Mechanisms*. Dordrecht: Kluwer Academic.
- Manocha, D., and J. F. Canny. 1994. "Efficient Inverse Kinematics for General 6R Manipulators." *IEEE Transactions on Robotics and Automation* 10(5), 648–657.
- Mavroidis, C., and B. Roth. 1994. "Structural Parameters Which Reduce the Number of Manipulator Configurations." *Journal of Mechanical Design* 116, 3–10.
- Murray, R. M., Z. Li, and S. S. Sastry. 1994. *A Mathematical Introduction to Robotic Manipulation*. London: CRC Press. Chapter 3.
- Park, F. C., and K. Okamura. 1994. "Kinematic Calibration and the Product of Exponentials Formula." In *Advances in Robot Kinematics and Computational Geometry*. Ed. A. J. Lenarcic and B. B. Ravani. Dordrecht: Kluwer Academic. 119–128.
- Pieper, D. L., and B. Roth. 1969. "The Kinematics of Manipulators under Computer Control." In *Proceedings of 2nd International Congress for the Theory of Machines and Mechanisms*, Zakopane, Poland. Vol. 2. 159–168.
- Raghavan, M., and B. Roth. 1993. "Inverse Kinematics of the General 6R Manipulator and Related Linkages." *Transactions of the ASME* 115, 502–508.
- Ruoff, C. 1981. "Fast Trigonometric Functions for Robot Control." *Robotics Age* (November).
- Salmon, G. 1964. *Lessons Introductory to the Modern Higher Algebra*. New York: Chelsea.
- Selfridge, R. G. 1989. "Analysis of 6-Link Revolute Arms." *Mechanism and Machine Theory* 24(1), 1–8.
- Spong, M. W., and M. Vidyasagar. 1989. *Robot Dynamics and Control*. New York: John Wiley & Sons.
- Turner, T., J. Craig, and W. Gruver. 1984. "A Microprocessor Architecture for Advanced Robot Control." Paper presented at 14th ISIR, Stockholm, October.
- Vukobratovic, M., and M. Kircanski. 1986. *Kinematics and Trajectory Synthesis of Manipulation Robot*. New York: Springer-Verlag. 53–77.
- Walker, M. W. 1985. "Kinematics and Dynamics." In *Handbook of Industrial Robots*. 1st ed. Ed. S. Y. Nof. New York: John Wiley & Sons. Chapter 6.
- Wampler, C., and A. P. Morgan. 1991. "Solving the 6R Inverse Position Problem Using a Generic-Case Solution Methodology." *Mechanisms and Machine Theory* 26(1), 91–106.
- Westmacott, G. D. 1993. "The Application of Symbolic Equation Manipulation to High Performance Multibody Simulation." In *Robotics: Applied Mathematics and Computational Aspects*. Ed. Kevin Warwick. Oxford: Oxford University Press. 527–540.
- Whitney, D. E. 1969. "Resolved Motion Rate Control of Manipulators and Human Prostheses." *IEEE Transactions on Man-Machine Systems* MMS-10(2), 47–53.
- Wilkinson, J. H. 1959. "The Evaluation of the Zeros of Ill-Conditioned Polynomials, Parts I and II." *Numerical Methods* 1, 150–180.
- Yuan, M. S. C., and F. Freudentstein. 1971. "Kinematic Analysis of Spatial Mechanisms by Means of Screw Coordinates, Part 1—Screw Coordinates." *Transactions of the ASME* 93, 61–66.

# CHAPTER 7

---

## ROBOT HANDS AND END-EFFECTORS

Kazuo Tanie

Mechanical Engineering Laboratory  
AIST-MITI  
Tsukuba, Japan

### 1 INTRODUCTION

The robot hand is a tool that enables robots to interact with environments. It is expected to perform tasks like a human hand. The objective of the interaction is generally to execute a required task through applying actions to a task environment. Because it can be considered a tool for creating an effect on the environment and is generally located at an end of a robotic arm, it is often called an *end-effector*. One of the best ways of making a good robot end-effector would be to develop a hand like a human hand, which has five fingers that can move dexterously and perform various complex tasks. However, such a hand requires complex mechanisms and control algorithms, causing development difficulties and increases in cost. Robots in industrial applications are often required to handle only limited shapes of objects or parts and do limited kinds of tasks. For these requirements, human-like hands are not economical. Various types of single-purpose hands with simple grasping function or task-oriented tools are commonly used instead. A device to handle only limited shapes of objects is sometimes called a *gripper* or *gripping device*. In some applications simplification of gripping function is more important than the limited versatility and dexterity of such devices. In other applications handling and manipulating many different objects of varying weights, shapes, and materials is required, and an end-effector that has complex functions will be more suitable. This type of end-effector is called a *universal hand*. Extensive research is currently being carried out on the design and manipulation of universal hands, but to date few practical versions exist.

This chapter describes several kinds of end-effectors in practical use and discusses recent developments in universal hands and their control algorithms. The chapter also explains the practical implementation and design criteria of end-effectors. Gripper selection is explained in Chapter 48.

### 2 CLASSIFICATION OF END-EFFECTORS

End-effectors have several variations, depending on the many ways in which they are required to interact with environments in carrying out required tasks. This brings about an increasing number of mechanisms used to design end-effectors and the functions installed in them. End-effectors can also be designed using several kinds of actuators if actively controlled elements are needed. This causes more variations to be developed. This section discusses the classifications of end-effectors based on the functions installed. The next section describes drive systems.

In general, end-effectors can be classified by function as follows:

1. Mechanical hands
2. Special tools
3. Universal hands

The most common tasks given to end-effectors involve grasping functions. The tool for grasping—that is, a hand—is thus the most commonly used. *Class I* refers to hands with fingers whose shape cannot be actively controlled. The fingers in such a hand are generally

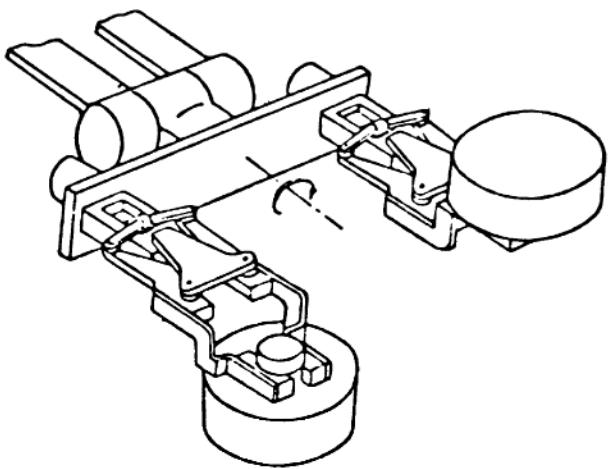


Figure 1 Multihand system.

unjointed and have a fixed shape designed specifically for the object to be handled. Class 1 devices are less versatile and less dexterous than class 3 devices, but more economical to produce. Finer classifications of class 1 can be made, using, for example, the number of fingers. Two-, three-, and five-finger types exist. For industrial applications the two-finger hand is the most popular. Three- and five-finger hands, with some exceptions, are customarily used for prosthetic hands for amputees. Another classification is by the number of hands—single or multiple—mounted on the wrist of the robot arm. Multihand systems (Figure 1) enable effective simultaneous execution of more than two different jobs. Design methods for each individual hand in a multihand system are subject to those for single hands. Another classification, by mode of grabbing, is between external and internal systems. An external gripper (Figure 2) grasps the exterior surface of objects with closed fingers, whereas an internal gripper (Figure 3) grips the internal surface of objects with open fingers. There are two finger-movement classifications: translational finger hands and swinging finger hands. Translational hands can move their own fingers, keeping them parallel. Swinging hands employ a swinging motion of the fingers. Another classification is by the number of degrees of freedom (d.o.f.) implemented in hand structures. Typical mechanical hands are classified as 1 d.o.f. A few hands have more than 2 d.o.f.

Class 2 refers to special-purpose devices for specific tasks. Vacuum cups and electromagnets are typical devices in this class. In some applications the objects to be handled may be too large or thin for a hand to grasp them. In such cases a special tool suitable for holding the object has a great advantage over the other types of device. Also, in some applications it will be more efficient to install a specific tool according to the required

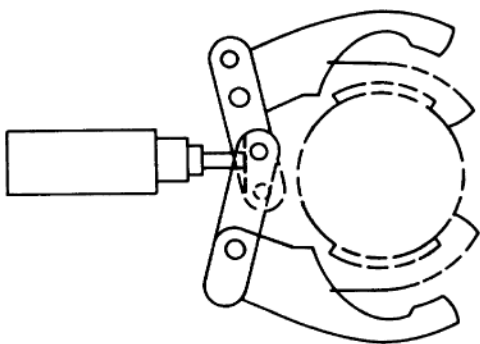
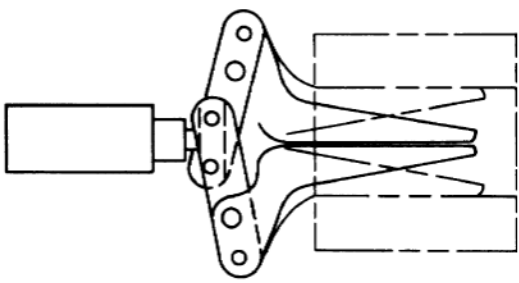


Figure 2 External gripper.



**Figure 3** Internal gripper.

task. Spot welders for spot welding, power drills for drilling, paint sprayers for spray-painting, and so on are popularly used as end-effectors for industrial robots.

*Class 3* is composed of multipurpose hands with usually more than three fingers and /or more than one joint on each finger, providing the capability of performing a wide variety of grasping and manipulative assignments. To develop this type of hand, however, many problems must be solved in the design of mechanisms and controls. Currently several mechanical designs have been proposed for universal hands, some of which are commercially available, and several efficient control algorithms for stable grasp and manipulation have been proposed, though not many applications have been found.

The following sections describe the three end-effector classes.

### 3 ACTUATOR SYSTEM FOR END-EFFECTORS

In robot systems three kinds of drive methods are practically available: pneumatic, electric, and hydraulic. Actuators are mainly used in hand-type end-effectors.

Pneumatic drive can be found in end-effectors of almost all industrial robots. The main actuator systems in pneumatic drive are the cylinder and motor. They are usually connected to on/off solenoid valves that control their direction of movement by electric signal. For adjusting the speed of actuator motion, airflow regulation valves are needed. A compressor is used to supply air (maximum working pressure  $10 \text{ kg/cm}^2$ ) to actuators through valves. The pneumatic system has the advantage of being less expensive than other methods, which is the main reason that many industrial robots use it. Another advantage of the pneumatic system derives from the low stiffness of the air-drive system. This feature of the pneumatic system can be used effectively to achieve compliant grasping, which is one of the most important functions of the hand: it refers to grasping objects with delicate surfaces carefully. On the other hand, the relatively limited stiffness of the system makes precise position control difficult. Air servo-valves are being developed for this purpose. However, they increase the cost and result in some loss of economic advantage of the air drive.

The electric system is also popular. There are typically three kinds of actuators: DC motor, AC motors, and stepping motors. AC motors are becoming more popular because of brushless structure, which reduces the maintenance cost and makes the system applicable to tasks in combustible environments. In general, each motor requires appropriate reduction gear systems to provide proper output force or torque. Direct-drive torque motors (DDMs) are commercially available, but their large size makes designing compact systems difficult. Few robot hands use DDM. In the electric system a power amplifier is also needed to provide a complete actuation system. Electric drive has several benefits:

1. A wide variety of products are commercially available.
2. Constructing flexible signal-processing and control systems becomes very easy because they can be controlled by electric signals, enabling the use of computer systems as control devices.
3. Electric drive can be used for both force and position control.

Drawbacks of the electric system are that it is somewhat more expensive than the pneumatic system and has less power generation and less stiffness than the hydraulic system.

The hydraulic drives used in robot systems are electrohydraulic drive systems. A typical hydraulic drive system consists of actuators, control valves, and power units. There

are three kinds of actuators in the system: piston cylinder, swing motor, and hydraulic motor. To achieve position control using electric signals, electrohydraulic conversion devices are available. For this purpose electromagnetic or electrohydraulic servo-valves are used. The former provides on/off motion control, and the latter provides continuous position control. Hydraulic drive gives accurate position control and load-invariant control because of the high degree of stiffness of the system. On the other hand, it makes force control difficult because high stiffness causes high pressure gain, which has a tendency to make the force control system unstable. Another claimed advantage of hydraulic systems is that the ratio of the output power per unit weight can be higher than in other systems if high pressure is supplied. This drive system has been shown to provide an effective way of constructing a compact high-power system.

Other than the preceding three types of drive, there are a few other drive methods for hand type end-effector. One method uses a springlike elastic element. A spring is commonly used to guarantee automatic release action of gripping mechanisms driven by pneumatic or hydraulic systems. Figure 4 shows a spring-loaded linkage gripping mechanism using a pneumatic cylinder (Sheldon, 1972). Gripping action is performed by means of one-directional pneumatic action, while the spring force is used for automatic release of the fingers. This method considerably simplifies the design of the pneumatic or hydraulic circuit and its associated control system. The spring force can also be used for grasping action. In this case, because the grasping force is influenced by the spring force, to produce a strong grasping force a high-stiffness spring is necessary. This usually causes the undesirable requirement of high-power actuators for the release action of the fingers. Therefore the use of spring force for grasping action is limited to low-grasping-force gripping mechanisms for handling small machine parts such as pins, nuts, and bolts. The spring force can be used for a one-directional motion of the pneumatic and the hydraulic actuator because the piston can be moved easily by the force applied to the output axis (piston rod). The combination of a spring and electric motor is not viable because normal electric motors include a high reduction gear system which makes it difficult to transmit the force inversely from the output axis.

Another interesting method uses electromagnets. The electromagnet actuator consists of a magnetic head constructed with a ferromagnetic core, conducting coil, and actuator rod made of ferrous materials. When the coil is activated, the magnetic head attracts the actuator rod, and the actuator displacement is locked at a specified position. When the coil is not activated, the actuator rod can be moved freely. This type of actuator is usually employed with a spring and produces two output control positions. Figure 5 shows a hand using the electromagnetic drive. The electromagnetic actuator 1 produces the linear motion to the left along the L-L line. The motion is converted to grasping action through the cam 2. The releasing action is performed by the spring 3. The actuator displacement that this kind of actuator can make is commonly limited to a small range because the

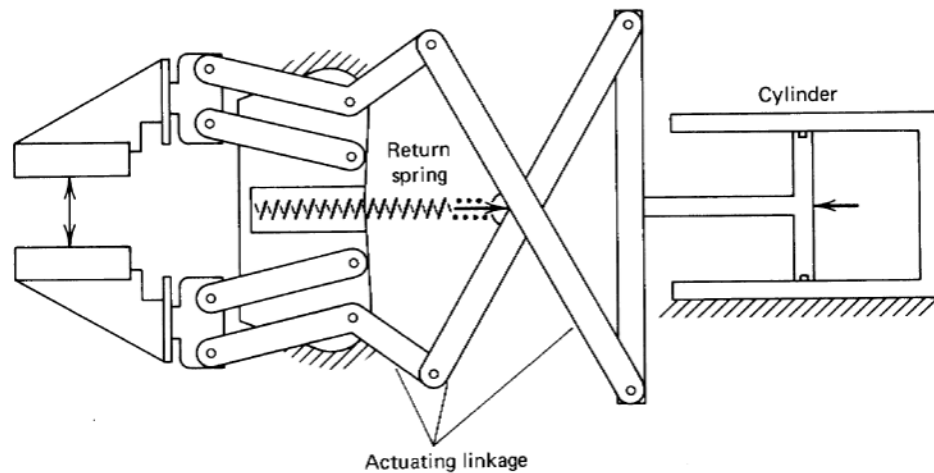
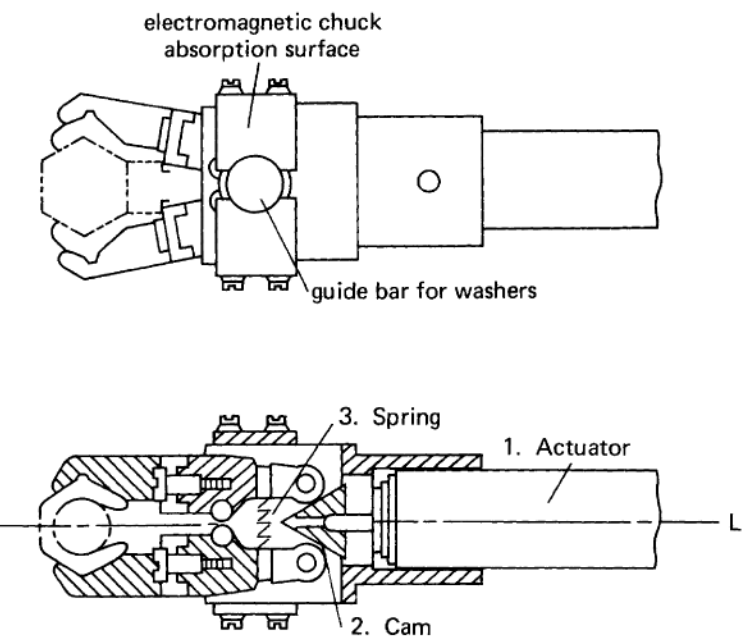


Figure 4 Spring-loaded linkage gripper (courtesy Dow Chemical Co., Ltd.).



**Figure 5** Hand using an electromagnetic drive (courtesy Seiko-seiki Co., Ltd.).

force produced by the magnetic head decreases according to the increase of the actuator displacement. This drive method can therefore be effectively used only for gripping small workpieces.

In the design of effective robotic end-effectors, the selection of drive system is very important. Selection depends on the jobs required of the robot. Briefly, if an end-effector has some joints that need positional control, the electric motor is recommended. If force-control function is needed at some joints—for example, to control grasping force—electric or pneumatic systems are recommended. If high power is needed, the hydraulic drive is recommended.

#### 4 MECHANICAL HANDS

Human-hand grasping is divided into six different types of prehension (Schlesinger, 1919): palmar, lateral, cylindrical, spherical, tip, and hook. See Figure 6. Crossley and Umholts (1977) classified manipulation functions by the human hand into nine types: trigger grip, flipping a switch, transfer pipe to grip, use cutters, pen screw, cigarette roll, pen transfer, typewrite, and pen write. Human hand can perform various grasping functions using five fingers with joints. In designing a hand, a subset of the types of human grasp and hand manipulation is considered, according to the required task. To achieve minimum grasping function, a hand needs two fingers connected to each other using a joint with 1 d.o.f. for its open–close motion. If the hand has two rigid fingers, it has the capability of grasping only objects of limited shapes and is not able to enclose objects of various shapes. Also, this type of hand cannot have manipulation function because all degrees of freedom are used to maintain prehension. There are two ways to improve the capability for accommodating the change of object shapes. One solution is to put joints on each finger that can move according to the shape of the grasped object. The other is to increase the number of fingers. The manipulation function also emerges from this design. To manipulate objects the hand must usually have more fingers and joints driven externally and independently than does the hand designed for grasping objects. The more fingers, joints, and degrees of freedom the hand has, the more versatile and dexterous it can be. With this principle in mind, the type of hand can be selected and the mechanical design considered.

Several kinds of grasping functions described above can be realized using various mechanisms. From observation of the usable pair elements in gripping devices, the following kinds, among others, have been identified (Chen, 1982): linkage, gear-and-rack,

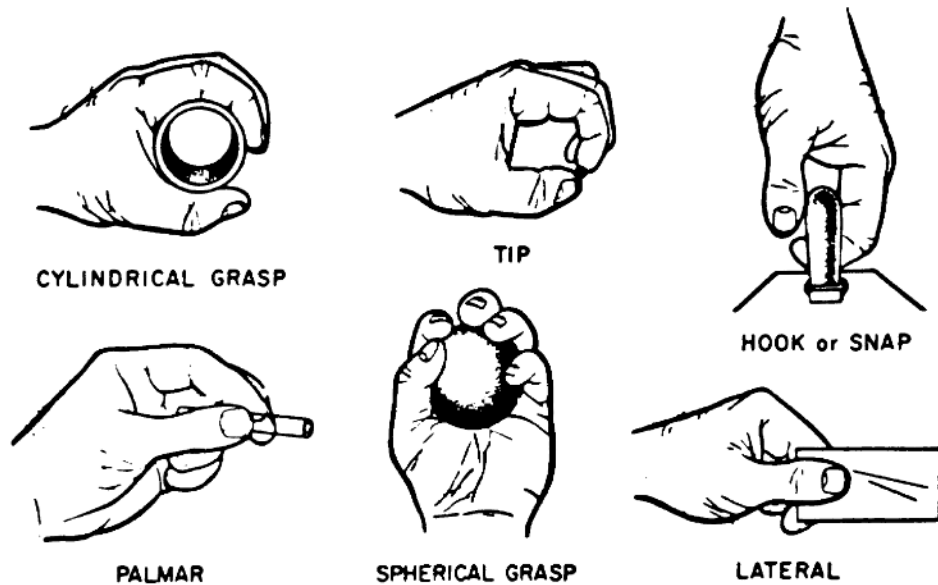


**Figure 6** The various types of hand prehension. (From G. Schlesinger, *Der Mechanische Aufbau der künstlichen Glieder*, Part 2 of *Ersatzglieder und Arbeitshilfen*. Berlin: Springer, 1919.)

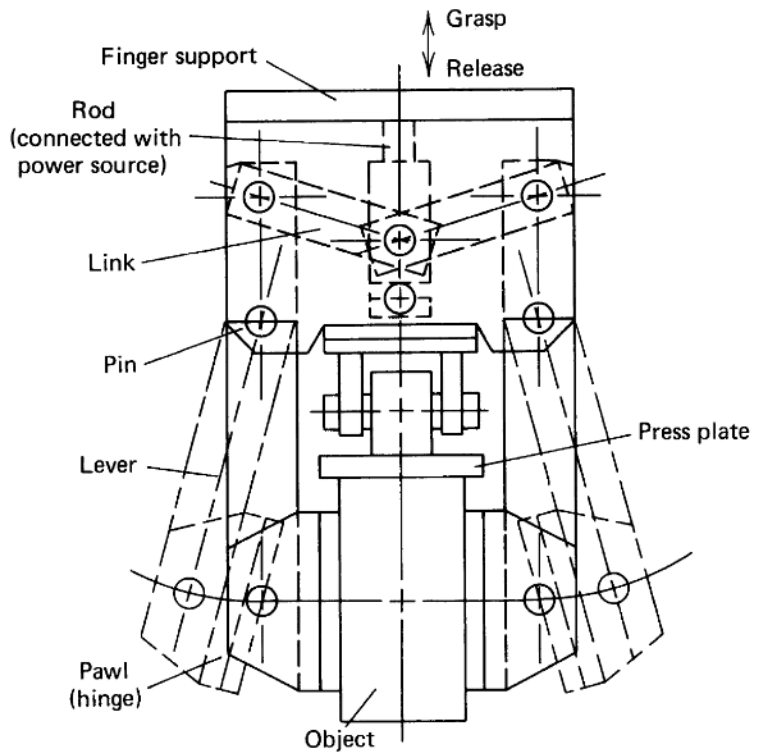
cam, screw, and cable and pulley. The selection of these mechanisms is affected by the kind of actuators and grasping modality to be used. Many hand mechanisms have been proposed. The following sections explain the hand mechanisms in practical use. Chen (1982) lists other possible hand mechanisms.

#### 4.1 Mechanical Hands with Two Fingers

##### 4.1.1 Swinging Gripping Mechanisms

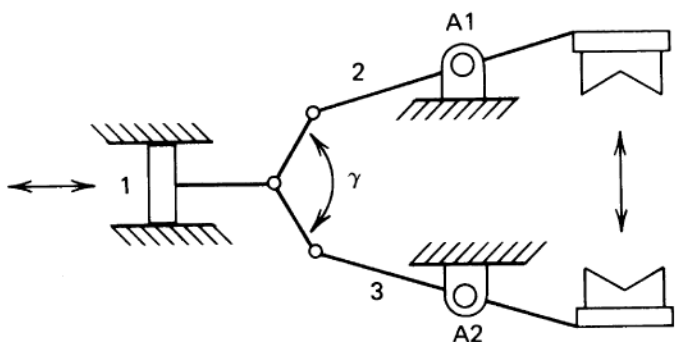
One of the most popular mechanical hands uses the swinging gripping mechanism. The hand has the swing motion mechanism in each finger. It is useful for grasping objects of limited shape, especially cylindrical workpieces. Figure 7 shows a typical example of such a hand. This type of hand is driven by linear motion actuator, such as a pneumatic cylinder, because it uses a slider-crank mechanism. The design of the mechanism that makes the finger swing motion will depend on the type of actuator used. If actuators are used that produce linear movement, such as pneumatic or hydraulic piston cylinders, the device contains a pair of slider-crank mechanisms. Figure 8 shows a simplified drawing of a pair of slider-crank mechanisms commonly used in hands with pneumatic or hydraulic piston cylinder drive. When the piston 1 is pushed by hydraulic or pneumatic pressure to the right, the elements in the cranks 2 and 3 rotate counterclockwise with the fulcrum A1 and clockwise with the fulcrum A2, respectively, when  $\gamma$  is less than  $180^\circ$ . These rotations make the grasping action at the extended end of the crank elements 2 and 3. The releasing action can be obtained by moving the piston to the left. The motion of this mechanism has a dwell position at  $\gamma = 180^\circ$ . For effective grasping action,  $\gamma = 180^\circ$  must be avoided. An angle  $\gamma$  ranging from  $160^\circ$  to  $170^\circ$  is commonly used. Figure 9 shows another example of a mechanism for a hand with swing finger motion that uses a piston cylinder and two swing-block mechanisms. The sliding rod 1, actuated by a pneumatic or a hydraulic piston, transmits motion by way of the two symmetrically arranged swinging-block linkages 1-2-3-4 and 1-2-3'-4' to grasp or release the object by means of the subsequent swinging motions of links 4 and 4' at their pivots A1 and A2.

Figure 10 shows a typical example of a hand with swing motion fingers using a rotary actuator in which an actuator is placed at the cross point of the two fingers. Each finger is connected to the rotor and the housing of the actuator, respectively. The actuator movement directly produces grasping and releasing actions. This type of hand includes a revolutionary pair mechanism, which is schematically illustrated in Figure 11a. According



**Figure 7** Hand with swing motion mechanisms (courtesy Yasukawa Electric Mfg. Co., Ltd.).

to the different types of actuator used instead of the rotary actuator, there are several variations in this type of hand. Two are shown in Figure 11b and c. Figure 11b uses a cylinder–piston actuator instead of a rotary actuator. Figure 11c shows a hand that uses a cam to convert the linear piston motion to the grasping–releasing action. An application example of this mechanism has been shown in Fig. 5. Figure 12a shows a cross-four-bar link mechanism with two fulcrums, A and B. This mechanism is sometimes used to make a finger-bending motion. Figure 12b shows a typical example of a finger constructed with the cross-four-bar link. There are two ways of activating this mechanism. First, a rotary actuator can be used at point A or B to rotate the element AD or BC. The actuator movement produces the rotation of the link element CD, which produces a bending motion of the finger. Second, a slider-crank mechanism activated by a cylinder piston can



**Figure 8** Schematic of a pair of slider-crank mechanisms.

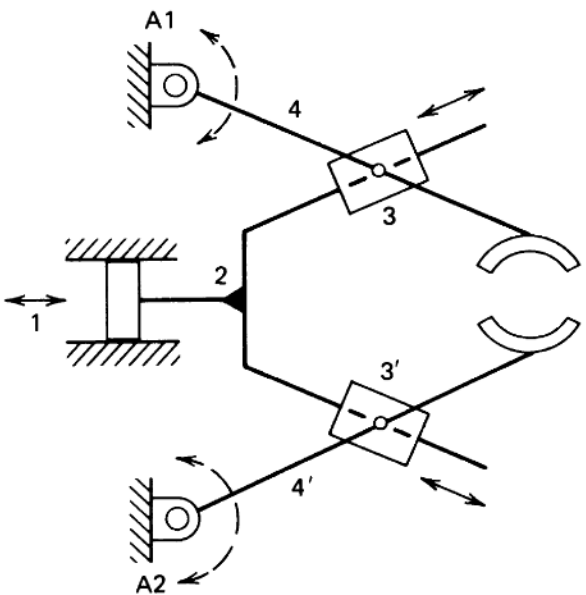


**Figure 9** Schematic of swing-block mechanism.

be used to rotate the element AD or BC. The lower illustration in Figure 12b depicts this type of drive. The finger-bending motion can be obtained in the same way as with rotary actuators. The use of a cross-four-bar link offers the capability of enclosing the object with the finger. This mechanism can be used for a hand that has more than two fingers.

#### 4.1.2 Translational Hand Mechanisms

The translational mechanism is another popular gripping mechanism widely used in hands for industrial robots. It enables the finger to be closed and opened without the attitude being changed. The mechanism is usually somewhat more complex than the swinging type. The simplest translational hand uses the direct motion of the piston–cylinder type actuator. Figure 13 shows such a hand using a hydraulic or pneumatic piston cylinder.

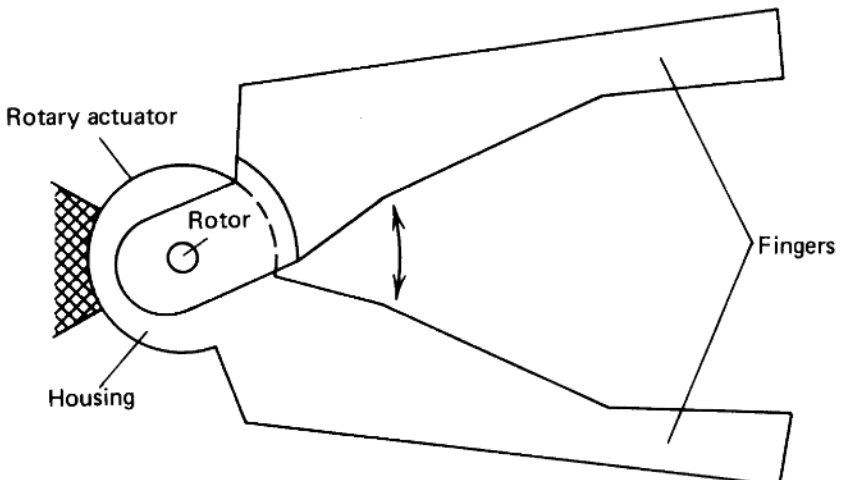


**Figure 10** Hand using a rotary actuator.

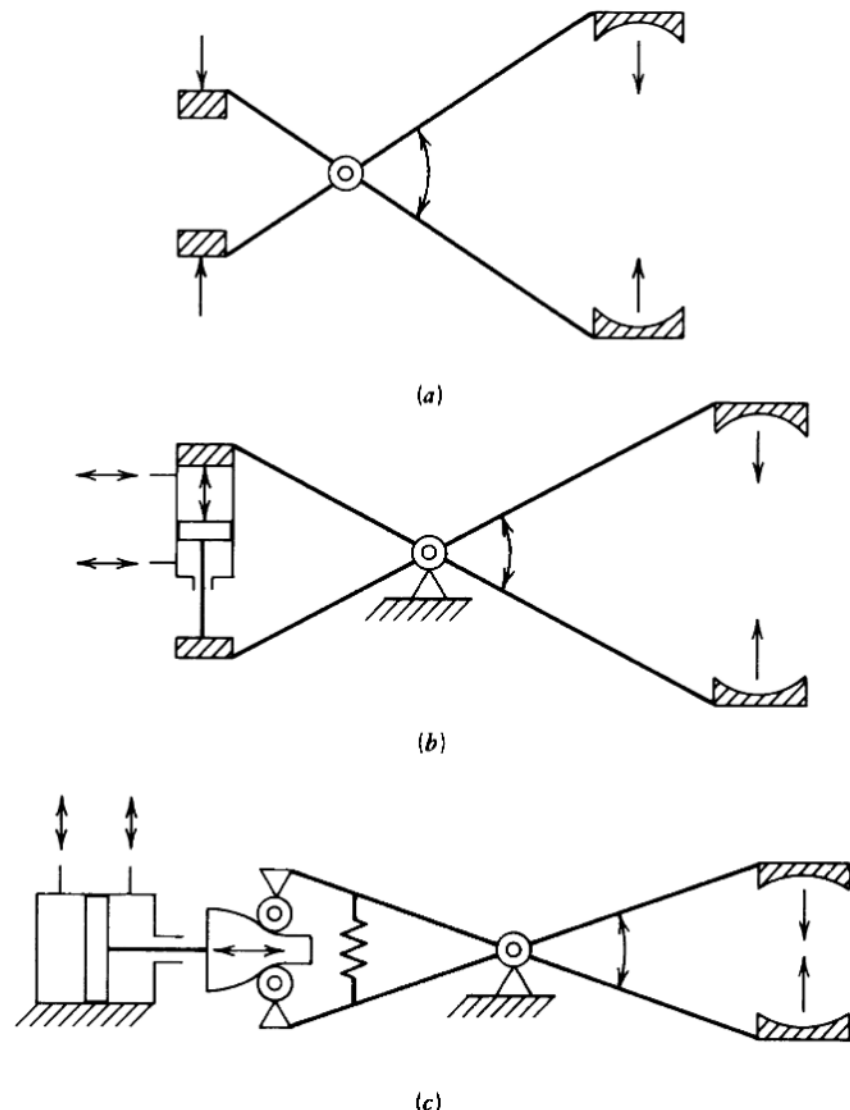


**Figure 11** (a) Hand mechanism that includes a revolute pair. (b) Hand using a revolute pair and a piston cylinder. (c) Hand using a cam and a piston cylinder.

As depicted in the figure, the finger motion corresponds to the piston motion without any connecting mechanisms between them. The drawback of this approach is that the actuator size determines the size of the hand, which sometimes makes it difficult to design the desired size of hand, though it is suitable for the design of wide-opening translational hands. Figure 14 shows a translational hand using a pneumatic or hydraulic piston cylinder, which includes a dual-rack gear mechanism and two pairs of the symmetrically arranged parallel-closing linkages. This is a widely used translational hand mechanism. The pinion gears are connected to the elements A and A', respectively. When a piston rod moves toward the left, the translation of the rack causes the two pinions to rotate clockwise and counterclockwise, respectively, and produces the release action, keeping each finger direction constant. The grasping action occurs when the piston rod moves to the right in the same way. There is another way to move the parallel-closing linkages in Figure 14. Figure 15 shows a mechanism using a rotary actuator and gears in lieu of the

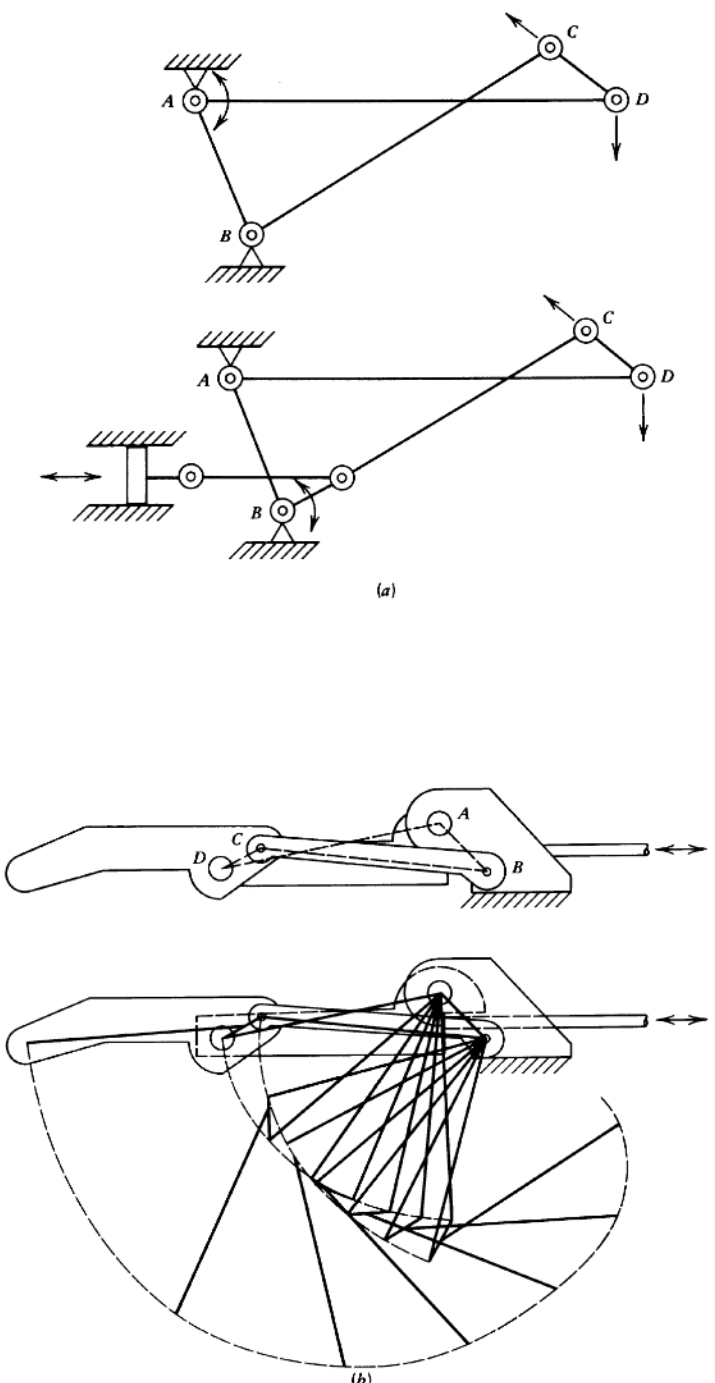


**Figure 12** (a) Schematic of cross-four-bar link mechanism. (b) A finger using cross-four-bar link mechanism.

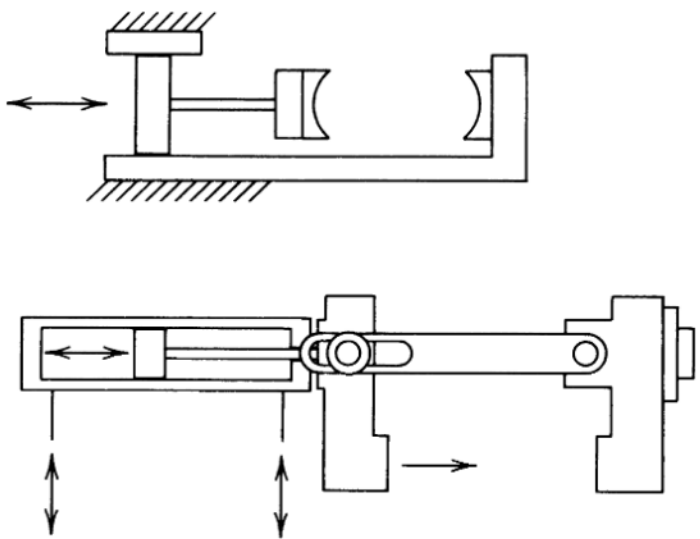


**Figure 13** Translational hand using a cylinder piston.

combination of a piston cylinder and two racks in Figure 14. Figure 16 shows two other examples of translational hand mechanism using rotary actuators. Figure 16a consists of an actuator and rack-and-pinion mechanism. The advantage of this hand is that it can accommodate a wide range of dimensional variations. Figure 16b includes two sets of ball-screw mechanisms and an actuator. This type of hand enables accurate control of finger positions.

#### 4.1.3 Single-Action Hand

Where fewer actuators are installed in the hand than the hand has fingers, each finger cannot be moved independently. This is true of most of the hands reviewed above. For

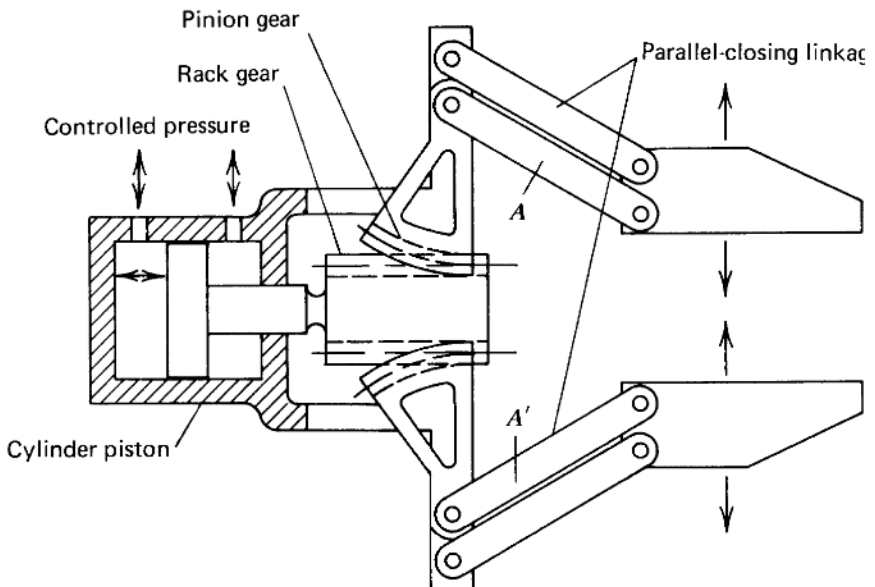


**Figure 14** Translational hand including parallel-closing linkages driven by a cylinder piston and a dual-rack gear.

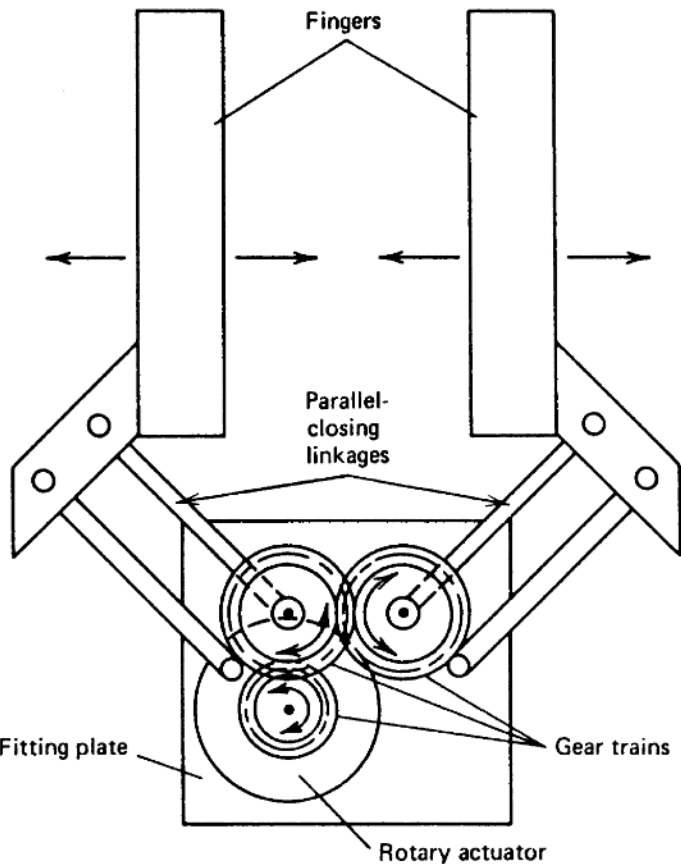


**Figure 15** Translational hand including parallel-closing linkages driven by a rotary actuator and gears.

example, the mechanical hand shown in Figure 8 has only one actuator used to move two fingers. Figure 13 shows a hand with one stationary finger or fixed finger and one moving finger, commonly referred to as a *single-action* hand. When this kind of hand picks up an object rigidly fixed on the base, the hand must be exactly position-controlled to the position that will allow the two fingers to touch the surface of the part to be grasped with one actuator motion. Otherwise, coordinated motion of robot arm and fingers will be needed. The use of a hand in which each finger can be driven by an independent actuator will avert such a situation, but such a hand increases the cost. To reach a compromise solution, some precautions will generally be required in the task environment. A method of making the part to be handled free to move during pickup or release is often introduced.

#### 4.1.4 Consideration of Finger Configuration

##### **Design of Object-Shaped Cavity**

When rigid fingers are used, the finger configuration must be contrived to accommodate the shape of the object to be handled. For grasping the object tightly, object-shaped cavities on the contact surface of the finger, as shown in Figure 17a, are effective. A cavity is designed to conform to the periphery of the object of a specified shape. For example, if cylindrical workpieces are handled, a cylindrical cavity should be made. A finger with this type of cavity can grasp single-size workpieces more tightly with a wider contact surface. However, such a structure will limit the hand's ability to accommodate change in the dimension of an object to be handled. Versatility can be slightly improved

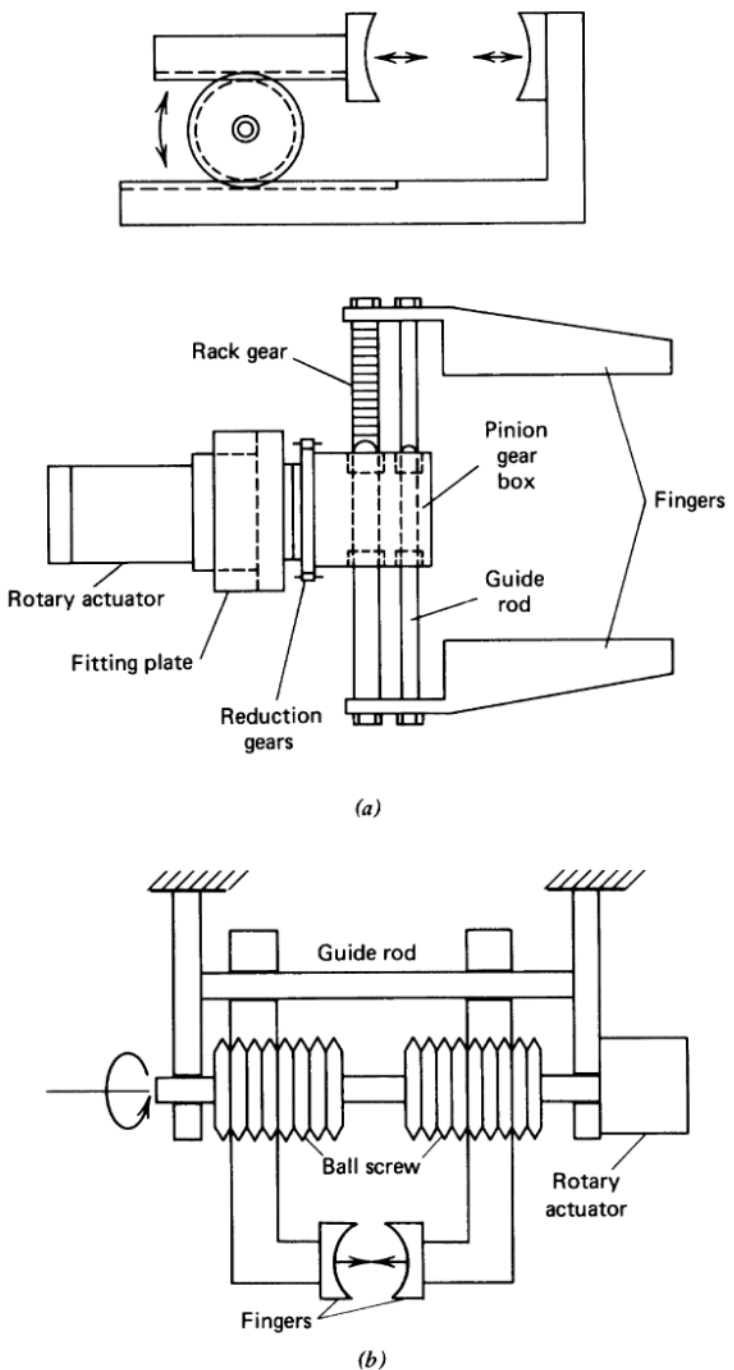


**Figure 16** (a) A translational hand operated by a rotary actuator with rack-and-pinion mechanism (courtesy Tokiko Co., Ltd.). (b) A translational hand using a rotary actuator and ball-screw mechanism.

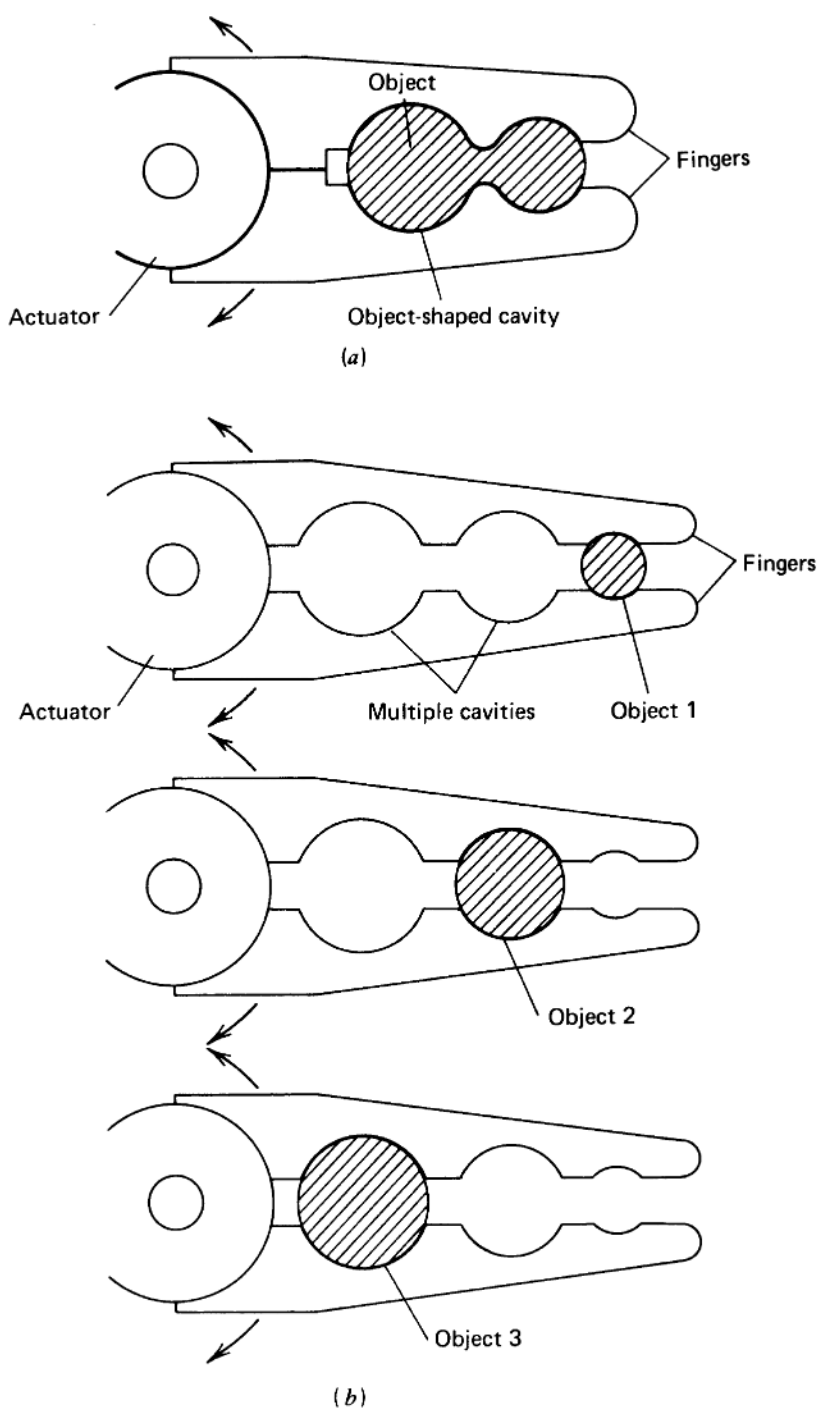
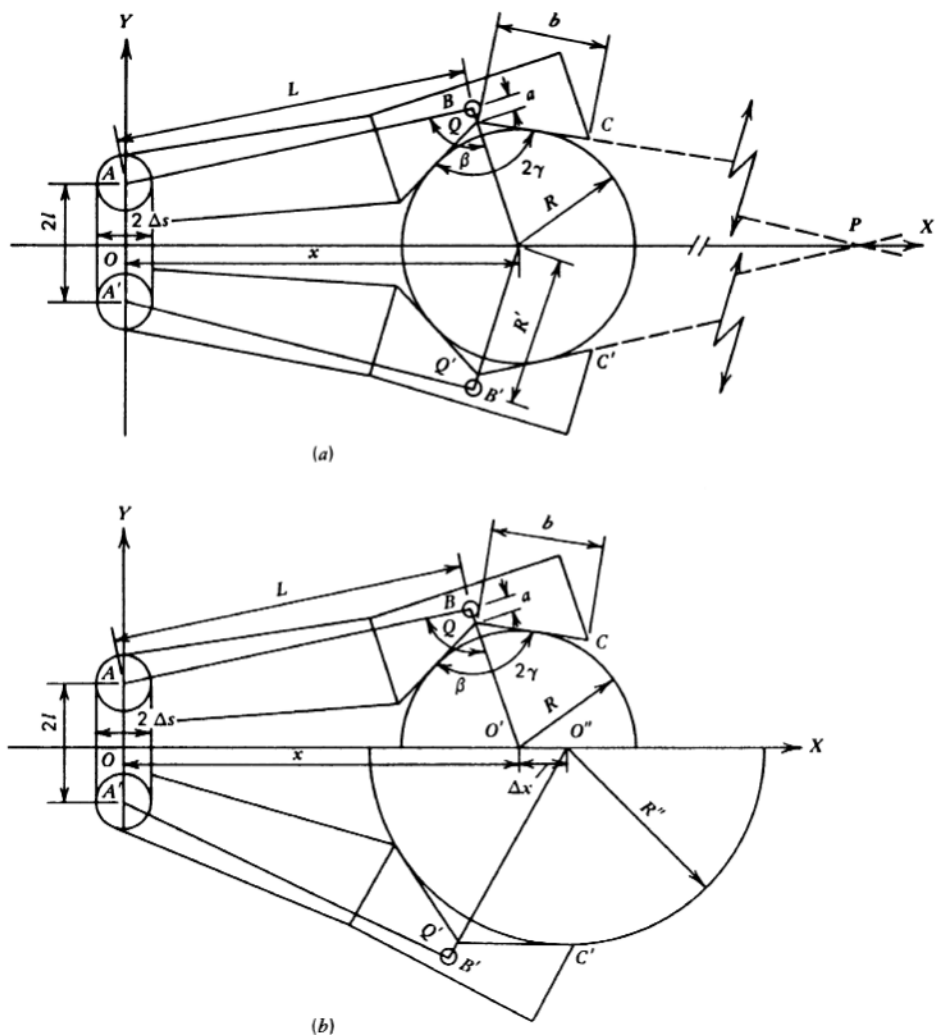


Figure 17 (a) Finger with an object-shaped cavity. (b) Finger with multiple object-shaped cavities.

by the use of a finger with multiple cavities for objects of differing size and shape. Figure 17b shows examples of fingers with multiple cavities.

### Design of V-Shaped Cavity

In manufacturing, many tasks involve cylindrical workpieces. For handling cylindrical objects, a finger with a V-shaped cavity instead of an object-shaped cavity may be adopted. Each finger contacts the object at two spots on the contact surface of the cavity during the gripping operation. The two-spot contact applies a larger grasping force to a limited surface of the grasped object and may sometimes distort or scratch the object. However, in many tasks this problem is not significant, and this device has great advantages over a hand with object-shaped cavities. One advantage is that it can accommodate a wide range of diameter variations in the cylindrical workpiece, allowing the shape of the cavity to be designed independent of the dimensions of the cylindrical object. Another advantage is that it is easier to make, resulting in reduced machinery costs. Figure 18a shows a typical geometrical configuration of a grasping system for a cylindrical object using a V-shaped cavity finger hand. Some relation exists between the configuration pa-



**Figure 18** (a) Geometrical configuration of grasping system for a cylindrical object using two-finger hand with a V-shaped cavity. (b) The deviation of center position of grasped objects.

rameters of the V-shaped cavity and the diameter of possible cylindrical workpieces to be grasped (Osaki and Kuroiwa, 1969). Suppose that parameters of the grasping system  $\gamma$ ,  $\beta$ ,  $R$ ,  $R'$ ,  $L$ ,  $a$ , and  $b$ , symbols  $B$ ,  $C$ ,  $Q$ ,  $B'$ ,  $C'$ ,  $Q'$ , and  $O'$ , and the coordinate system  $O-xy$  are defined as shown in the figure. Since the cylindrical workpiece grasped and the hand construction cannot intersect, the following inequality is obtained:

$$x - R < \Delta s \quad (1)$$

where  $\Delta s$  is the  $\frac{1}{2}$  width of the hand element and  $x$  is the distance between the center of cylindrical workpiece and the origin  $O$ , as shown in Figure 18a. The distance  $x$  is expressed by the following equation:

$$x = \sqrt{\left[ L^2 + \left( \frac{R}{\sin \gamma} + a \right)^2 - 2L \left( \frac{R}{\sin \gamma} + a \right) \cos \beta \right] - l^2} \quad (2)$$

In the swinging-type hand, the hand will be often designed so that  $\beta$  is a constant value. If  $\beta = 90^\circ$ , as it generally is, Equation (2) becomes

$$x = \sqrt{L^2 + \left( \frac{R}{\sin \gamma} + a \right)^2 - l^2} \quad (3)$$

In a translational hand in which each cavity block is kept parallel to every other is used, i.e.,  $\angle BO'O = 90^\circ$ , the following equation can be obtained:

$$\cos \beta = \frac{R' - l}{L} \quad \left( R' = \frac{R}{\sin \gamma} + a \right) \quad (4)$$

After substitution of Equation (4) into Equation (2),  $x$  can be expressed by the following:

$$x = \sqrt{L^2 - \left( \frac{R}{\sin \gamma} + a - l \right)^2} \quad (5)$$

For the object to contact each finger at the two spots on the surface of the cavity,  $D$ ,  $\gamma$ , and  $b$  must satisfy the following inequality:

$$D < 2b \tan \gamma \quad (6)$$

where  $D$  is the diameter of the cylindrical object and equals  $2R$ . If the swinging gripper is assumed, another condition must be considered because the longitudinal direction of each finger varies with objects of differing size. To hold an object safely in the hand without slippage, the extended line  $QC$  must cross the extended line  $Q'C'$  at point P in front of the hand. From this constraint, the upper diameter limit of the object that can be grasped by the hand is expressed with some parameters of the cavity as follows:

$$D < 2 \sin \gamma \cdot \left[ L \cdot \tan \left( \frac{\pi}{2} - \gamma \right) + \frac{l}{\tan(\pi/2 - \gamma)} \right] \quad (7)$$

In the special case in which  $l = 0$ , as in Figure 10, Equation (7) becomes

$$D < 2 \sin \gamma \cdot L \tan \left( \frac{\pi}{2} - \gamma \right) \quad (8)$$

If the translational hand is used, inequalities (7) or (8) can be ignored because the attitudes of the finger and the V-shaped cavity are kept constant. Equations (1), (6), (7), and (8) provide the basic parameter relations to be considered when the V-shape cavity is designed. The other consideration in designing the V-shape cavity is that the  $x$  coordinate of the center of the cylindrical object varies with the diameter. This can be recognized from Equations (2), (3), and (5). Figure 18b explains the deviation ( $O'O'' = \Delta x$ ) of the center positions of two different-sized objects grasped by a hand. The deviation

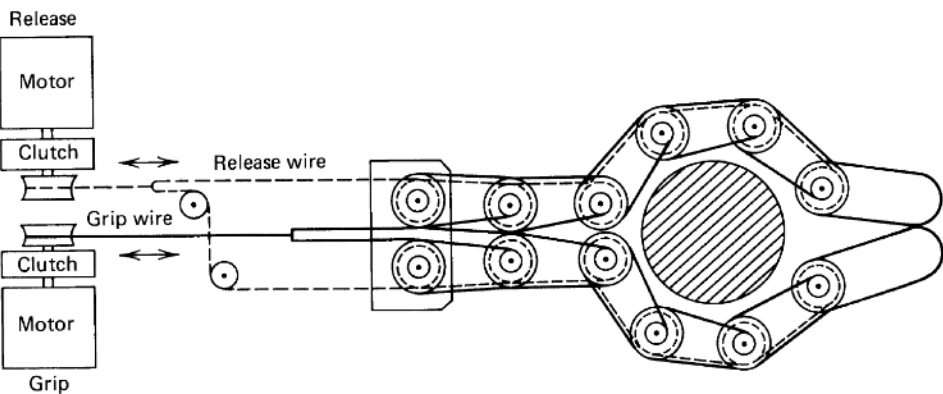


**Figure 19** The soft gripper. (From S. Hirose and Y. Umetani, "The Development of a Soft Gripper for the Versatile Robot Hand," in *Proceedings of the Seventh International Symposium on Industrial Robots*, Tokyo, 1977, 353–360.)

will be undesirable for some tasks. The reduction must be considered (Osaki and Kuroiwa, 1969). The deviation is generally smaller if a translational hand is used than if a swinging hand is used, if fingers of the same size are employed. A well-designed translational hand using a rack-and-pinion or ball-screw mechanism, as shown in Figure 16, can make the deviation almost zero. The hand shown in Figure 13 yields the same effect. For a swinging hand, longer fingers will help to reduce the deviation.

#### Soft-Gripping Mechanism

To provide the capability to completely conform to the periphery of objects of any shape, a soft-gripping mechanism has been proposed. See Figure 19 (Hirose and Umetani, 1977). The segmental mechanism is schematically illustrated in Figure 20. The adjacent links and pulleys are connected with a spindle and are free to rotate around it. This mechanism is manipulated by a pair of wires, each of which is driven by an electric motor with gear reduction and clutch. One wire, called the *grip wire*, produces the gripping movement. The other, the *release wire*, pulls antagonistically and produces the release movement from the gripping position. When the grip wire is pulled against the release wire, the

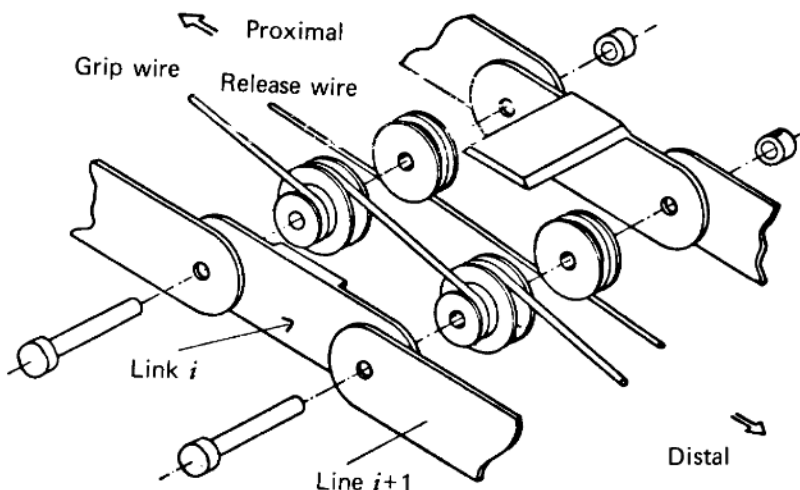


**Figure 20** Segmental mechanism of the soft gripper. (From S. Hirose and Y. Umetani, "The Development of a Safe Gripper for the Versatile Robot Hand," in *Proceedings of the Seventh International Symposium on Industrial Robots*, Tokyo, 1977, 353–360.)

finger makes a bending motion from the base segment. During this process of wire traction, the disposition of each finger's link is determined by the mechanical contact with an object. When the link  $i$  makes contact with an object and further movement is hindered, the next link,  $(i + 1)$ , begins to rotate toward the object until it makes contact with the object. This results in a finger motion conforming to the peripheral shape of the object. In this system it is reported that the proper selection of pulleys enables the finger to grasp the object with uniform grasping pressure.

#### 4.1.5 Calculation of Grasping Force or Torque

The maximum grasping force or grasping torque is also an important specification in hand design. The actuator output force or torque must be designed to satisfy the conditions the task will require. How hard the hand should grasp the object depends on the weight of the object, the friction between the object and the fingers, how fast the hand is expected to move, and the relation between the direction of the hand movement and the attitude of the object grasped. In the worst case, the direction of the gravity and the acceleration force vectors applied to the grasped object are parallel to the grasp surface of the fingers. Then friction alone must hold the object. This situation is thus assumed in evaluating the maximum grasping force or grasping torque. After the maximum grasping force or torque has been determined, the force or torque that the actuator must generate can be considered. The calculation of those values requires the conversion of the actuator output force or torque to the grasping force or torque, which depends on the kind of actuators and mechanisms employed. Table 1 shows the relation between the actuator output force or torque and the grasping force for the hand with various kinds of mechanisms and actuators.

### 4.2 Mechanical Hands with Three or Five Fingers

#### 4.2.1 Three-Finger Hand

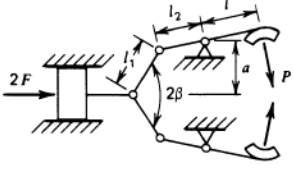
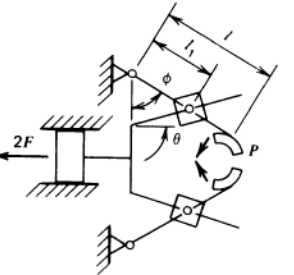
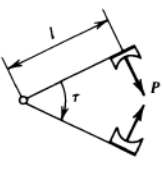
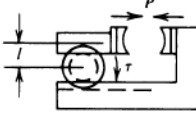
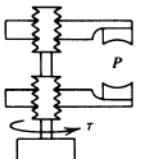
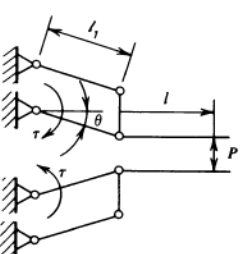
Increasing the number of fingers and degrees of freedom will greatly improve the versatility of the hand, but will also complicate the design process. The design methods for three-finger hands are not yet well established from the practical point of view. However, several examples have been developed, mainly for experimental or research uses. The simplest example is a hand with three fingers and one joint driven by an appropriate actuator system.

The main reason for using the three-finger hand is its capability of grasping the object in three spots, enabling both a tighter grip and the holding of spherical objects of differing size while keeping the center of the object at a specified position. Three-point chuck mechanisms are typically used for this purpose (see Figure 21). Each finger motion is performed using a ball-screw mechanism. Electric motor output is transmitted to screws attached to each finger through bevel gear trains that rotate the screws. When each screw is rotated clockwise or counterclockwise, the translational motion of each finger will be produced, resulting in the grasping-releasing action. Figure 22 shows another three-finger hand with the grasping-mode switching system (Skinner, 1974). This includes four electric motors and three fingers and can have four grasping modes, as shown in Figure 23, each of which can be achieved by the finger-turning mechanism. All fingers can be bent by motor-driven cross-four-bar link mechanisms, and each finger has one motor. The finger-turning mechanism is called a *double-dwell* mechanism, as shown in Figure 24 (Skinner, 1974). Gears that rotate the fingers are shown, and double-headed arrows indicate the top edge of the finger's bending planes for each prehensile mode. This mechanism transfers the state of the hand progressively from three-jaw to wrap to spread to tip prehension. The gears for fingers 2 and 3 are connected to the motor-driven gear directly, whereas the gear for finger 1 is connected to the motor-driven gear through a coupler link. Rotating the motor-driven gear in three-jaw position, finger 1 rotates, passes through a dwell position, and then counterrotates to reach the wrap position. Similarly, finger 1 is rotated out of its spread position but is returned as the mechanism assumes tip prehension. Finger 2 is rotated counterclockwise 60° from its three-jaw position to the wrap position, then counterclockwise 120° into the spread position, then counterclockwise 150° into the tip position. Finger 3 rotates through identical angles but in a clockwise direction. A multi-prehension system of this type is effective for picking up various-shaped objects.

#### 4.2.2 Five-Finger Hand

A small number of five-finger hands have been developed, with only a few for industrial use. Almost all are prosthetic hands for amputees. In the development of prosthetic arms, cosmetic aspects are more important to the mental state of the disabled than functions.

**Table 1** Relations Between the Actuator Output Force or Torque and The Grasping Force

Type of Gripper Mechanism and Configuration Parameters	Relations between Actuator Output and Grasping force
	$IP = I_2 \left[ \tan \beta \sqrt{1 - \left( \frac{l_1 \sin \beta - a}{l} \right)^2} - \frac{l_1 \sin \beta - a}{l} \right] \cdot F$
	$IP = I_1 \frac{\cos(\phi - \theta)}{\cos \theta} \cdot F$
	$IP = \tau$
	$P = \frac{\tau}{l}$
	$P = \frac{\tau}{r \tan \alpha}$
<p><math>r</math>: the pitch radius of the thread</p> <p><math>\alpha</math>: pitch angle of the thread (rectangular)</p> 	$P = \frac{\tau}{l_1 \cos \theta}$

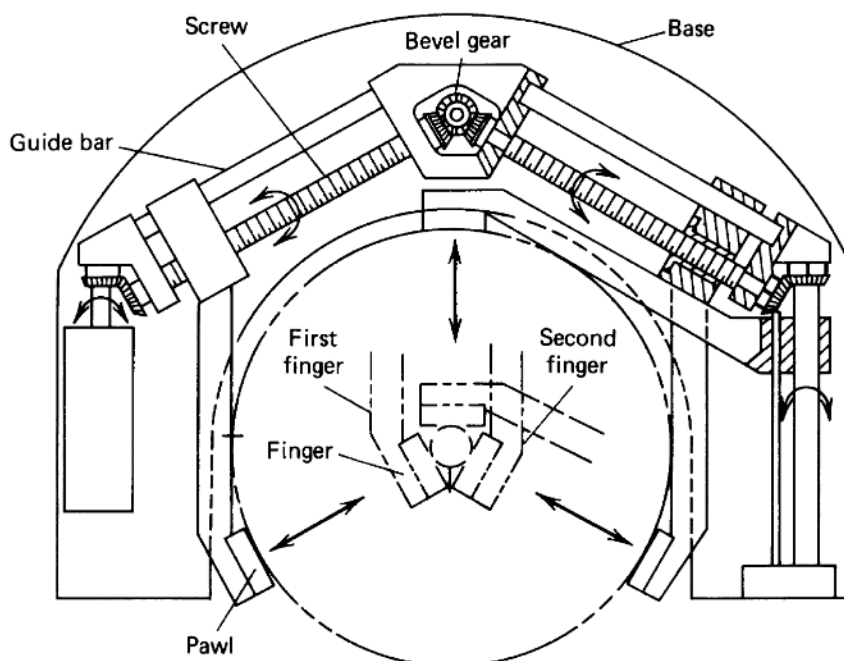


**Figure 21** Hand using three-point chuck mechanism (courtesy Yamatake Honeywell Co., Ltd.).

Anthropomorphism is thus required in their design. For industrial use, function is more important than cosmetic aspects, and anthropomorphism is beyond consideration. This is why there are few five-finger industrial hands. Nevertheless, an example of a five-finger hand developed for prosthetic use is described below because such hands include many mechanisms that will be effective in the design of industrial hands. A disabled person must produce control signals for operation of a prosthetic arm. The number of independent control signals available determines how many degrees of freedom the prosthetic device can have. Typical models of a five-finger hand for prostheses have only 1 d.o.f. Each finger is connected to a motor by appropriate mechanisms. Figure 25 shows an example, called the WIME Hand (Kato et al., 1969). Each finger is constructed using a cross-four-bar link mechanism that gives the finger proper bending motion. One element of each of the five sets of cross-four-bar links includes a crank rod. All crank rods are connected to the spring-loaded plate 1, which is moved translationally by an electric motor drive-screw mechanism 2. When the motor rotates clockwise or counterclockwise, the plate 1 moves toward the left or the right, respectively, and activates the cross-four-bar link of each finger to bend the finger and produce the grasping operation. To ensure that the hand holds the object with the equilibrium of the forces between the fingers and the object, the arrangement of fingers must be carefully considered. In typical five-finger hands, the thumb faces the other four fingers and is placed equidistant from the index finger and middle finger so the tips of the fingers can meet at a point when each finger is bent (see Figure 26). If each finger connects to the drive system rigidly, finger movements are determined by the motion of the drive system. The finger configuration cannot accommodate the shape change of grasped objects. To remedy this problem, the motor output can be transmitted to each finger through flexible elements.

#### 4.3 Mechanical Hands for Precision Tasks

For tasks that require manipulation of microobjects, such as microassembly in microindustry or manipulating cells in bioindustry, hands that can manipulate very precise objects are needed. The technology for developing such hands has drawn much attention since the beginning of the 1990s. With the advancement of microelectronics, manufacturing technologies for microobjects are becoming popular. Several very small microgripping devices have been developed. These are discussed in Chapter 10 and 11. This section

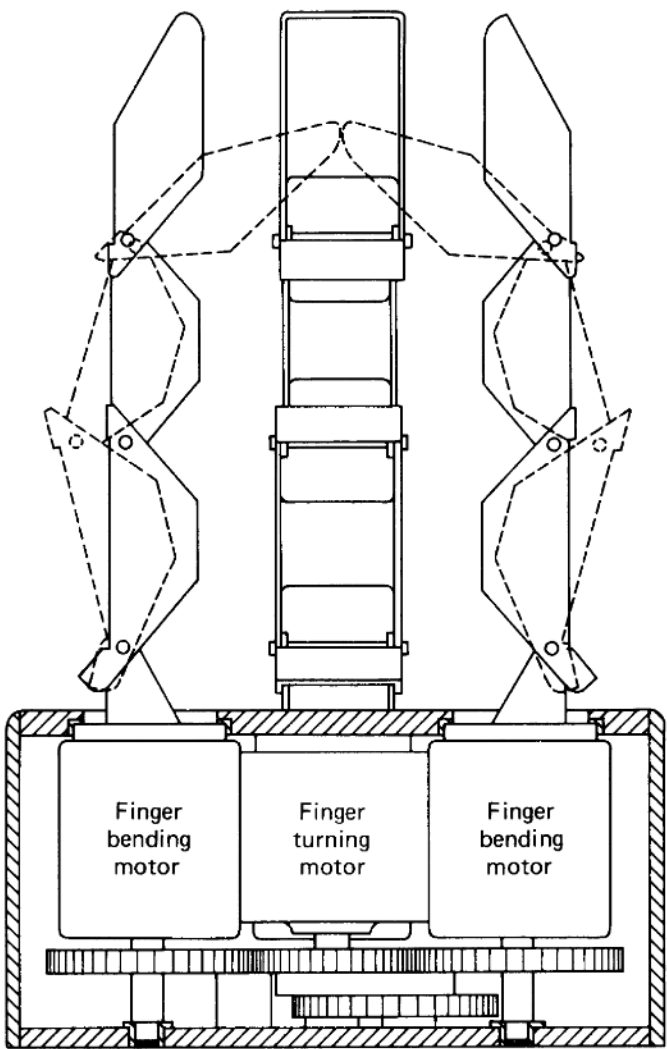


**Figure 22** Multiple prehension hand system. (From F. Skinner, "Design of a Multiple Prehension Manipulator System," ASME Paper 74-det-25, 1974.)

discusses gripping devices that, though not small themselves, can precisely manipulate very small objects.

There are several ways of designing such hands. One way employs a flexure structure using thin metal plate. See Figures 27 and 28 (Ando et al., 1990; Kimura et al., 1995). For the actuator, a piezoelectric stack element (PZT) is used. It is inserted in the central section of the hand. The PZT deforms when voltage is applied, and the deformation is amplified through the structure, composed of several arms and hinges that are spring joints, causing grasping motion at the fingertip. Opening motion is caused by the spring effect in the structure when the applied voltage is turned off to zero. At the hinge near the tip, a strain gauge is installed for grasp force detection. It is also used to compensate for the hysteresis that the PZT actuator generally has. The hand shown in Figure 28 can grasp a load less than 0.8 mm in diameter. The maximum grasping force is about 40 mN.

Another efficient design for gripping devices for microobject handling uses a parallel mechanism. The parallel arm, like the Stewart platform-type arm, provides the benefit of precise positioning functions at the fingertip, since the joints relating to the fingertip motion are arranged in parallel, with the result that the positioning error at each joint will

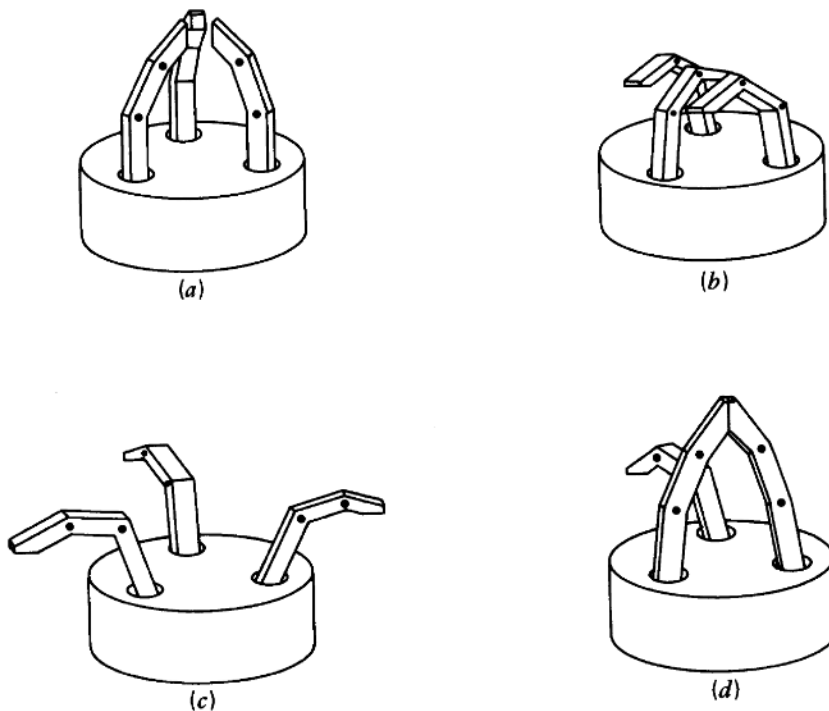


**Figure 23** Mechanical equivalent prehensile modes. (a) Three-jaw position; (b) wrap position; (c) spread position; (d) tip position. (From F. Skinner, "Design of a Multiple Prehension Manipulator System," ASME Paper 74-det-25, 1974.)

not be stacked at the fingertip. Figure 29 shows a finger for such a gripping device using a parallel link mechanism (Arai, Larssoneur, and Jaya, 1993; Tanikawa, Arai, and Matsuda, 1996). A piezoelectric actuator is installed on each link located between the base plate and the upper plate attached to the end-effector (finger). Both ends of each link are connected to the base through a ball joint. The deformation of each link that is made by the actuator produces 6-d.o.f. fingertip motion. Thus, using two fingers, microobjects can be grasped and manipulated in three-dimensional space (Figure 30). Positioning two fingertips at exactly the same location, as is necessary for grasping very small objects easily, is difficult. To address this problem, a two-finger microhand, in which the link for a finger is fixed on the other finger's upper base, has been developed, as shown in Figures 31 and 32. It is called the *chopstick-type microgripper*. Because the finger set installed on the upper plate of one finger is positioned relative to the other, the hand can be controlled more simply and with higher reliability in grasping an object. Using such a hand, successful manipulation of a 2-mm glass ball has been reported.

## 5 SPECIAL TOOLS

As mentioned above in Section 2, there are two functional classifications of end-effector for robots: gripping devices for handling parts, and tools for doing work on parts. In some tasks, especially handling large objects, designing gripping mechanisms with fingers is difficult. Also, in some applications dealing with only a specific object, a special tool for the required task will be much easier and more economical to design than the gripping devices. As mentioned above, specific tools such as drills and spot welders are popularly used. Details are discussed in other chapters of this handbook. The following sections describe special tools especially for part handling used in industrial robots instead of mechanical hands.

### 5.1 Attachment Devices

Attachment devices are simply mounting plates with brackets for securing tools to the tool mounting plate of the robot arm. In some cases attachment devices may also be

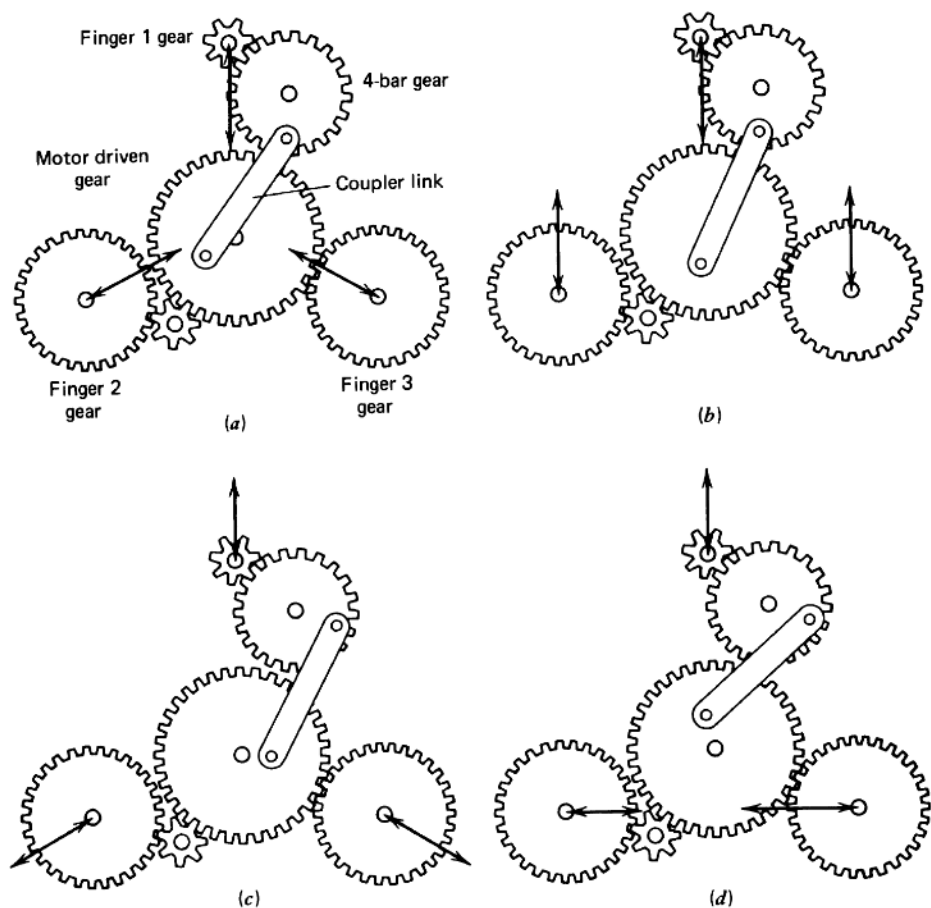


**Figure 24** The double-dwell finger-turning mechanism. (From F. Skinner, "Design of a Multiple Prehension Manipulator System," ASME Paper 74-det-25, 1974.)

designed to secure a workpiece to the robot tool mounting plate, as with a robot manipulating a part against a stationary tool where the cycle time is relatively long. In this case the part is manually secured and removed from the robot tool mounting plate for part retention.

## 5.2 Support and Containment Devices

Support and containment devices include lifting forks, hooks, scoops, and ladles. See Figure 33. No power is required to use this type of end-effector; the robot simply moves to a position beneath a part to be transferred, lifts to support and contain the part or material, and performs its transfer process.

## 5.3 Pneumatic Pickup Devices

The most common pneumatic pickup device is a vacuum cup (Figure 34), which attaches to parts to be transferred by suction or vacuum pressure created by a Venturi transducer or a vacuum pump. Typically used on parts with a smooth surface finish, vacuum cups are available in a wide range of sizes, shapes, and materials. Parts with nonsmooth surface finishes can be picked up by a vacuum system if a ring of closed-cell foam rubber is bonded to the surface of the vacuum cup. The ring conforms to the surface of the part and creates the seal required for vacuum transfer. Venturi vacuum transducers, which are relatively inexpensive, are used for handling small, lightweight parts where a low vacuum flow is required. Vacuum pumps, which are quieter and more expensive, generate greater vacuum flow rates and can be used to handle heavier parts.

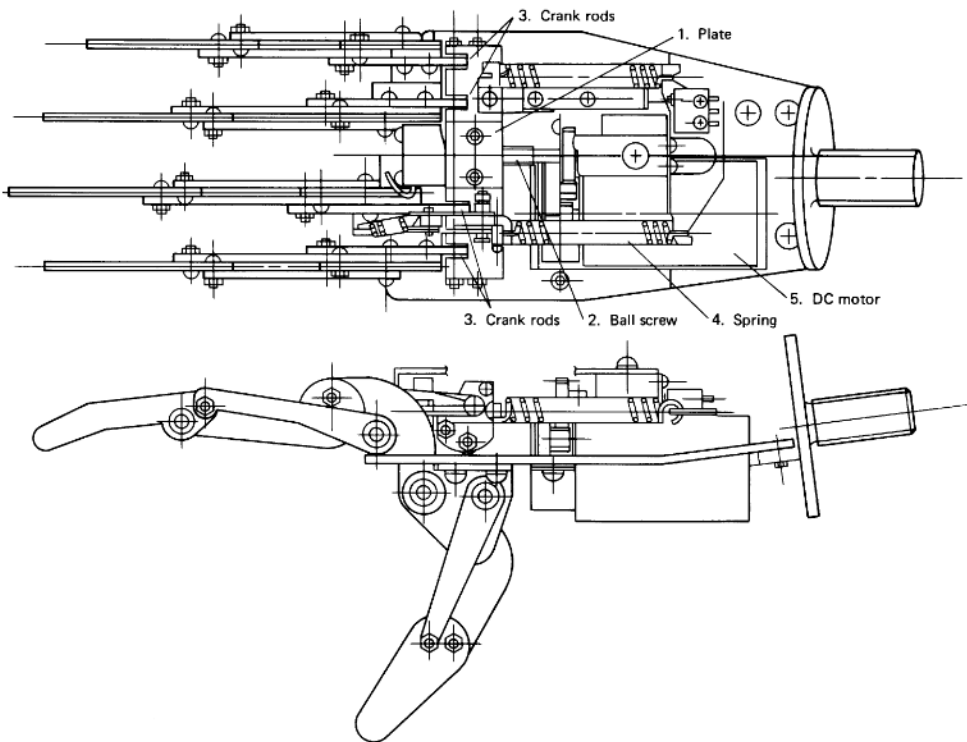


**Figure 25** Prosthetic hand for forearm amputee, WIME hand (courtesy Imasen Engineering Co., Ltd.).

With any vacuum system, the quality of the surface finish of the part being handled is important. If parts are oily or wet, they will tend to slide on the vacuum cups. Therefore some additional type of containment structure should be used to enclose the part and prevent it from sliding on the cups. In some applications a vacuum cup with no power source can be utilized. Pressing the cup onto the part and evacuating the air between the cup and part creates a suction capable of lifting the part. However, a stripping device or valve is required to separate the part from the cup during part release. When a Venturi or vacuum pump is used, a positive air blow-off may be used to separate the part from the vacuum cup. Vacuum cups have temperature limitations and cannot be used to pick up relatively hot parts.

Another example of a pneumatic pickup device is a pressurized bladder, which is generally specially designed to conform to the shape of the part. A vacuum system is

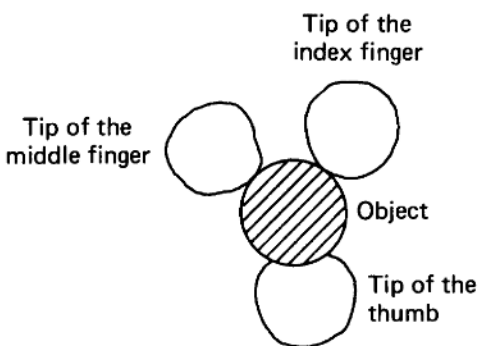


**Figure 26** Three-point pinch.

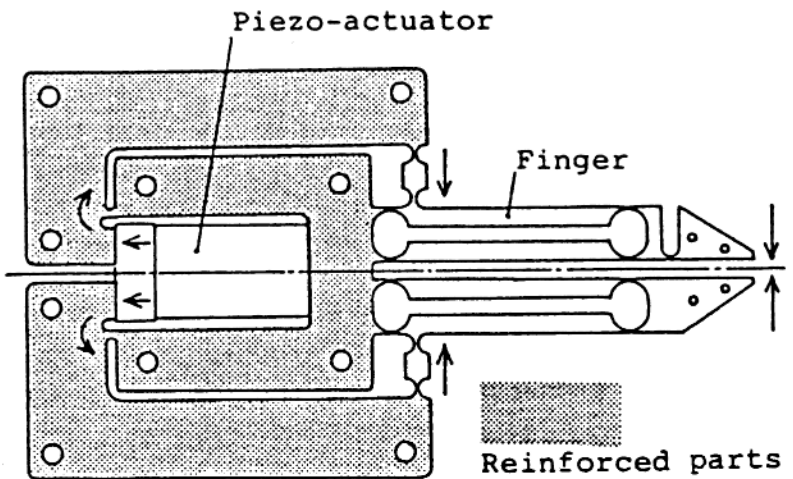


**Figure 27** Microgripper using thin flexure structure. (Courtesy Mechanical Engineering Laboratory, AIST-MITI, Japan.)

used to evacuate air from the inside of the bladder so that it forms a thin profile for clearance in entering the tooling into a cavity or around the outside surface of a part. When the tooling is in place inside or around the part, pressurized air causes the bladder to expand, contact the part, and conform to the surface of the part with equal pressure exerted on all points of the contacted surface. Pneumatic bladders are particularly useful where irregular or inconsistent parts must be handled by the end-effector.

Pressurized fingers (see Figure 35) are another type of pneumatic pickup device. Similar to a bladder, pneumatic fingers are more rigidly structured. They contain one straight half, which contacts the part to be handled; one ribbed half; and a cavity for pressurized

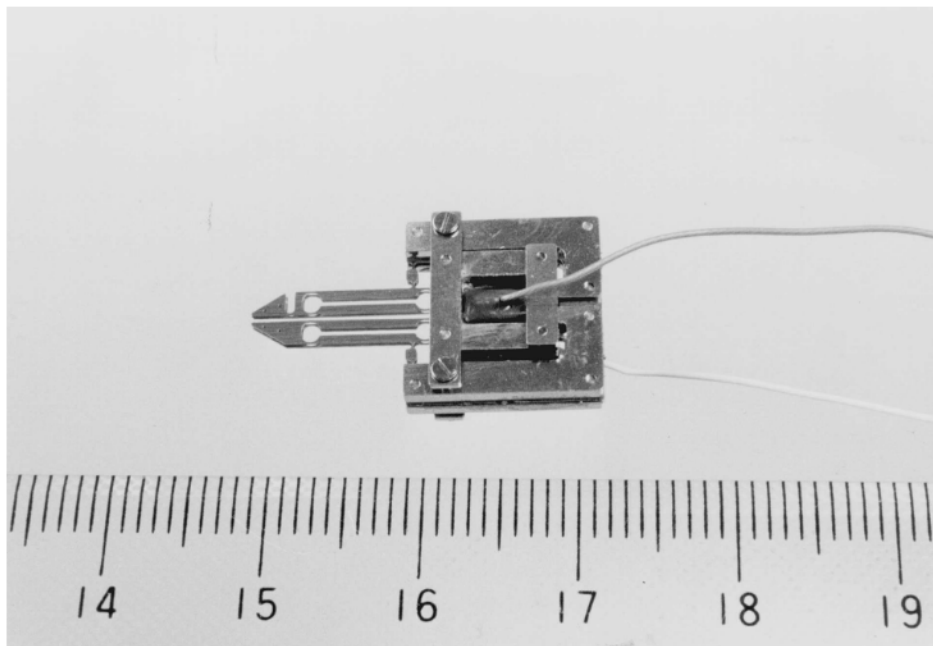


**Figure 28** An example of microgripper using thin flexure structure. (Courtesy Mechanical Engineering Laboratory, AIST-MITI, Japan.)

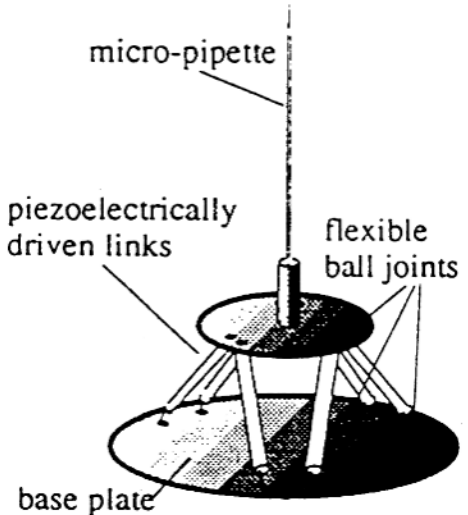


**Figure 29** Microgripper finger using a parallel link mechanism. (Courtesy Mechanical Engineering Laboratory, AIST-MITI, Japan.)

air between the two halves. Air pressure filling the cavity causes the ribbed half to expand and “wrap” the straight side around a part. With two fingers per end-effector, a part can thus be gripped by the two fingers wrapping around the outside of the part. These devices can also conform to various shape parts and do not require a vacuum source to return to their unpressurized position.

#### 5.4 Magnetic Pickup Devices

Magnetic pickup devices are the fourth type of end-effector. They can be considered when the part to be handled is of ferrous content. Either permanent magnets or electromagnets are used, with permanent magnets requiring a stripping device to separate the part from the magnet during part release. Magnets normally contain a flat part-contact surface but can be adapted with a plate to fit a specific part contour. A recent innovation in magnetic pickup devices uses an electromagnet fitted with a flexible bladder containing iron filings, which conforms to an irregular surface on a part to be picked up. As with vacuum pickup

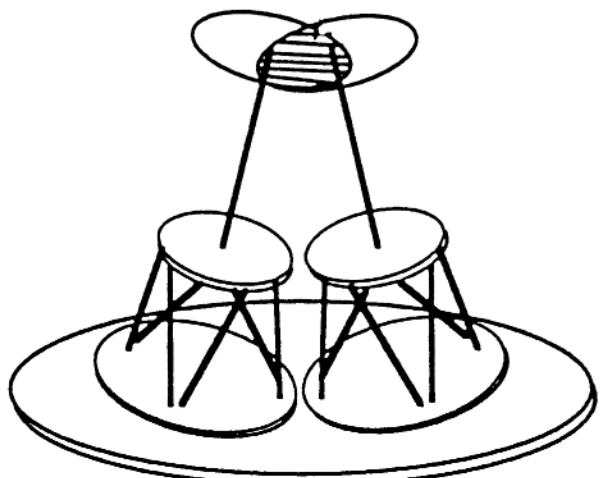


**Figure 30** Microgripper using two parallel link fingers. (Courtesy Mechanical Engineering Laboratory, AIST-MITI, Japan.)

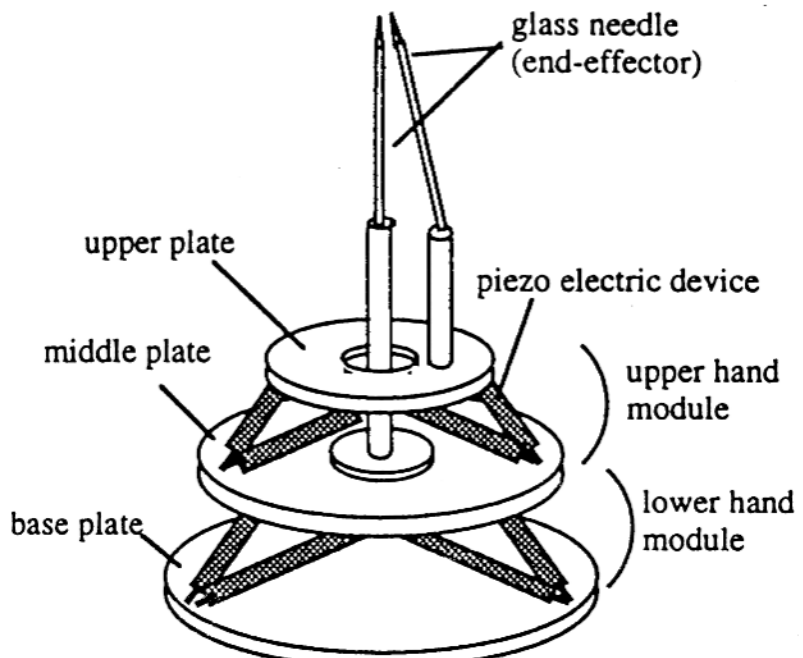


**Figure 31** "Chopstick-type" microgripper. (Courtesy Mechanical Engineering Laboratory, AIST-MITI, Japan.)

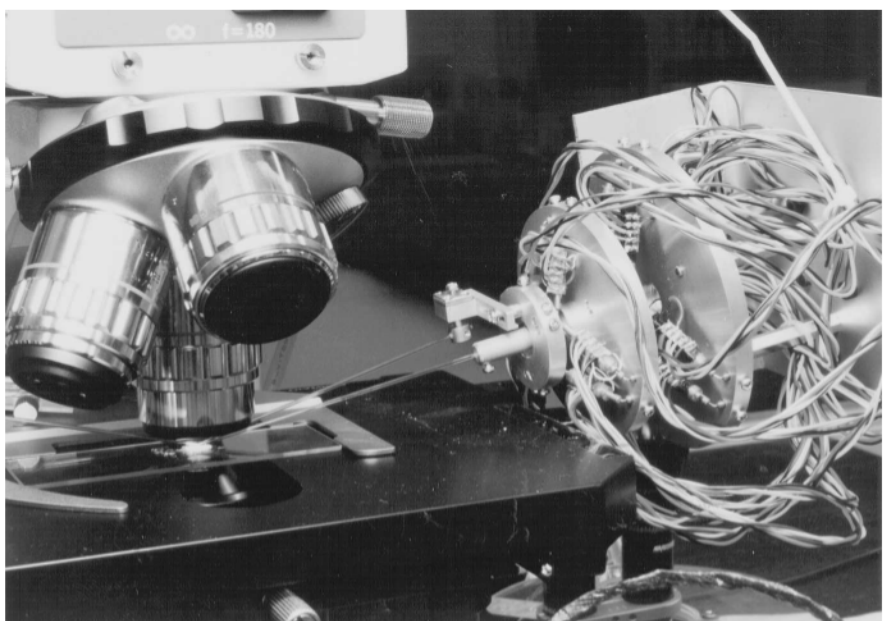


**Figure 32** Microobject manipulation by chopstick-type microgripper. (Courtesy Mechanical Engineering Laboratory, AIST-MITI, Japan.)

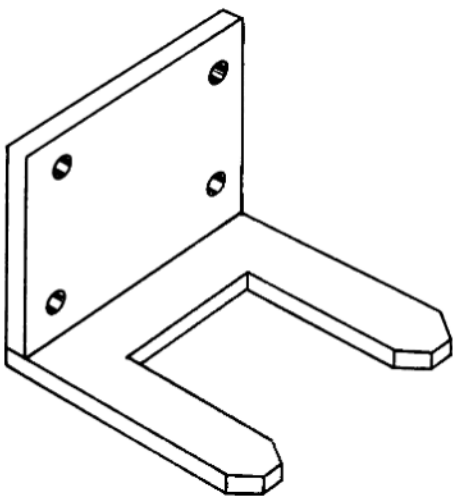


Figure 33 Support and containment device.

devices, oily or wet part surfaces may cause the part to slide on the magnet during transfer. Therefore containment structures should be used in addition to the magnet to enclose the part and prevent it from slipping.

Three additional concerns arise in handling parts with magnets. First, if a metal-removal process is involved in the application, metal chips may also be picked up by the magnet. Provisions must be made to wipe the surface of the magnet in this event. Next, residual magnetism may be imparted to the workpiece during pickup and transfer by the magnetic end-effector. If this is detrimental to the finished part, a demagnetizing operation may be required after transfer. Finally, if an electromagnet is used, a power failure will cause the part to be dropped immediately, which may produce an unsafe condition. Although electromagnets provide easier control and faster pickup and release of parts, permanent magnets can be used in hazardous environments requiring explosion-proof electrical equipment. Normal magnets can handle temperatures up to 60°C (140°F), but magnets can be designed for service in temperatures up to 150°C (300°F).

## 6 UNIVERSAL HANDS

### 6.1 Design of Universal Hands

Universal hands have many degrees of freedom, like the human hand. They have been researched by several investigators. Figure 36 shows the joint structure in a typical uni-

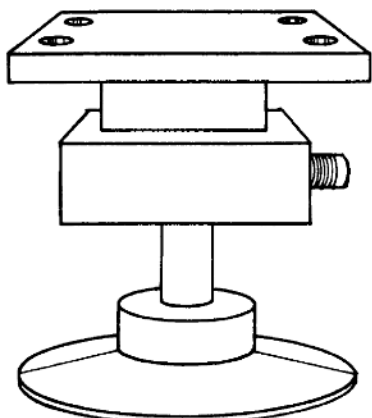
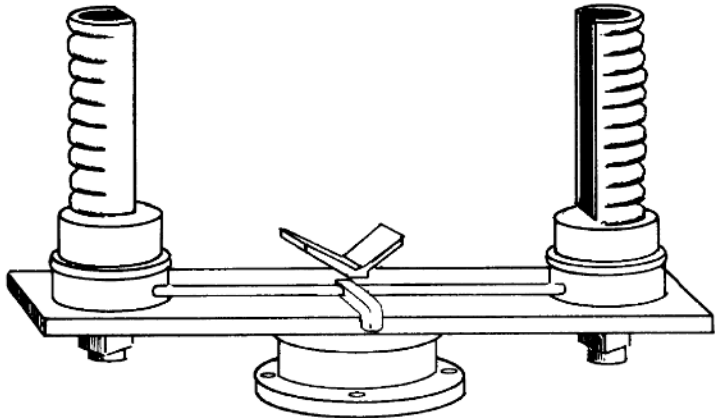


Figure 34 Vacuum cup pickup device.



**Figure 35** Pneumatic pickup device (pressurized fingers).

versal hand. The example uses 4-d.o.f. fingers, but 3-d.o.f. fingers are often used. In such fingers the joint nearest to the fingertip will be removed. The number of fingers is three or four, though three fingers usually provide enough functions for universal hands.

Increasing the number of degrees of freedom causes several problems. One difficult problem is how to install in the hand the actuators necessary to activate all degrees of freedom. This requires miniature actuators that can produce enough power to drive the hand joint. A few universal hands have finger joints directly driven by small, specially designed actuators. See Figure 37 (Umetsu and Oniki, 1993). The fingers in this hand each have 3 d.o.f. A miniature electric motor with a high reduction gear to produce sufficient torque is directly installed at each joint. The direct drive joint is very effective for simplifying the hand structure. However, suitable actuators are not always commercially available. An actuator with sufficient power generation will usually be too large to attach at each joint of the finger. The most frequent solution is to use a tendon drive

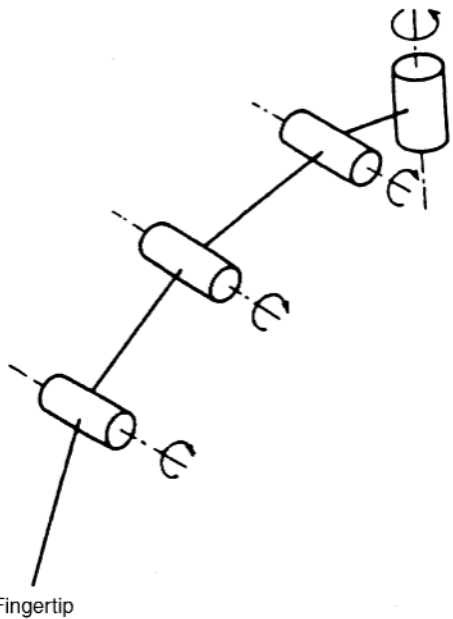


**Figure 36** Multijoint structure in a typical universal hand.

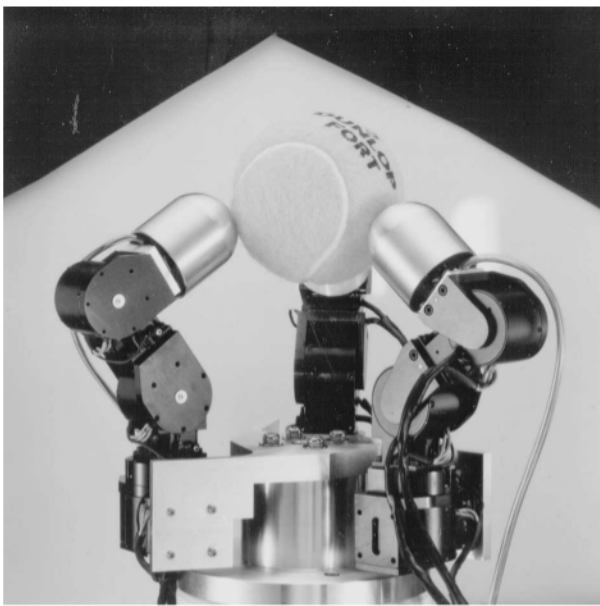


**Figure 37** Yaskawa universal hand. (Courtesy Yaskawa Electric Corporation.)

mechanism that enables actuators to be placed at an appropriate position away from the joint. There are two tendon drive mechanisms. One uses tendon-pulley mechanisms. Figure 38 shows the Utah/MIT Hand, which has four fingers (Jacobsen et al., 1981). Tendon-pulley mechanisms are shown in Figure 39. One end of the tendon is fixed at a hinge located on a finger segment to be moved. The other end is connected to a pneumatic actuator (cylinder). Between the ends, the tendon is guided through several guided pulleys, which can be passively rotated by tendon motion. Two tendons, agonistic and antagonistic, are used to drive each joint. A tendon tension sensor is attached to each actuator to control tendon tension and interaction among the tendons. This sensor is used to control the tendon tension and the interaction among the tendons (Jacobsen et al., 1981). The other tendon drive mechanism uses a combination of pulleys and hoses to guide the tendons. This mechanism has the advantage of reducing the complexity of the guidance mechanisms. The drawback is that it increases the friction in a power transmission system. Figure 40 shows a hand using this drive mechanism. The hand has three fingers: a thumb, index finger, and middle finger (Okada, 1982). Each finger contains two or three segments made of 17-mm brass rods bored to be cylindrical. The tip of each segment is truncated at a slope of 30° so that the finger can be bent at a maximum angle of 45° at each joint, both inward and outward. The workspace of the finger is thus more extensive than that of the human finger. The thumb has three joints and the index and middle fingers each have four joints. Each joint has 1 d.o.f. and is driven using a tendon-pulley mechanism and electric motors. A pulley is placed at each joint, around which two tendons are wound after an end of each tendon is fixed to the pulley. The tendon is guided through coil-like hoses so that it cannot interfere with the complicated finger motion. Using coil-like hoses protects the tendon and makes possible the elimination of relaying points for guiding tendons. To make the motions of the fingers flexible and the hand system more compact, the tendons and hoses are installed through the finger tubes. The section drawing of the hand system in Figure 41 explains the joint drive mechanisms. Motors for driving the respective joints are located together within a trunk separated from the hand system.

One solution proposed to solve the problem of friction between hoses and wires is to support the hoses with flexible elements such as springs (Sugano et al., 1984). Figure 42 shows the construction of a tendon-pulley drive system with tendon-guiding hoses supported by springs. Bending a hose whose ends are rigidly fixed will extend the hose. This reduces the cross-section area of the hose, which increases the friction. In the system

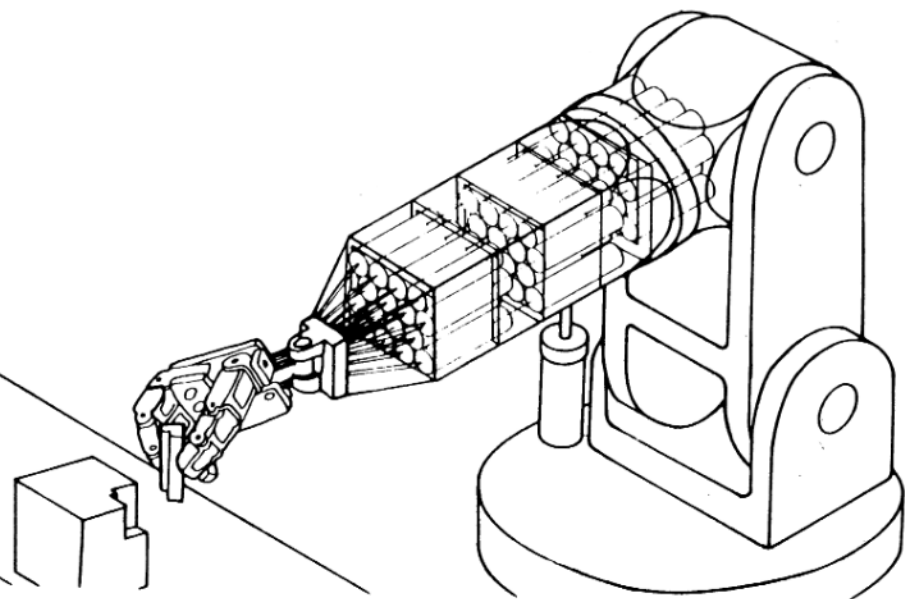


**Figure 38** Utah-MIT hand. (From M. Brady and R. Paul, *Robotics Research*. Cambridge: MIT Press, 1984, p. 602.)

shown in Figure 42, the spring, rather than the hose, will be extended when the hose is bent, and the cross-section area of the hose will not be affected by the change of hose configuration. This prevents friction from increasing.

Another problem with the tendon drive method is controlling the tendon tension properly during motion. Tension control using sensors is used to avoid relaxing of tension. Coupled tendon drive mechanisms are also effective. These mechanisms use a network of tendons, each of which interferes with the others. Figure 43 shows such a tendon drive system for a finger with three joints. The hand using it, the Stanford/JPL Hand (Figure 44) (Mason and Salisbury, 1985), uses four tendons and electric motors to drive three joints. Each motor is installed so that it interferes with the others through tendons. The tendon tension can thus be adjusted by controlling each motor cooperatively. This structure raises control complexity, but is useful for controlling tendon tension.

## 6.2 Control of Universal Hands

To grasp an object stably and manipulate it dexterously using universal hands, each finger joint in the hand must be moved cooperatively. For this purpose a stable grasp control algorithm has been proposed (Li and Sastry, 1990; Yoshikawa, 1990). From the principle of statics, the requirements of fingertip force for each finger are as follows:

1. Fingertip force should be applied to the grasped object within the friction cone.
2. For the object to be grasped statically, the sum of fingertip forces and their moments around a specific point must be zero. Also proper internal forces at each fingertip should be generated to support the gravity force of the grasped object when the object is grasped statically.
3. For the grasped object to be manipulated, proper additional forces at each fingertip must be generated to produce the desired motion of the object, keeping the above conditions.

To meet the above requirements, each finger in the universal hand will be required to have force control functions as well as position control. Proper compliance at the fingertip also plays an important role in achieving robust stable grasp. Almost all universal hands developed so far therefore have force and position control functions.

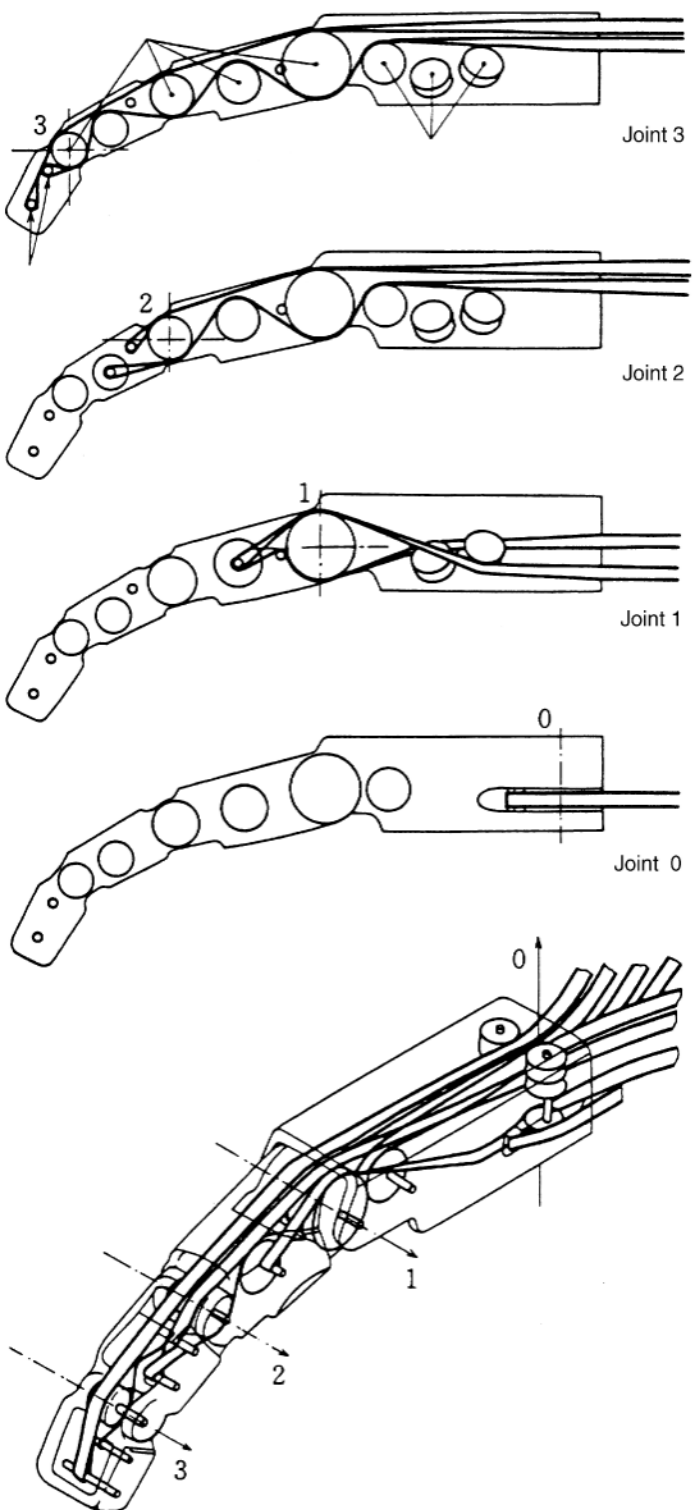


**Figure 39** Tendon-Pulley Mechanisms in a finger of Utah-MIT hand. (From M. Brady and R. Paul, Robotics Research, Cambridge: MIT Press, 1984, p. 606–607.)

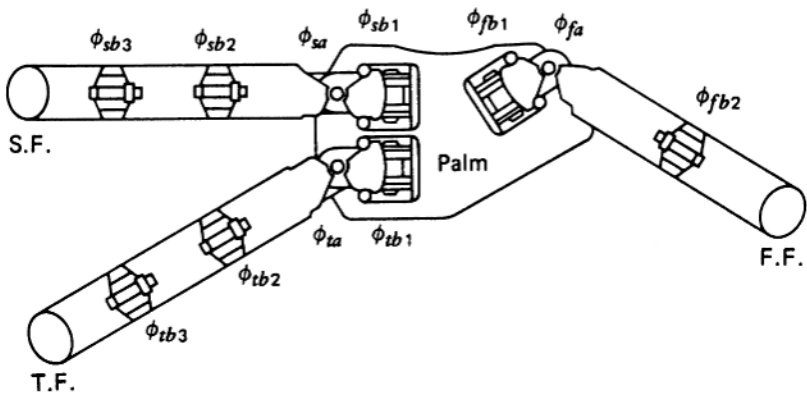


**Figure 40** Versatile hand system. (From T. Okada, "Computer Control of Multijointed Finger System for Precise Object-Handling," *IEEE Transactions on Systems, Man and Cybernetics SMC-12(3)*, 1982, 289–299.)

Humans can do various complex tasks using dexterous finger motions. Sometimes they will manipulate the object by using slip motion of the grasped object on the finger surface. For a universal hand to perform such skilled operations, more complex requirements should be satisfied in addition to those listed above. For dexterous universal hand control to be achieved, many problems must be solved relating to grasp planning, grasp location finding, adaptive grasp force control, and so on. For details about grasp and manipulation control using universal hands, see Murray, Li, and Sastry (1994) and Maekawa, Tanie, and Komoriya (1997).

## 7 PRACTICAL IMPLEMENTATION OF ROBOT END-EFFECTORS

The end-effector practically used in industrial robots is commonly made up of four distinct elements (see Figure 45):

1. Attachment of the hand or tool to the robot end-effector mounting plate
2. Power for actuation of end-effector tool motions
3. Mechanical linkages
4. Sensors integrated into the end-effector

The role of the element and how to implement power and sensors are discussed below from the practical point of view.

### 7.1 Mounting Plate

The means of attaching the end-effector to an industrial robot are provided by a robot end-effector mounting plate located at the end of the last axis of motion on the robot arm. This mounting plate contains either threaded or clearance holes arranged in a pattern for attaching a hand or tools. For a fixed mounting of a hand or tool, an adapter plate with a hole pattern matching the robot end-effector mounting plate can be provided. The remainder of the adapter plate provides a mounting surface for the hand or tool at the proper distance and orientation from the robot end-effector mounting plate. If the task of the robot requires it to automatically interchange hands or tools, a coupling device can be provided. An adapter plate is thus attached to each of the hands or tools to be used, with a common lock-in position for pickup by the coupling device. The coupling device may also contain the power source for the hands or tools and automatically connect the power when it picks up the end-effector. Figures 46, 47, and 48 illustrate this power connection end-effector tool change application. An alternative to this approach is for each tool to have its own power line permanently connected and the robot simply to pick up the various tools mounted to adapter plates with common lock-in points.

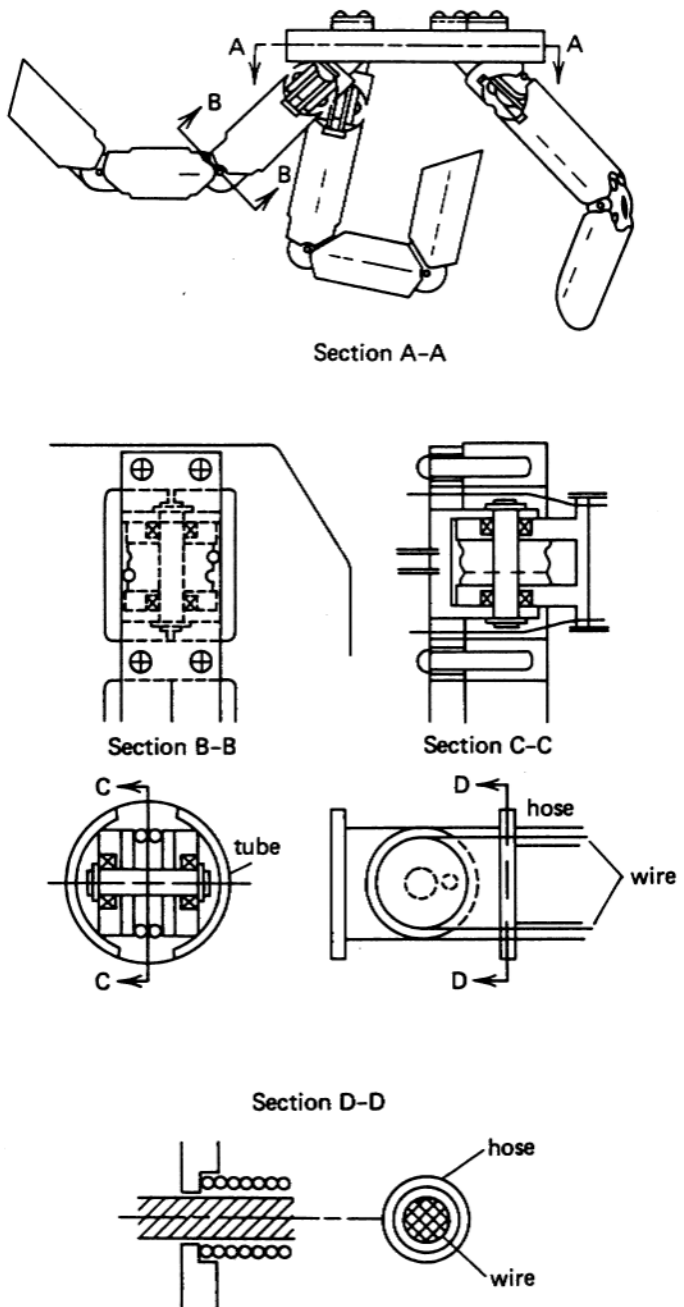


**Figure 41** Joint drive mechanism of the versatile hand. (From T. Okada, "Computer Control of Multijointed Finger System for Precise Object-Handling," *IEEE Transactions on Systems, Man, and Cybernetics SMC-12(3)*, 1982, 289–299.)

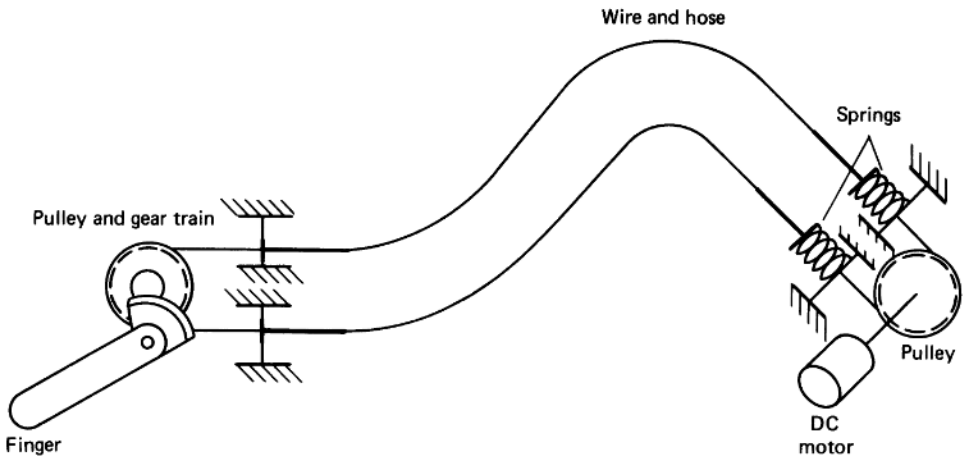


**Figure 42** Tendon-pulley drive system with tendon-guiding hoses supported by springs. (From S. Sugano et al., "The Keyboard Playing by an Anthropomorphic Robot," in *Preprints of Fifth ISM-IFTOMM Symposium on Theory and Practice of Robots and Manipulators*, Udine, 1984.)

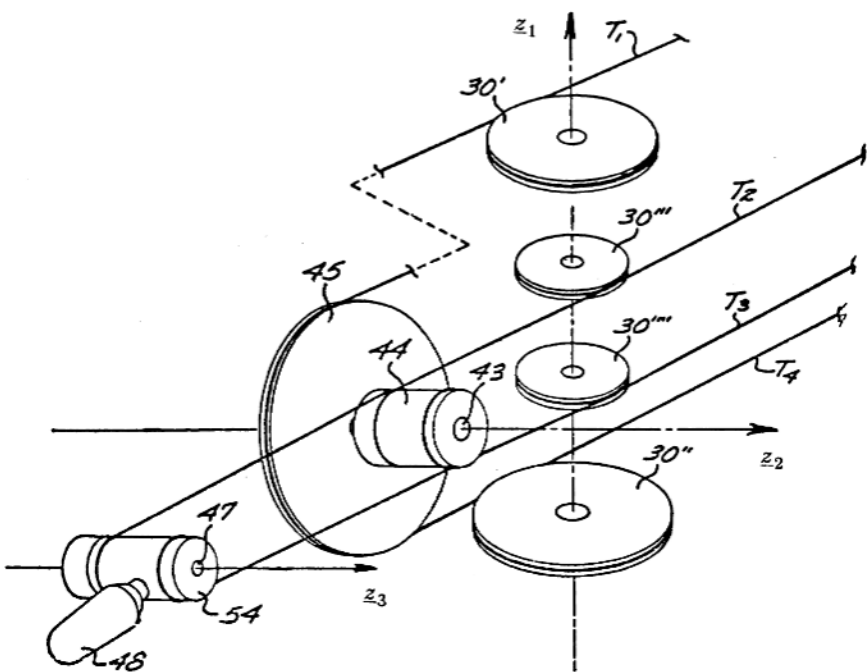


**Figure 43** Coupled tendon-pulley drive mechanisms in Stanford/JPL hand. (From M. T. Mason and J. K. Salisbury, *Robot Hands and the Mechanics of Manipulation*. Cambridge: MIT Press, 1985, p. 80.)

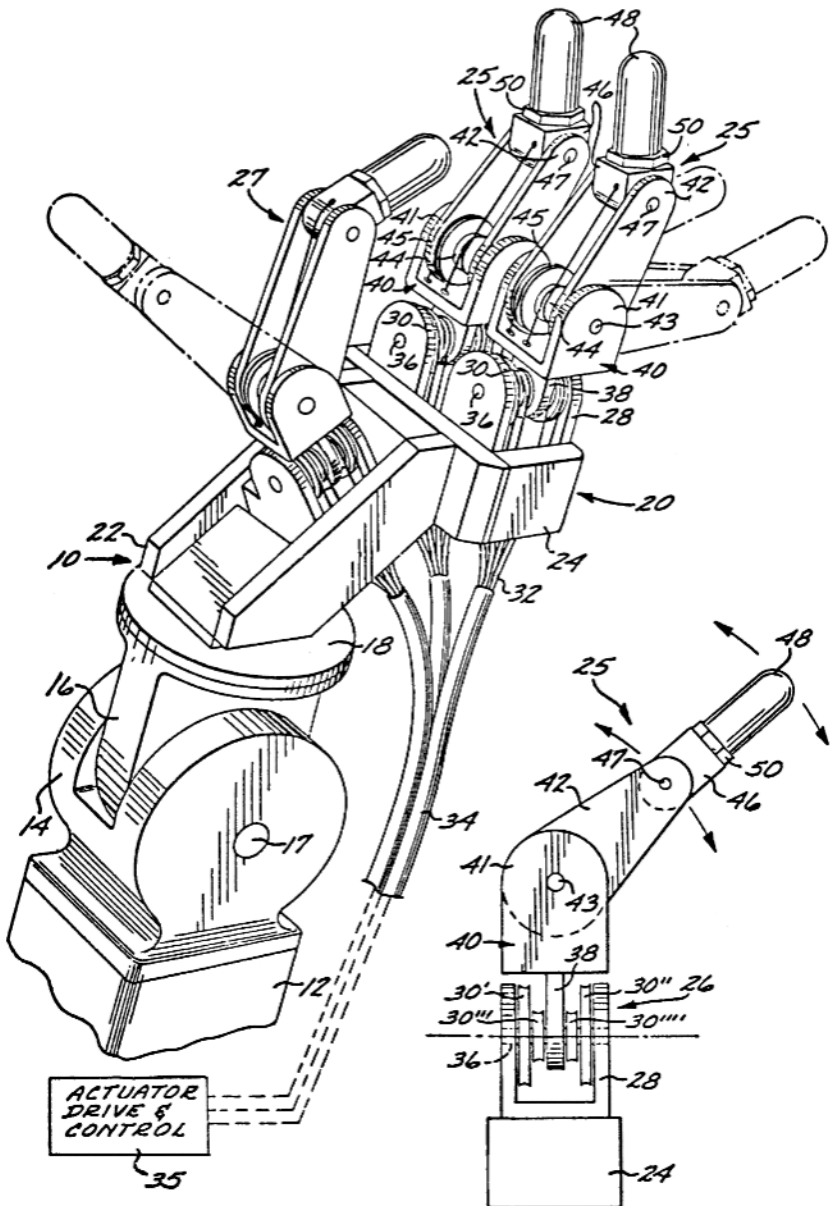


**Figure 44** Stanford/JPL hand. (From M. T. Mason and J. K. Salisbury, *Robot Hands and the Mechanics of Manipulation*. Cambridge: MIT Press, 1985, p. 81.)

## 7.2 Power Implementation

Power for actuation of end-effector motions can be pneumatic, hydraulic, or electrical, as mentioned above, or the end-effector may not require power, as in the case of hooks or scoops. Generally, pneumatic power is used wherever possible because of its ease of installation and maintenance, low cost, and light weight. Higher-pressure hydraulic power is used where greater forces are required in the tooling motions. However, contamination of parts due to leakage of hydraulic fluid often restricts its application as a power source for tooling. Although it is quieter, electrical power is used less frequently for tooling power, especially in part-handling applications, because of its lower applied force. Several

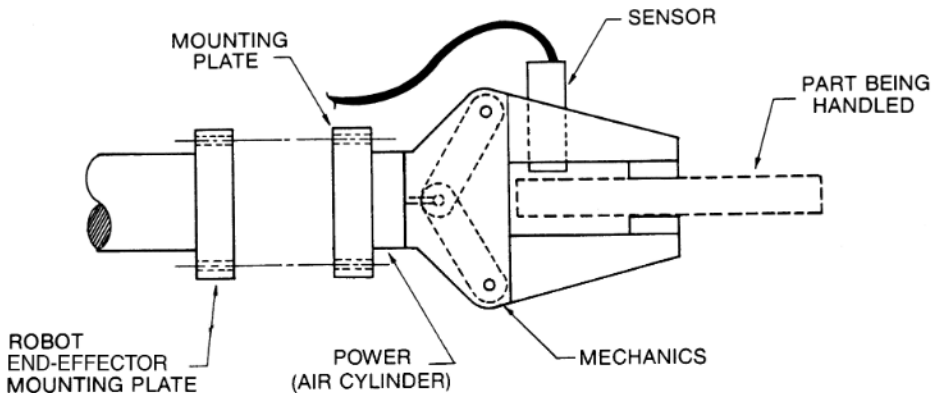


**Figure 45** Elements of end-effector.

light payload assembly robots utilize electrical tooling power because of its control capability. In matching a robot to an end-effector, consideration should be given to the power source provided with the robot. Some robots have provisions for tooling power, especially in part-handling robots, and it is an easy task to tap into this source for actuation of tool functions. As previously mentioned, many robots are provided with a pneumatic power source for tool actuation and control.

### 7.3 Mechanical Linkages

End-effectors for robots may be designed with a direct coupling between the actuator and workpiece, as in the case of an air cylinder that moves a drill through a workpiece, or may use indirect couplings or linkages to gain mechanical advantage, as in the case of a pivot-type gripping device. A gripper-type hand may also have provisions for mounting interchangeable fingers to conform to various part sizes and configurations. In turn, fingers attached to hands may have provisions for interchangeable inserts to conform to various part configurations.

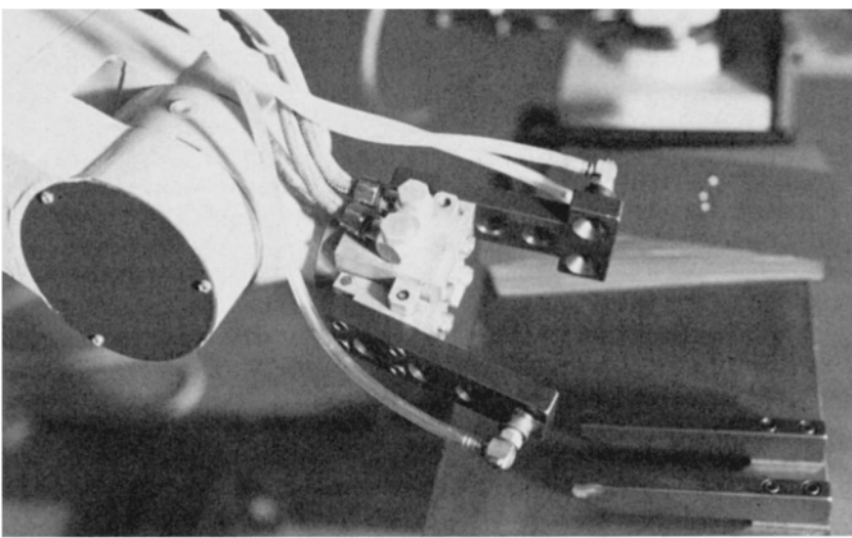


**Figure 46** Pickup hand for tool change. Power for tool actuation is ported through the fingers for connection to the various tools to be picked up. (From R. D. Potter, "End-of-Arm Tooling," in *Handbook of Industrial Robotics*, ed. Shimon Y. Nof. New York: John Wiley & Sons, 1985.)

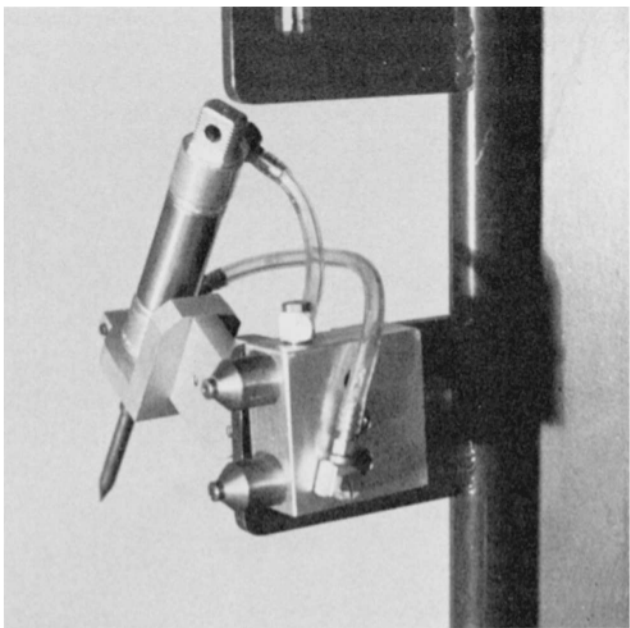


**Figure 47** Tool is rack-ready to be picked up by robot. Note cone-shaped power connection ports in tool mounting block. (From R. D. Potter, "End-of-Arm Tooling," in *Handbook of Industrial Robotics*, ed. Shimon Y. Nof. New York: John Wiley & Sons, 1985.)

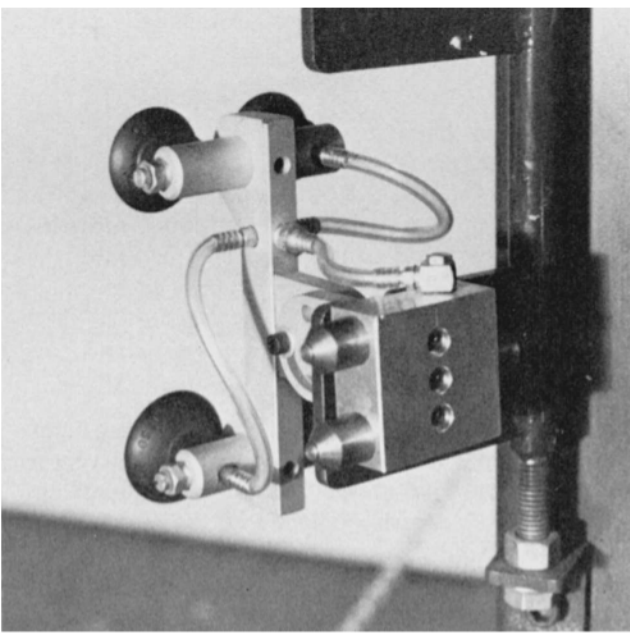


**Figure 48** Another tool with power connection block ready for robot pickup. (From R. D. Potter, "End-of-Arm Tooling," in *Handbook of Industrial Robotics*, ed. Shimon Y. Nof. New York: John Wiley & Sons, 1985.)

#### 7.4 Sensors

Sensors are incorporated in end-effectors to detect various conditions. For safety considerations sensors are normally designed into tooling to detect workpiece or tool retention by the robot during the robot operation. Sensors are also built into end-effectors to monitor the condition of the workpiece or tool during an operation, as in the case of a torque sensor mounted on a drill to detect when a drill bit is dull or broken. Sensors are also used in tooling to verify that a process is completed satisfactorily, such as wire-feed detectors in arc welding torches and flow meters in dispensing heads. More recently, robots specially designed for assembly tasks contain force sensors (strain gauges) and dimensional gauging sensors in the end-effector.

### 8 PRACTICAL DESIGN FOR ROBOT END-EFFECTORS

This section first explains general criteria for robot end-effector design, including the importance of analyzing the object to be handled or worked on. The analysis relates to preengineering and data collection. The development of end-effector concept and design will proceed only after the analysis is completed. Second, the preengineering phase, involving analysis of the workpiece and process, with emphasis on productivity considerations, will be explained. Third, some important guidelines for actual end-effector design will be summarized.

#### 8.1 General End-Effector Design Criteria

Although robot end-effectors vary widely in function, complexity, and application area, certain design criteria pertain to almost all of them. First, the end-effector should be as lightweight as possible. Weight affects the performance of the robot. The rated load-carrying capacity of the robot, or the amount of weight that can be attached to the robot end-effector mounting plate, includes the weight of the end-effector and of the part being carried. The load that the robot is carrying also affects the speed of its motions. Robots can move faster carrying lighter loads. Therefore, for cycle time considerations, the lighter the tool, the faster the robot is capable of moving. The use of lightening holes, whenever possible, and lightweight materials such as aluminum or magnesium for hand components are common solutions for weight reduction. Figure 49 shows a double-action pickup hand with lightening holes.

Second, the end-effector should be as small in physical size as possible. Minimizing the dimensions of the tool also helps to minimize weight. Minimizing the size of the

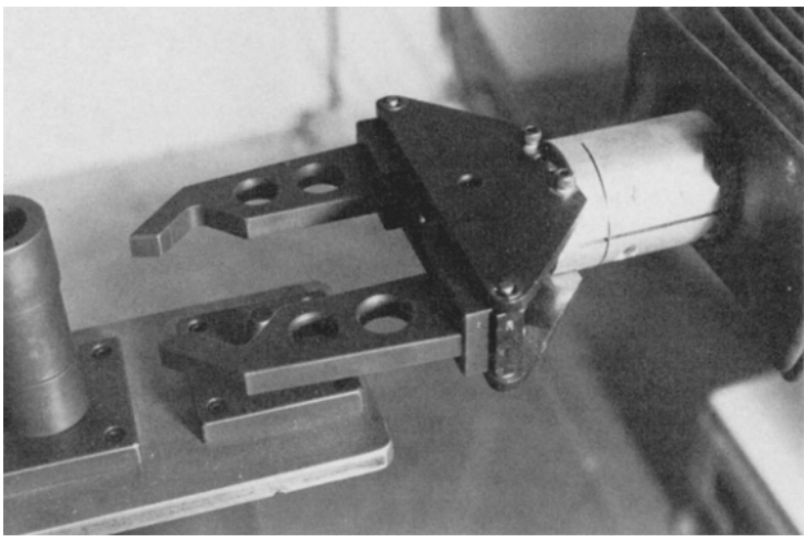


**Figure 49** Double-action pickup hand showing interchangeable fingers with lightening holes and V-block locating features. (From R. D. Potter, "End-of-Arm Tooling," in *Handbook of Industrial Robotics*, ed. Shimon Y. Nof. New York: John Wiley & Sons, 1985.)

tooling provides for better clearances in workstations in the system. Load-carrying capacities of robots are usually based on moment of inertia calculations of the last axis of motion; that is, a given load capacity at a given distance from the tool mounting plate surface. Minimizing the size of the end-effector and the distance from the end-effector mounting plate to the center of gravity of the end-effector thus enhances robot performance. At the same time, it is desirable to handle the widest possible range of parts with the robot end-effector. This minimizes changeover requirements and reduces costs for multiple tools. Although minimizing the size of the end-effector somewhat limits the range of parts that can be handled, there are techniques for accomplishing both goals. Adjustable motions may be designed into the end-effector so that it can be quickly and easily manually changed to accommodate different-sized parts. Interchangeable inserts may be put in the end-effector to change the hand from parts of one size or shape to another. The robot may also automatically interchange hands or tools to work on a range of parts, with each set of end-effectors designed to handle a certain portion of the entire range of parts. This addresses weight and size considerations and reduces the total number of tools required. Figure 50 shows a standard dual part-handling end-effector for gripping parts varying within a certain size range.

*Maximizing rigidity* is another criterion that should be designed into the end-effector. Again, this relates to the task performance of the robot. Robots have specified repeatabilities and accuracies in handling a part. If the end-effector is not rigid, this positioning accuracy will not be as good and, depending on part clearances and tolerances, problems in the application may result. Excessive vibration may also be produced when a nonrigid or flimsy end-effector is attached to the end-effector mounting plate. Because robots can move the end-effector at very high rates of speed, this vibration may cause breakage or damage to the end-effector. Attaching a rigid end-effector eliminates these vibrations.

*The maximum applied holding force* should be designed into the end-effector. This is especially important for safety reasons. Robots are dynamic machines that can move parts at high velocities at the end of the arm, with only the clamp force and frictional force holding the parts in the hand. Because robots typically rotate the part about a fixed robot

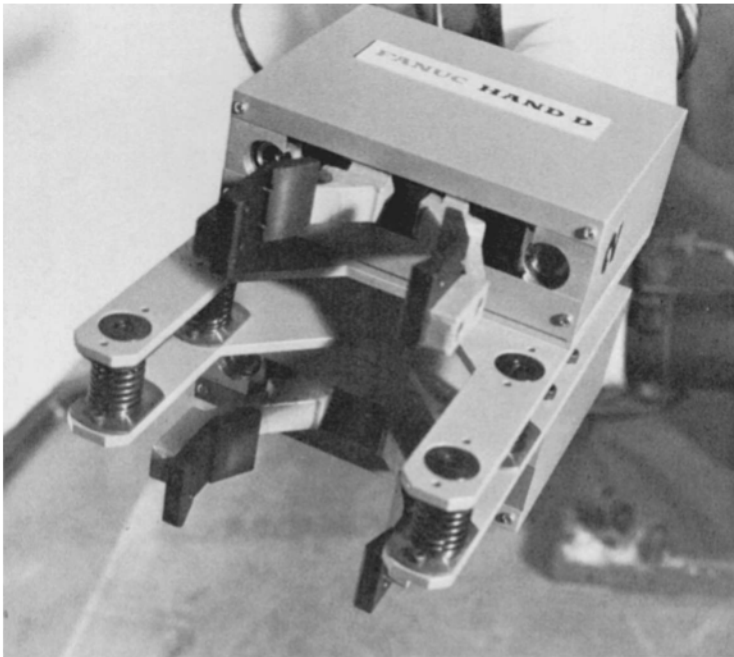


**Figure 50** Standard tooling for parts-handling applications, with such features as parallel motion fingers, dual part-handling capability, and compliance in hand. (From R. D. Potter, "End-of-Arm Tooling," in *Handbook of Industrial Robotics*, ed. Shimon Y. Nof. New York: John Wiley & Sons, 1985.)

base centerline, centrifugal forces are produced. Acceleration and deceleration forces also result when the robot moves from one point to another. The effect of these forces acting on the part makes it critical to design in an applied holding force with a safety factor great enough to ensure that the part is safely retained in the hand during transfer and not thrown as a projectile, with the potential of causing injury or death to personnel in the area or damage to periphery equipment. On the other hand, the applied holding force should not be so great that it actually causes damage to a more fragile part being handled. Another important consideration in parts transfer relating to applied holding force is the orientation of the part in the hand during transfer. If the part is transferred with the hand axis parallel to the floor, the part, retained only by the frictional force between the fingers and part, may have a tendency to slip in the hand, especially at programmed stop points. By turning the hand axis perpendicular to the floor during part transfer, the required holding force may be decreased, and the robot may be able to move at higher speed because the hand itself acts as a physical stop for the part.

*Maintenance and changeover* considerations should be designed into the tooling. Perishable or wear details should be designed to be easily accessible for quick change. Change details such as inserts or fingers should also be easily and quickly interchangeable. The same type of fastener should be used wherever possible in the hand assembly, thereby minimizing the number of maintenance tools required.

## 8.2 Preengineering and Data Collection

### 8.2.1 Workpiece Analysis

The part being transferred or worked on must be analyzed to determine critical parameters to be designed into the end-effector. The dimensions and tolerances of the workpiece must be analyzed to determine their effect on end-effector design. The dimensions of the workpiece will determine the size and weight of the end-effector required to handle the part. It will also determine whether one tool can automatically handle the range of part dimensions required, whether interchangeable fingers or inserts are required, or whether tool change is required. The tolerances of the workpieces will determine the need for compliance in the end-effector. Compliance allows for mechanical “float” in the end-effector in relation to the robot end-effector mounting plate to correct misalignment errors encountered when parts are mated during assembly operations or loaded into tight-fitting fixtures or periphery equipment. If the part tolerances vary so that the fit of the part in fixture is less than the repeatability of the robot, a compliance device may have to be designed into the end-effector. Passive compliance devices such as springs may be incorporated into the end-effector to allow it to float to accommodate very tight tolerances. This reduces the rigidity of the end-effector. Other passive compliance devices, such as remote center compliance (RCC) units, are commercially available. These are mounted between the robot end-effector mounting plate and the end-effector to provide a multiaxis float. RCC devices, primarily designed for assembly tasks, allow robots to assemble parts with mating fits much tighter than the repeatability that the robot can achieve. Active compliance devices with sensory feedback can also be used to accommodate tolerance requirements.

The *material and physical properties* of the workpiece must be analyzed to determine their effect on end-effector design. The best method of handling the part, whether by vacuum, magnetic, or mechanical hand, can be determined. The maximum permissible grip forces and contact points on the part can be determined, as well as the number of contact points to ensure part retention during transfer. Based on the physical properties of the material, the need for controlling the applied force through sensors can also be resolved.

The *weight and balance* (center of gravity) of the workpiece should be analyzed to determine the number and location of grip contact points to ensure proper part transfer. This will also resolve the need for counterbalance or support points on the part in addition to the grip contact points. The static and dynamic loads and moments of inertia of the part and end-effector about the robot end-effector mounting plate can be analyzed to verify that they are within the safe operating parameters of the robot.

The *surface finish and contour* (shape) of the workpiece should be studied to determine the method and location of part grasp (i.e., vacuum for smooth, flat surfaces, mechanical hands for round parts, etc.). If the contour of the part is such that two or more independent grasp means must be applied, this can be accomplished by mounting separate gripping devices and/or special tools at different locations on the end-effector, each gripping or

attaching to a different section of the part. This may be a combination of vacuum cups, magnets, and/or mechanical hands. Special linkages may also be used to tie together two different grasp devices powered by one common actuator.

*Part modifications* should be analyzed to determine whether minor part changes that do not affect the functions of the part can be made to reduce the cost and complexity of the end-effector. Often, simple part changes, such as holes or tabs in parts, can significantly reduce the end-effector design complexity and build effort in the design of new component parts for automation and assembly by robots.

*Part inconsistencies* should be analyzed to determine the need for provision of out-of-tolerance sensors or compensating tooling to accommodate these conditions.

For *tool handling*, the tool should be analyzed to determine the characteristics of the end-effector required. This is especially true for the incorporation of protective sensors in the tool and end-effector to deal with part inconsistencies.

### 8.2.2 Process Analysis

In addition to a thorough analysis of the workpiece, an analysis of the application process should be made to determine the optimum parameters for the end-effector.

The *process method* itself should be analyzed, especially in terms of manual versus robot operation. In many cases physical limitations dictate that a person perform a task in a certain manner where a robot without these constraints may perform the task in a more efficient but different manner. An example of this involves the alternative of picking up a tool and doing work on a part or instead picking up the part and taking it to the tool. In many cases the size and weight-carrying capability of a person is limited, forcing the person to handle the smaller and lighter weight of the part or the tool. A robot, with its greater size and payload capabilities, does not have this restriction. Thus it may be used to take a large part to a stationary tool or take multiple tools to perform work on a part. This may increase the efficiency of the operation by reducing cycle time, improving quality, and increasing productivity. Therefore, in process analysis, consider the alternatives of having the robot take a part to a tool or a tool to a part and decide which approach is most efficient. When a robot is handling a part, rather than a tool, power-line connections to the tool, which experience less flexure and are less prone to problems when stationary than moving, are less of a concern.

Because of its increased payload capability, a robot may also be equipped with a multifunctional end-effector. This can simultaneously or sequentially perform work on a part that previously required a person to pick up one tool at a time to perform the operation, resulting in lower productivity. For example, the end-effector in a die-casting machine unloading application may not only unload the part, but also spray a die lubricant on the face of the dies.

The *range and quantity of parts or tools* in the application process should be analyzed to determine the performance requirements for the end-effector. This will dictate the number of hands or end-effectors that are required. The end-effector must be designed to accommodate the range of part sizes, whether automatically in the tool for the end-effector, through automatic tool change, or through manual changeover. Manual changeover could involve adjusting the tool to handle a different range of parts or interchanging fingers, inserts, or tools on a common hand. To reduce the manual changeover time, quick disconnect capabilities and positive alignment features such as dowel pins or locating holes should be provided. For automatic tool change applications, mechanical registration provisions, such as tapered pins and bushings, ensure proper alignment of tools. Verification sensors should also be incorporated in automatic tool change applications.

*Presentation and disposition* of the workpiece within the robot system affect the design of the end-effector. The position and orientation of the workpiece at either the pickup or release stations will determine the possible contact points on the part, the dimensional clearances required in the end-effector to avoid interferences, the manipulative requirements of the end-effector, the forces and moments of the end-effector and part in relation to the robot end-effector mounting plate, the need for sensors in the end-effector to detect part position or orientation, and the complexity of the end-effector.

The *sequence of events and cycle time requirements* of the process have a direct bearing on tooling design complexity. Establishing the cycle time for the operation will determine how many tools (or hands) are needed to meet the requirements. Hands with multiple parts-handling functions often allow the robot to increase the productivity of the operation by handling more parts per cycle than can be handled manually. The sequence of events may also dictate the use of multifunctional end-effectors that must perform

several operations during the robot cycle. For example, in machine unloading, mentioned above, the end-effector not only grasps the part, but sprays a lubricant on the molds or dies of the machine. Similarly, a robot end-effector could also handle a part and perform work on it at the same time, such as automatic gauging and drilling a hole. The sequence of events in going from one operation to another may cause the design of the end-effector to include some extra motions not available in the robot by adding extra axes of motion in the end-effector to accommodate the sequence of operations between various system elements.

*In-process inspection requirements* will affect the design of the end-effector. The manipulative requirements of the end-effector, the design of sensors or gauging into the end-effector, and the contact position of the end-effector on the part are all affected by the part-inspection requirements. Precision in positioning the workpiece is another consideration for meeting inspection requirements.

The *conditional processing* of the part will determine the need for sensors integrated into the end-effector, as well as the need for independent action by multiple-gripper systems.

The *environment* must be considered in designing the end-effector. The effects of temperature, moisture, airborne contaminants, corrosive or caustic materials, and vibration and shock must be evaluated, as will the material selection, power selection, sensors, mechanics, and provision for protective devices in the end-effector.

### 8.3 Guidelines for End-Effector Design

Guidelines for end-effector design to best meet the criteria discussed above are as follows:

1. Design for quick removal or interchange of the end-effector by requiring a small number of tools (wrenches, screwdrivers, etc.) to be used. Use the same fasteners wherever possible.
2. Provide locating dowels, key slots, or scribe lines for quick interchange, accuracy registration, and alignment.
3. Break all sharp corners to protect hoses and lines from rubbing and cutting and maintenance personnel from possible injury.
4. Allow for full flexure of lines and hoses to extremes of axes of motion.
5. To reduce weight, use lightening holes or lightweight materials wherever possible.
6. For wear considerations, hardcoat lightweight materials and put hardened, threaded inserts in soft materials.
7. Conceptualize and evaluate several alternatives in the end-effector.
8. Do not be “penny-wise and pound-foolish” in designing the end-effector; make sure enough effort and cost is spent to produce a production-worthy, reliable end-effector and not a prototype.
9. Design in extra motions in the end-effector to assist the robot in its task.
10. Design in sensors to detect part presence during transfer (limit switch, proximity, air jet, etc.).
11. For safety in part-handling applications, consider what effect a loss of power to the end-effector will have. Use toggle lock gripping devices or detented valves to promote safety.
12. Put shear pins or areas in end-effector to protect more expensive components and reduce downtime.
13. When handling tools with robot, build in tool inspection capabilities, either in the end-effector or peripheral equipment.
14. Design multiple functions into the end-effector.
15. Provide accessibility for maintenance and quick change of wear parts.
16. Use sealed bearings for the end-effector.
17. Provide interchangeable inserts or fingers for part changeover.
18. When handling hot parts, provide heat sink or shield to protect the end-effector and the robot.
19. Mount actuators and valves for the end-effector on the robot forearm.
20. Build in compliance in the end-effector fixture where required.

21. Design action sensors in the end-effector to detect open/close or other motion conditions.
22. Analyze inertia requirements, center of gravity of payload, centrifugal force, and other dynamic considerations in designing the end-effector.
23. Look at motion requirements for the gripping device in picking up parts (single-action hand must be able to move part during pickup; double-action hand centers part in one direction; three or four fingers center part in more than one direction).
24. When using an electromagnetic pickup hand, consider residual magnetism on parts and possible chip pickup.
25. When using vacuum cup pickup on oily parts, also use a positive blow-off.
26. Look at insertion forces of robot in using end-effector in assembly tasks.
27. Maintain orientation of the part in the end-effector by force and coefficient of friction or locating features.

## 9 SUMMARY

To date, most of the applications of industrial robots have involved a specially designed end-effector or simple gripping devices. In most practical applications the use of simple end-effector is the best solution from the point of view of productivity and economy. If more complex tasks will be required of the robot, universal hands with more dexterity will be needed. Several important contributions have been made so far in the theory of multifingered hand control, but the technology of designing multifingered hand hardware has not yet matured. Research is ongoing to develop more flexible general-purpose universal hand hardware that can adapt to a variety of sizes and shapes of parts. The advancement of this technology to make possible more dexterous robotic manipulation can be expected.

## ACKNOWLEDGMENTS

This chapter is revised from Chapter 8 of the first edition of this handbook, with some materials added from Chapter 37, "End-of-Arm Tooling," by R. D. Potter.

## REFERENCES

- Ando, Y., et al. 1990. "Development of Micro Grippers." In *Micro System Technologies 90*. Ed. H. Reichl. Berlin: Springer-Verlag. 855–849.
- Arai, T., R. Larssonneur, and Y. M. Jaya. 1993. "Basic Motion of a Micro Hand Module." In *Proceedings of the 1993 JSME International Conference on Advanced Mechatronics*, Tokyo. 92–97.
- Chen, F. Y. 1982. "Gripping Mechanisms for Industrial Robots." *Mechanism and Machine Theory* **17**(5), 299–311.
- Crossley, F. R. E., and F. G. Umholts. 1977. "Design for a Three-Fingered Hand." In *Robot and Manipulator Systems*. Ed. E. Heer. Oxford: Pergamon Press. 85–93.
- Hirose, S., and Y. Umetani. 1977. "The Development of a Soft Gripper for the Versatile Robot Hand." In *Proceedings of the Seventh International Symposium on Industrial Robots*, Tokyo. 353–360.
- Jacobsen, S. C., et al. 1981. "The Utah/MIT Dextrous Hand: Work in Progress." In *Robotics Research*. Ed. M. Brady and R. Paul. Cambridge: MIT Press. 601–653.
- Kato, I., et al. 1969. "Multi-functional Myoelectric Hand Prosthesis with Pressure Sensory Feedback System-Waseda Hand 4P." In *Proceedings of the Third International Symposium on External Control of Human Extremities*, Belgrade.
- Kimura, M., et al. 1995. "Force Control of Small Gripper Using Piezoelectric Actuator." *Journal of Advanced Automation Technology* **7**(5), 317–322.
- Li, Z., and S. Sastry. 1990. "Issues in Dextrous Robot Hands." In *Dextrous Robot Hands*. Ed. S. T. Venkataraman and T. Iberall. New York: Springer-Verlag. 154–186.
- Maekawa, H., K. Tanie, and K. Komoriya. 1997. "Tactile Feedback for Multifingered Dynamic Grasping." *Control Systems* **17**(1), 63–71.
- Mason, M.T., and J. K. Salisbury. 1985. *Robot Hands and the Mechanics of Manipulation*. Cambridge: MIT Press. 80–81.
- Murray, R. M., Z. Li, and S. S. Sastry. 1994. *A Mathematical Introduction to Robotic Manipulation*. London: CRC Press. 382–387.
- Okada, T. 1982. "Computer Control of Multijointed Finger System for Precise Object-Handling." *IEEE Transactions on Systems, Man and Cybernetics* **SMC-12**(3), 289–299.

- Osaki, S., and Y. Kuroiwa. 1969. "Machine Hand for Bar Works." *Journal of Mechanical Engineering Laboratory* 23(4). [In Japanese.]
- Schlesinger, G. 1919. *Der Mechanische Aufbau der künstlichen Glieder*. Part 2 of *Ersatzglieder und Arbeitshilfen*. Berlin: Springer.
- Sheldon, O. L. 1972. "Robots and Remote Handling Methods for Radioactive Materials." In *Proceedings of the Second International Symposium on Industrial Robots*, Chicago. 235–256.
- Skinner, F. 1974. "Design of a Multiple Prehension Manipulator System." ASME Paper 74-det-25.
- Sugano, S., et al. 1984. "The Keyboard Playing by an Anthropomorphic Robot." In *Preprints of Fifth CISM-IFTOMM Symposium on Theory and Practice of Robots and Manipulators*, Udine. 113–123.
- Tanikawa, T., T. Arai, and T. Matsuda. 1996. "Development of Micro Manipulation System with Two-Finger Micro Hand." In *Proceedings of the 1996 IEEE/RSJ International Conference on Robots and Intelligent Systems*, Osaka. 850–855.
- Umetsu, M., and K. Oniki. 1993. "Compliant Motion Control of Arm-Hand System." In *Proceedings of the 1993 JSME International Conference on Advanced Mechatronics*, Tokyo. 429–432.
- Yoshikawa, T., and K. Nagai. 1990. "Analysis of Multi-fingered Grasping and Manipulation." In *Dextrous Robot Hands*. Ed. S. T. Venkataraman and T. Iberall. New York: Springer-Verlag. 187–208.

#### ADDITIONAL READING

- Engelberger, J. F. *Robotics in Practice*. London: Kogan Page, 1980.
- Kato, I., ed. *Mechanical Hand Illustrated*. Tokyo: Survey Japan, 1982.